

Radiation Tolerant Silicon Detectors

Mara Bruzzi,
INFN and University of Florence, Italy
Gianluigi Casse
University of Liverpool, UK

Outline

- **Motivation to develop radiation harder detectors**
 - expected radiation levels at the upgraded LHC (sLHC)
 - Radiation induced degradation of detector performance
- **Radiation Damage in Silicon Detectors**
 - Microscopic damage (crystal damage), NIEL
 - Macroscopic damage (changes in detector properties: N_{eff} , I_R , $CC(V)$)
- **Changes with time after irradiation**
 - Annealing of the detector electrical properties: N_{eff} , I_R , $CCE(V)$
- **Radiation hardening of Silicon sensors**
 - Material Engineering
 - New silicon materials – FZ, MCZ, DOFZ, EPI
 - Device Engineering
 - p-in-n, n-in-n and n-in-p sensors, 3D sensors
- **Conclusions**

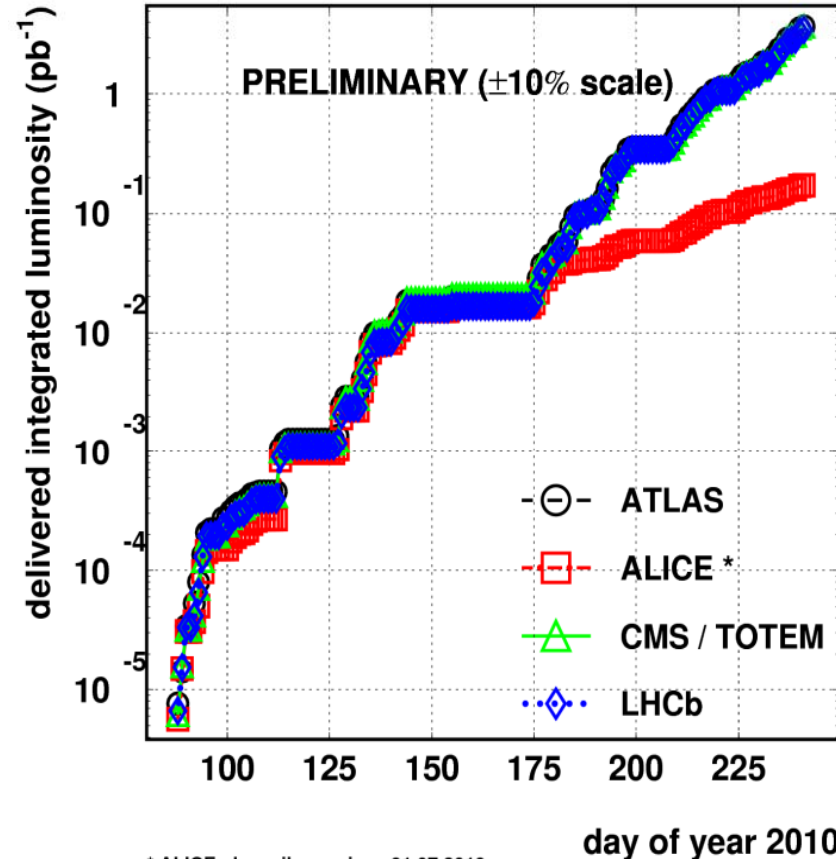
LHC Machine Performance in 2010

2010/09/06 08.36

LHC 2010 RUN (3.5 TeV/beam)

“Luminosity”, measured in $\text{b}^{-1}\text{s}^{-1}$ * or $\text{cm}^{-2}\text{s}^{-1}$ is an indication of how fast collisions are produced, it represents the flux as seen by all the protons in one beam of oncoming protons in the other.

Cross-section (σ): measure of the probability of a process per flux of incoming particles. \mathcal{L} multiplied by the total cross-section, gives the total event rate.



*1 barn = 10^{-28}m^2

The design number of protons per bunch, 1.1×10^{11} , was first achieved 10th June 2010 and is now routine. Emphasis now is on increasing number of bunches circulating at any time in the LHC and then further improve the final focus. Record luminosity: $\sim 4 \times 10^{31} \text{cm}^{-2}\text{s}^{-1}$ achieved 24th September.

Upgrading the LHC for High Luminosity

With modest investment, the **LHC can run at much higher collision rates**, greatly increasing the scope to search for new particles and study rare processes

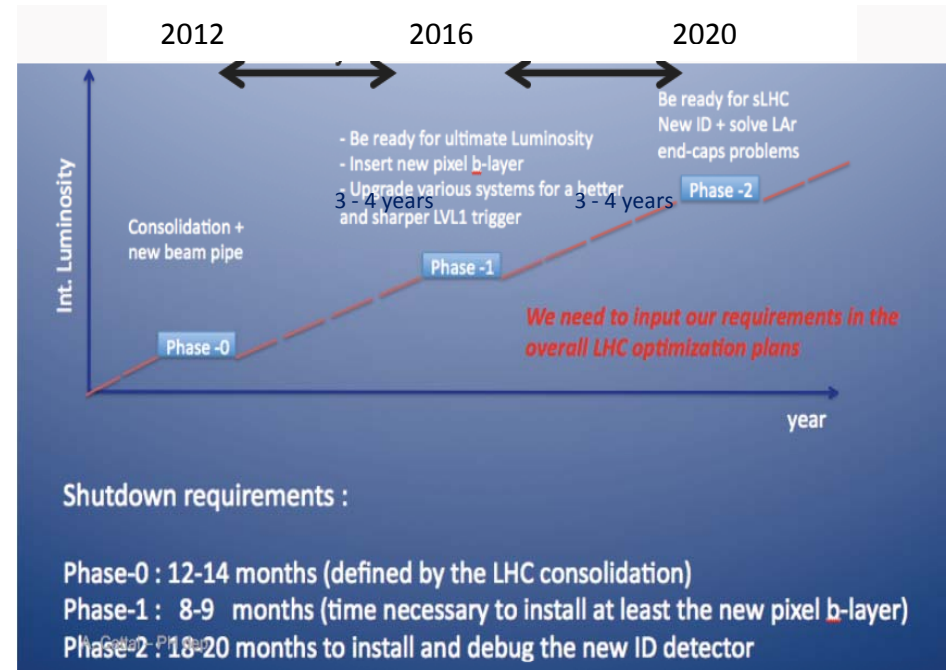
Expected Development in Luminosity

– Phase-I (after 5 years)

- Up to $\sim 60\text{fb}^{-1}/\text{year}$
- Experiments need:
 - **New vertex detectors**
 - **New off-line electronics**
 - ...

– Phase-II (after 10 years)

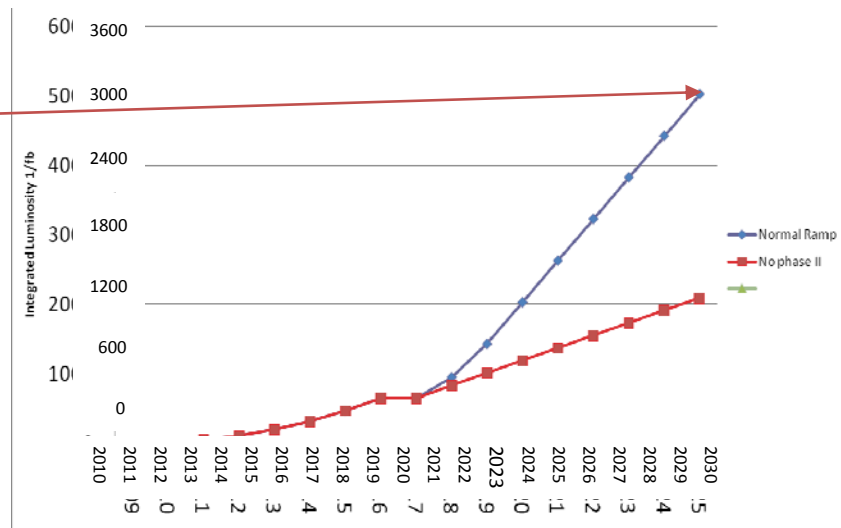
- Up to $\sim 300\text{fb}^{-1}/\text{year}$
- Experiments need:
 - **Complete tracker replacement**
 - **Much improved on-line filtering**
 - **New read-out for many subsystems**
 - ...



Upgrading the Experiments

To keep ATLAS and CMS running beyond ~10 years requires tracker replacement
Current trackers designed to survive up to 10Mrad in strip detectors ($\leq 700 \text{ fb}^{-1}$)
For the luminosity-upgrade the new trackers will have to cope with:

- much higher integrated doses
(need to plan for $\geq 3000 \text{ fb}^{-1}$)
- much higher occupancy levels (up to 400 collisions per beam crossing)
- Installation inside an existing 4π coverage experiment
- Budgets are likely to be such that replacement trackers, while needing higher performance to cope with the extreme environment, cannot cost more than the ones they replace

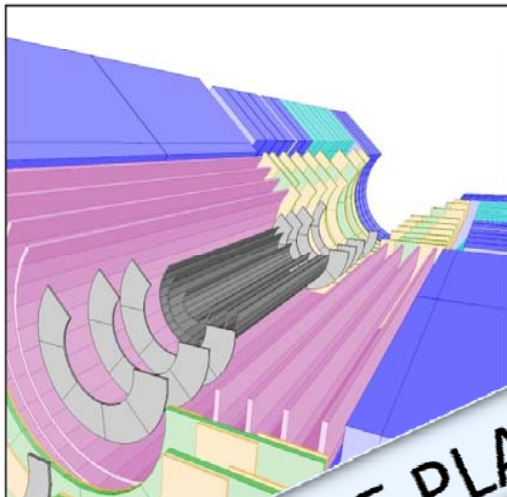


To install a new tracker in ~2020, require Technical Design Report 2014/15
(Note the ATLAS Tracker TDR: April 1997; CMS Tracker TDR: April 1998)

Technology in Current Highest Dose Regions

LHC vertex detectors close to the interaction point:

- Required to be very radiation hard and to be very finely segmented because of the very high density of tracks close to primary collisions
- Doses $5 - 10 \times 10^{14} n_{eq} cm^{-2}$ (~ 100 Mrad)
- $0.05mm \times 0.4mm$ pixels
(40 million images per second)

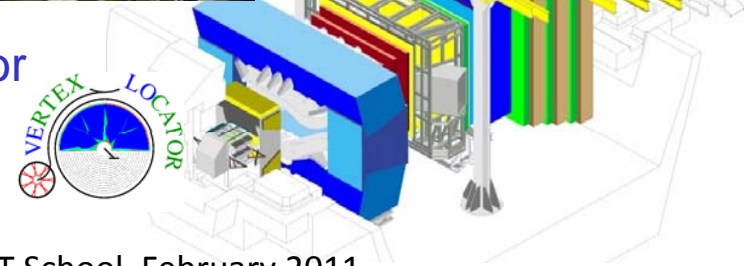


ATLAS
pixels

ALL USE PLANAR N-IN-N SILICON DETECTORS



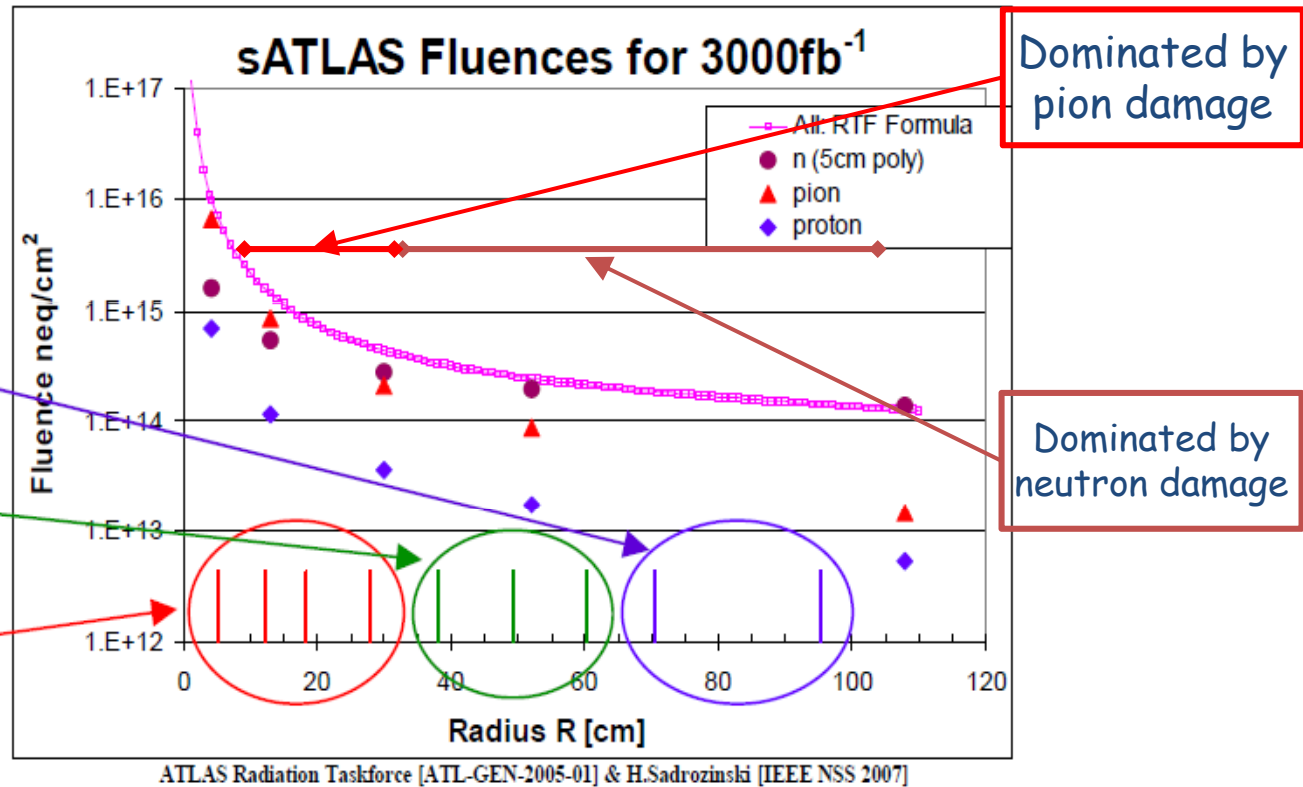
LHCb
Vertex Locator
Z(mm)=0-990



Radiation levels expected with sLHC

Radial distribution of sensors determined by Occupancy

- Long Strips (up to $4 \times 10^{14} \text{cm}^{-2}$)
- Short Strips (up to 10^{15}cm^{-2})
- Pixels (up to 10^{16}cm^{-2})

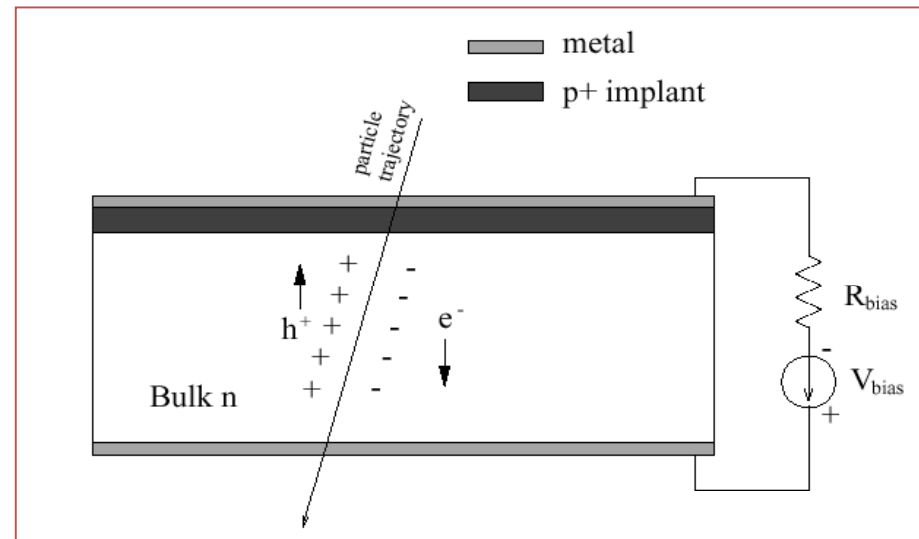
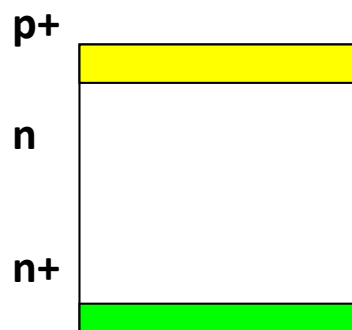


- Radiation hardness requirements (including safety factor of 2)
 - $2 \times 10^{16} \text{ n}_{\text{eq}}/\text{cm}^2$ for the innermost pixel layers
 - $1 \times 10^{15} \text{ n}_{\text{eq}}/\text{cm}^2$ for the innermost strip layers

[M.MoII]

Silicon Detector: Working Principles

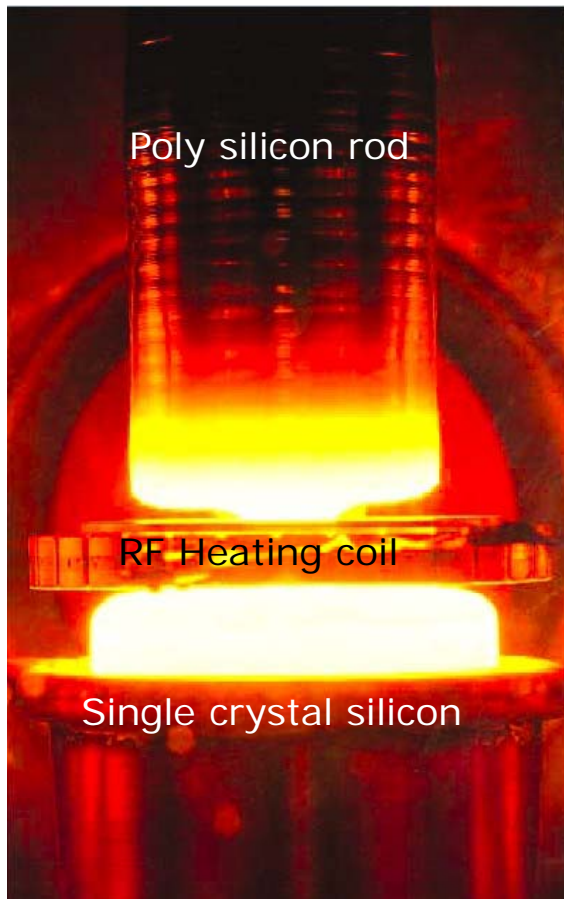
- Standard Si Detectors are **p⁺- n diodes made on high resistivity silicon:**
 - Float Zone silicon (FZ)
 - n-type: 2...20 KΩcm
 - [P] = 20...2×10¹¹ cm⁻³ (very low concentration !! below 1ppba = 5×10¹³cm⁻³)
 - [O] ≈ several 10¹⁵cm⁻³
 - [C] ≈ some 10¹⁵cm⁻³, usually [C] < [O]
 - crystal orientation: <111> or <100>



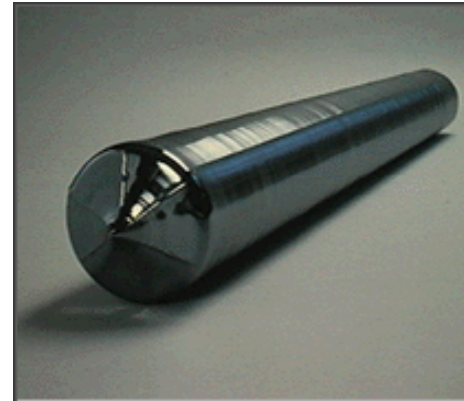
Material: Float Zone Silicon (FZ)

■ Float Zone process

- Using a single Si crystal seed, melt the vertically oriented rod onto the seed using RF power and “pull” the **monocrystalline ingot**



■ Mono-crystalline Ingot



■ Wafer production

- Slicing, lapping, etching, polishing



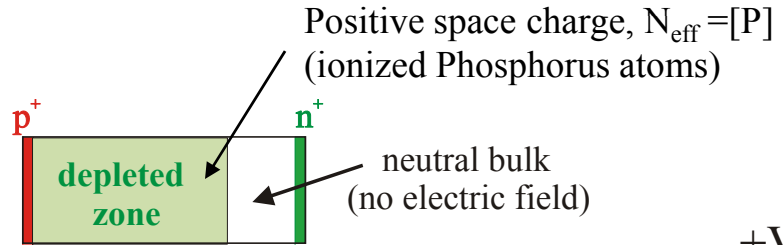
■ Highly pure crystal

- Low concentration of [O] and [C] 10^{15}cm^{-3}

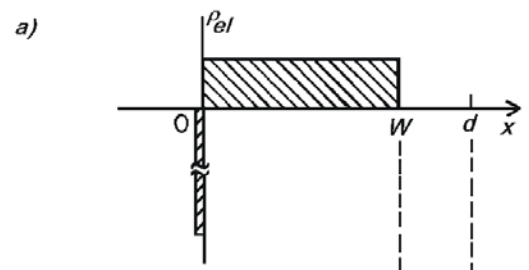
Reminder: Reverse biased abrupt p⁺-n junction

Poisson's equation

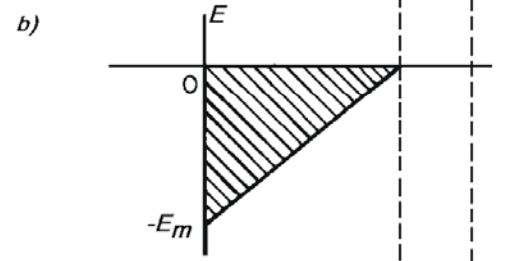
$$-\frac{d^2}{dx^2} \phi(x) = \frac{q_0}{\epsilon \epsilon_0} \cdot N_{eff}$$



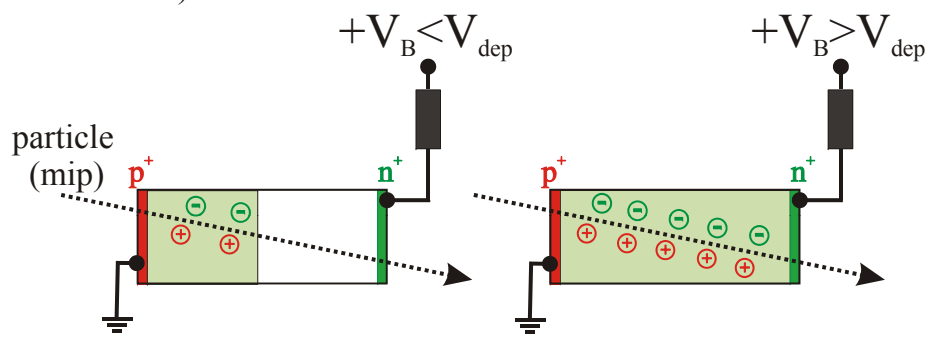
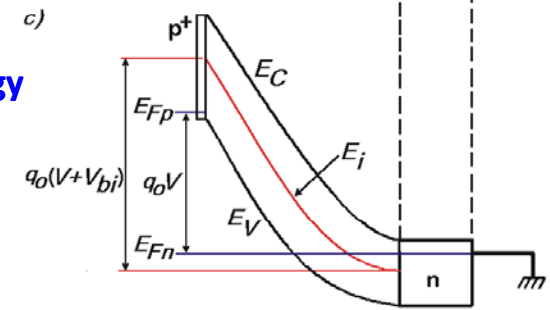
Electrical charge density



Electrical field strength



Electron potential energy



Full charge collection only for $V_B > V_{dep}$!

depletion voltage

$$V_{dep} = \frac{q_0}{\epsilon \epsilon_0} \cdot |N_{eff}| \cdot d^2$$

effective space charge density

Relevant parameters of the detector based on a p-n junction

Leakage Current

$$J_{rev} = \frac{1}{2} q \frac{n_i}{\tau_0} W \alpha \sqrt{V_{rev}}$$

Capacitance

$$C = \frac{\varepsilon \cdot Area}{d}$$

Depletion thickness

$$d = \sqrt{\frac{2\varepsilon}{qN_{eff}} (V_{rev} + V_{built-in})}$$

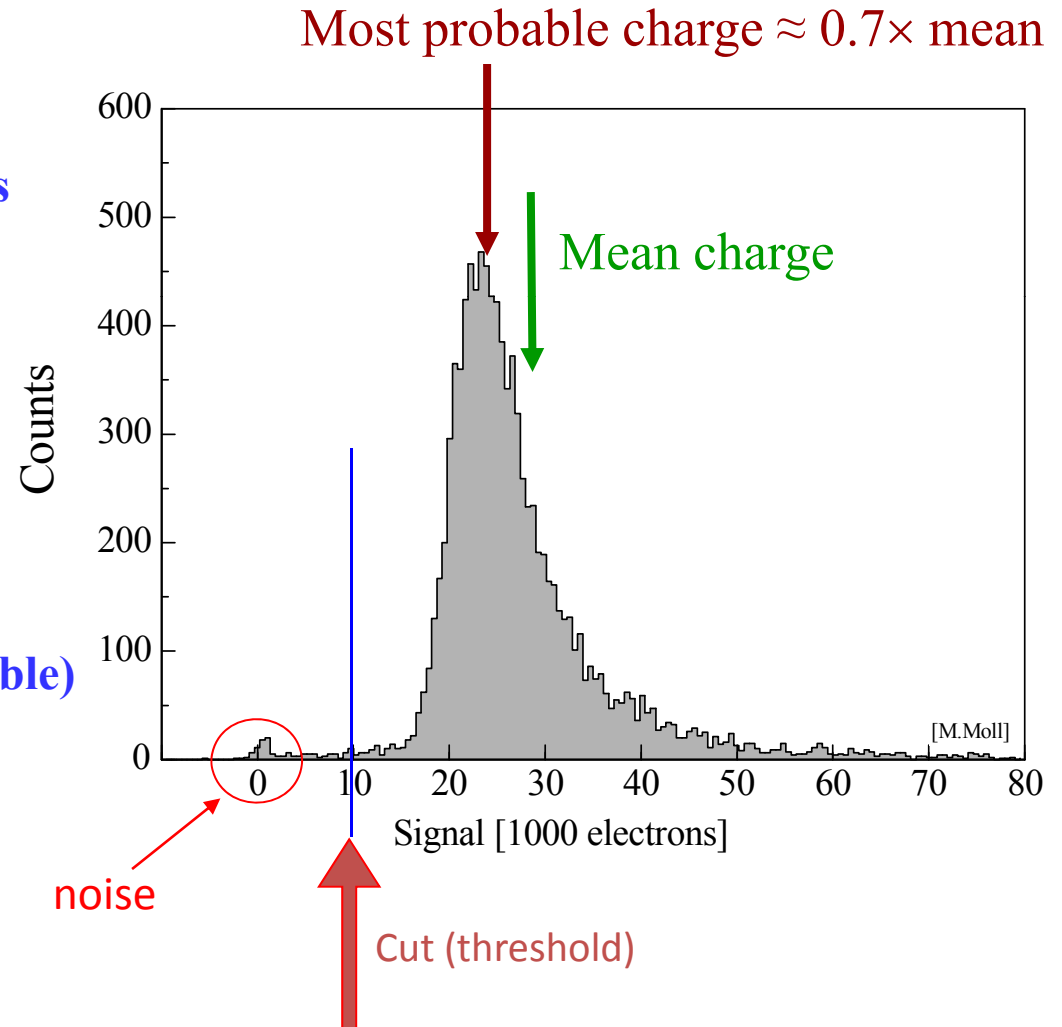
Effective space charge concentration in depleted region

$$N_{eff} = \frac{2 \cdot \varepsilon \cdot V_{dep}}{q \cdot W^2}$$

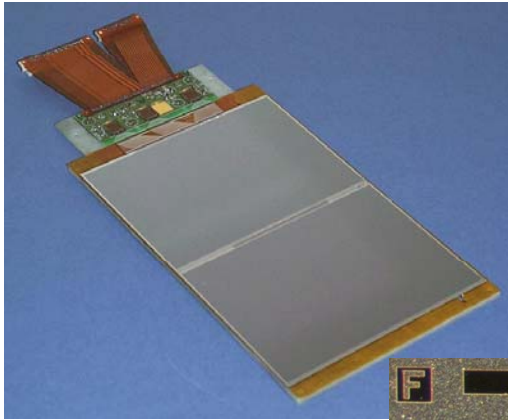
The charge signal

■ Collected Charge for a Minimum Ionizing Particle (MIP)

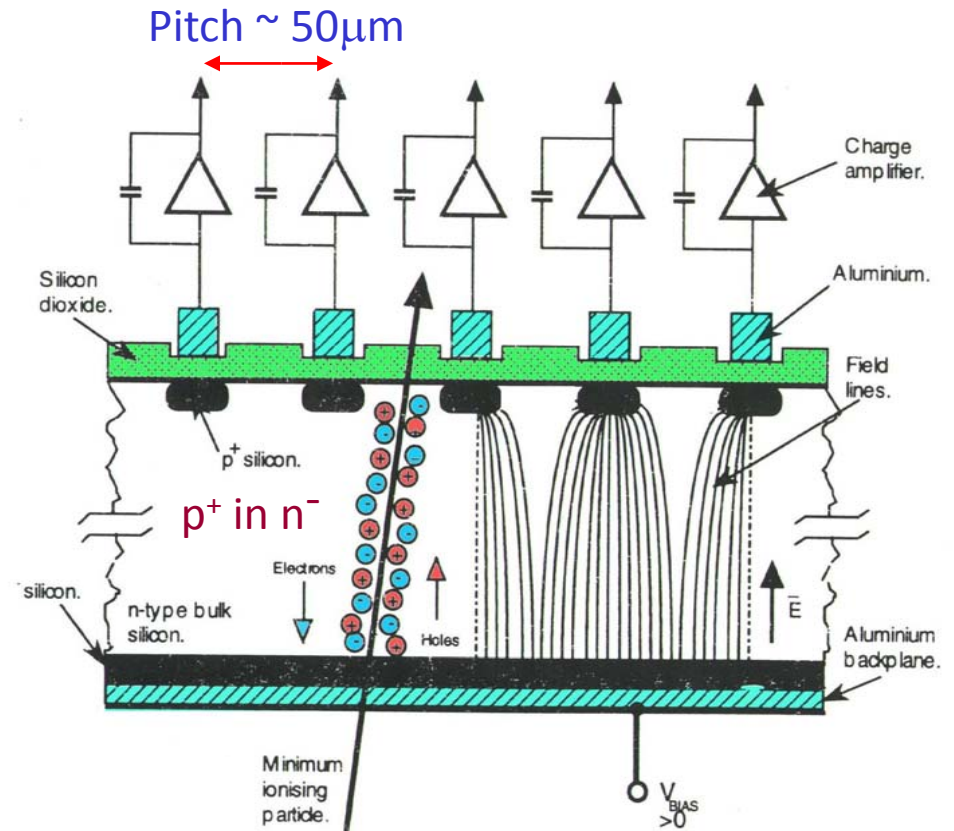
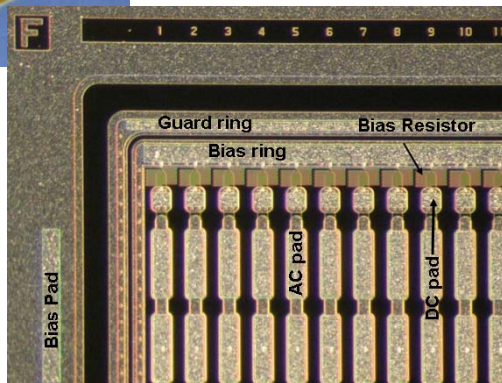
- **Mean energy loss**
 dE/dx (Si) = 3.88 MeV/cm
 \Rightarrow 116 keV for 300 μ m thickness
- **Most probable energy loss**
 $\approx 0.7 \times$ mean
 \Rightarrow 81 keV
- **3.6 eV to create an e-h pair**
 \Rightarrow 72 e-h / μ m (mean)
 \Rightarrow 108 e-h / μ m (most probable)
- **Most probable charge (300 μ m)**
 ≈ 22500 e ≈ 3.6 fC



Micro-strip Silicon Detectors



Highly segmented silicon detectors have been used in Particle Physics experiments for nearly 30 years. They are favourite choice for Tracker and Vertex detectors (high resolution, speed, low mass, relatively low cost)

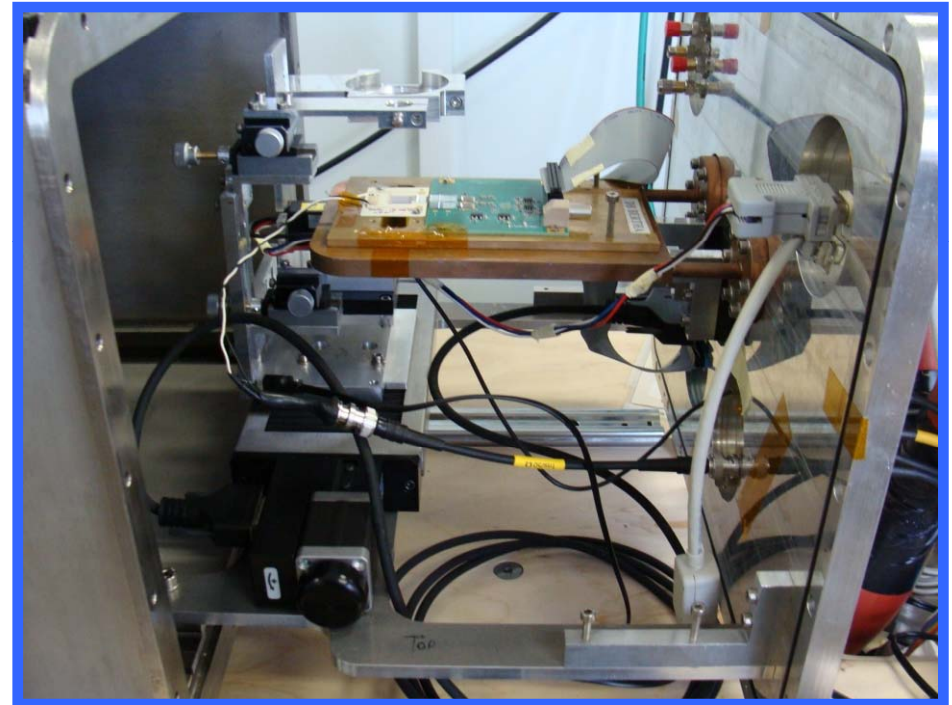


Main application: detect the passage of ionising radiation with high spatial resolution and good efficiency.
Segmentation \rightarrow position

Resolution $\sim 5\mu m$

The CERN CCE experimental system (strips)

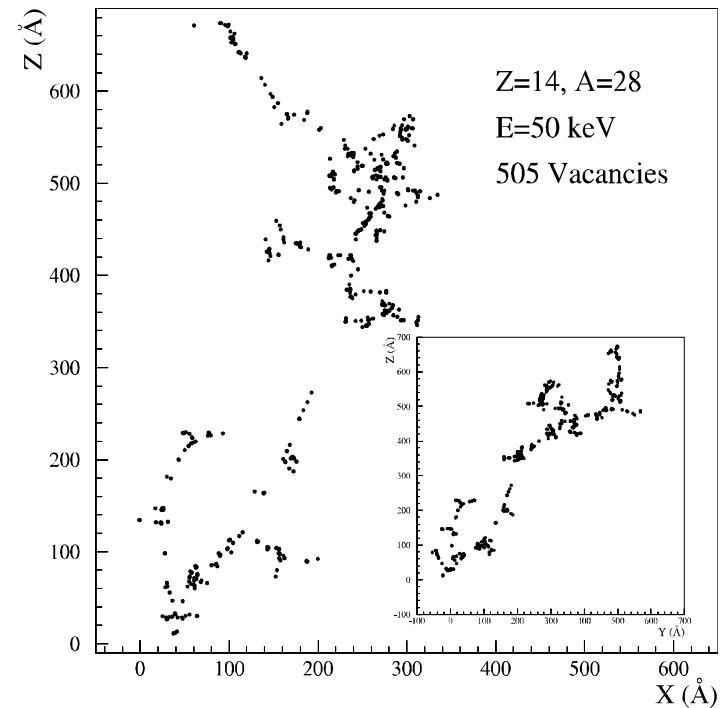
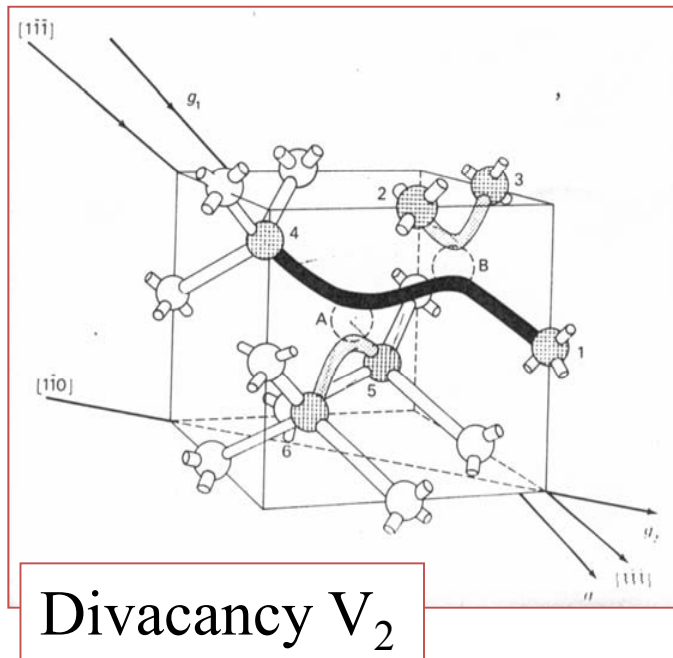
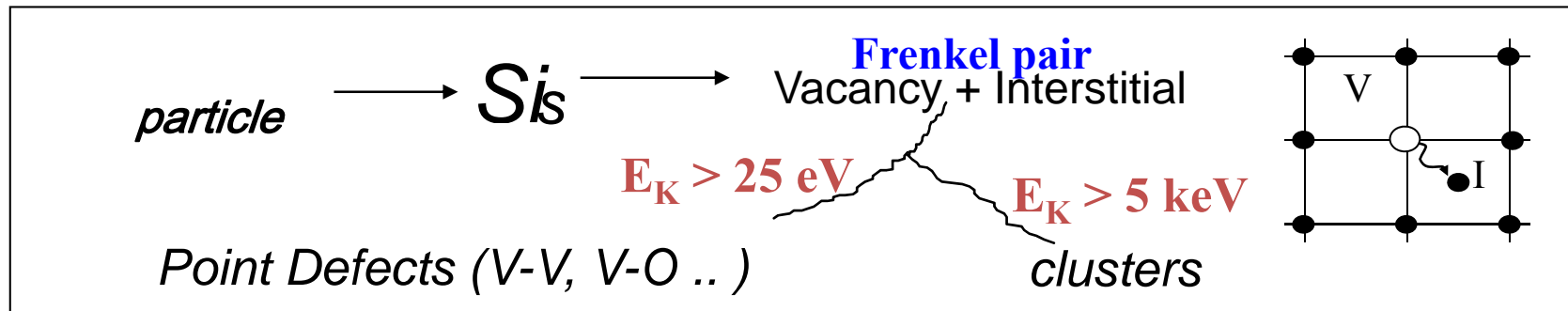
- Alibava based setup
- 3.6 MBq ^{90}Sr source
- $-30\pm 0.5^\circ\text{C}$ temperature (provided with closed circuit silicon-oil cooling) – Presented measurements performed at -20°C
- Single scintillator triggering (collimation provided by small cross section of the scintillator)
- Custom modified version of the Alibava DAQ software (0.1.5) with automatic voltage ramping implemented
- Custom version of the analysis root macros



Nicola Pacifico & al. - RESMDD10 Conference – Florence, October 2010

**More on Laboratory 3: Hands on Silicon Strip Detectors
by Richard Bates (Glasgow U.) , Irena Dolenc Kittelmann (CERN) , Marco Milanovic**

Radiation damage: a microscopic view



Vacancy amount and distribution depends on particle kind and energy

⁶⁰Co-gammas

–Compton Electrons
with max. $E_\gamma \approx 1$ MeV
(no cluster production)

Electrons

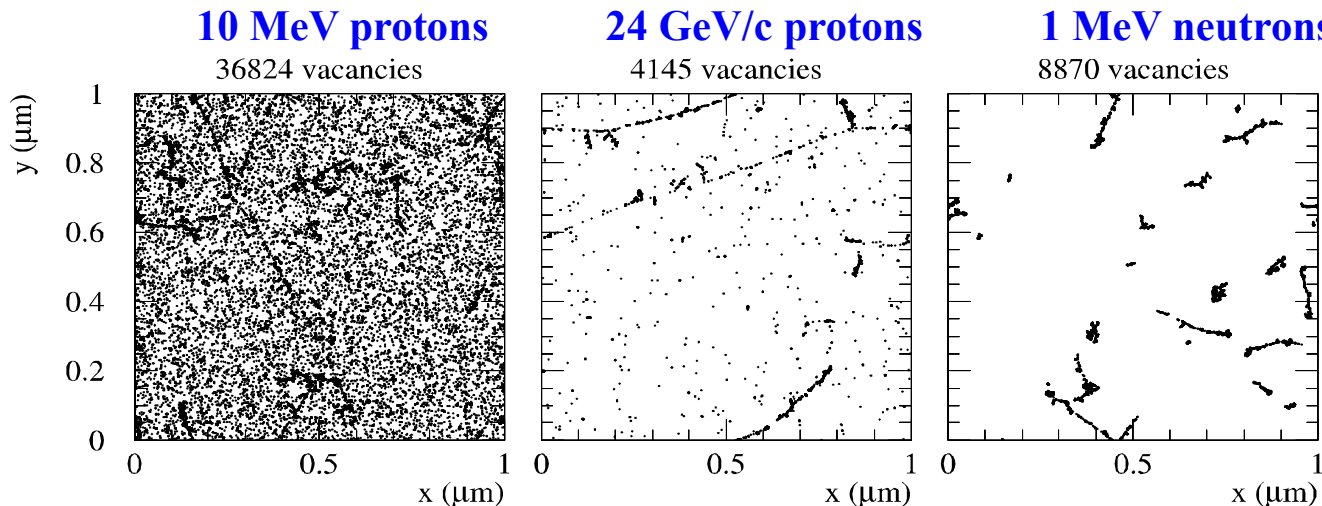
– $E_e > 255$ keV for displacement
– $E_e > 8$ MeV for cluster

Neutrons (elastic scattering)

– $E_n > 185$ eV for displacement
– $E_n > 35$ keV for cluster

Only point defects \longleftrightarrow point defects & clusters \longleftrightarrow Mainly clusters

Initial distribution of vacancies in $(1\mu\text{m})^3$ after 10^{14} particles/cm²



[Mika Huhtinen NIMA 491(2002) 194]

How to normalize radiation damage from different particles?

- NIEL - Non Ionizing Energy Loss scaling using hardness factors

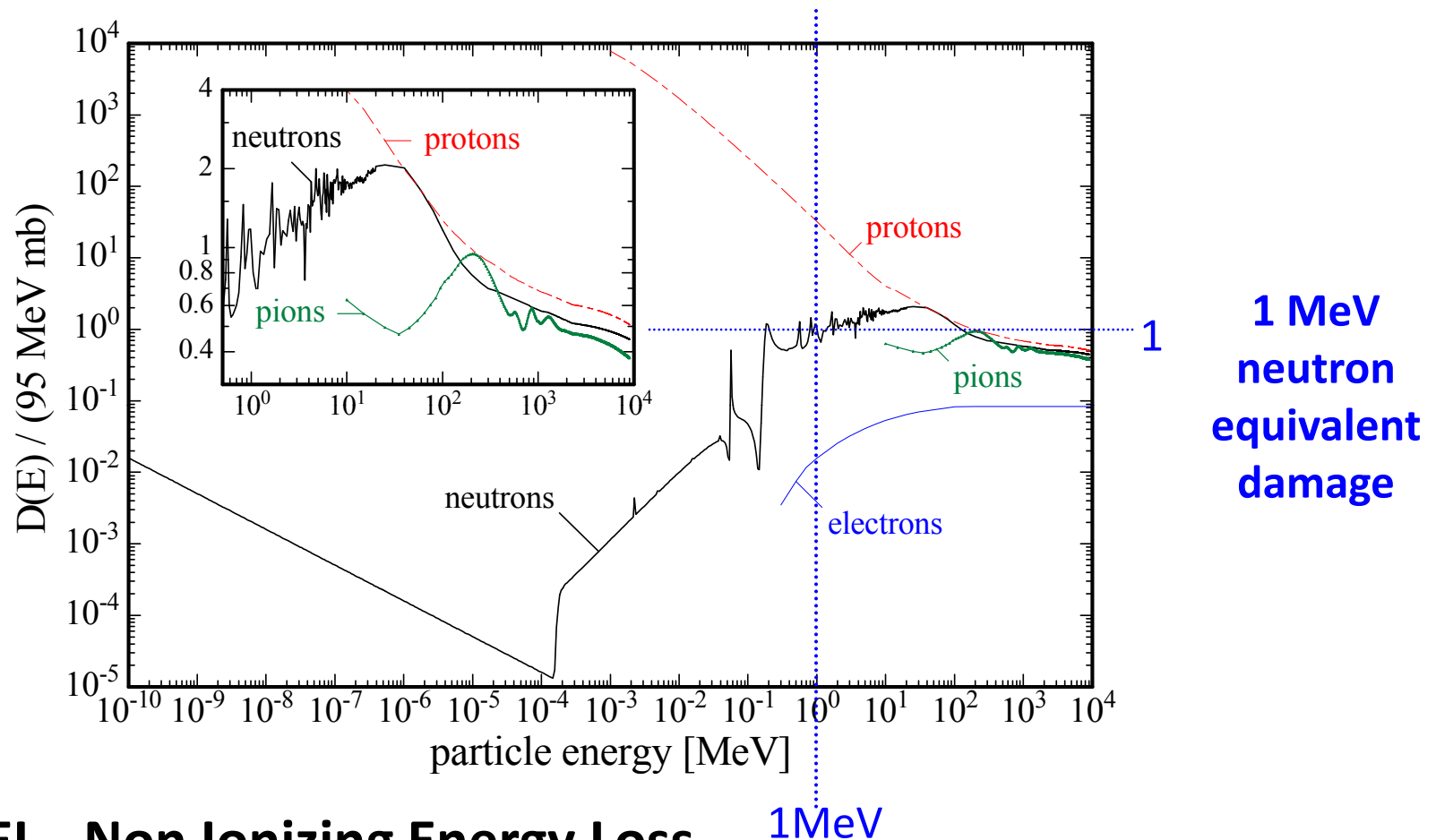
$$\kappa = \frac{1}{D(1\text{MeV neutrons})} \cdot \frac{\int D(E) \phi(E) dE}{\int \phi(E) dE}$$

Hardness factor κ of a radiation field (or monoenergetic particle) with respect to 1 MeV neutrons.

- **E** energy of particle
- **D(E)** displacement damage cross section for a certain particle at energy E
 $D(1\text{MeV neutrons})=95 \text{ MeV}\cdot\text{mb}$
- **$\phi(E)$** energy spectrum of radiation field

The integrals are evaluated for the interval $[E_{\text{MIN}}, E_{\text{MAX}}]$, being E_{MIN} and E_{MAX} the minimum and maximum cut-off energy values, respectively, and covering all particle types present in the radiation field

NIEL - Displacement damage functions



- NIEL - Non Ionizing Energy Loss
- NIEL - Hypothesis: Damage parameters scale with the NIEL
 - *Be careful, does not hold for all particles & damage parameters (see later)*

Primary Damage and Secondary Defect Formation

- Two basic defects

I - Silicon Interstitial V - Vacancy

- Primary defect generation

I, I₂ higher order I (?)
 ⇒ I-CLUSTER (?) ←

V, V₂, higher order V (?)
 ⇒ V-CLUSTER (?) ←

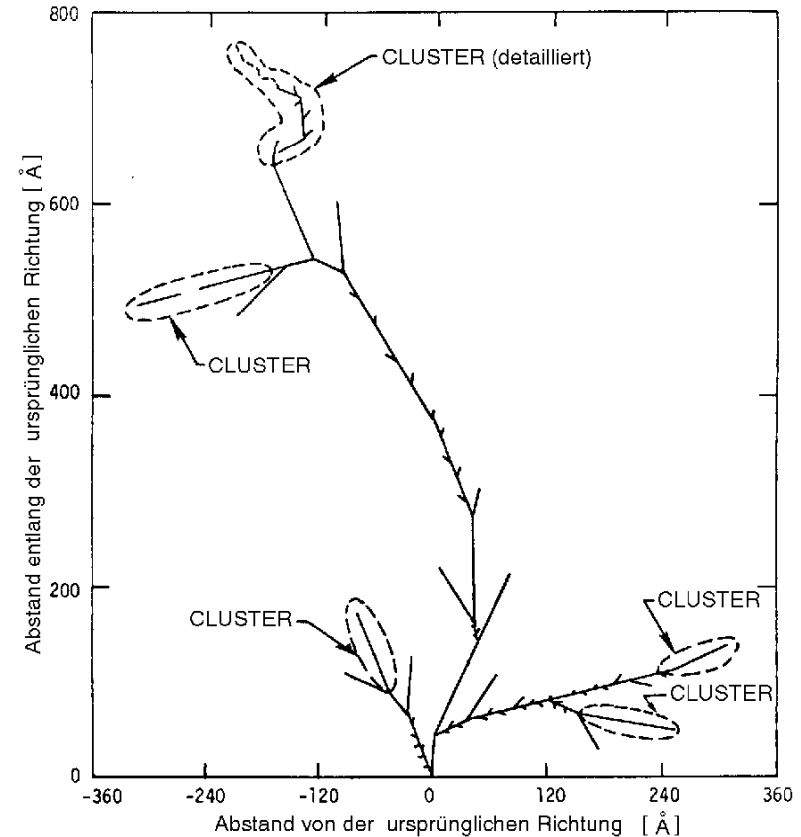
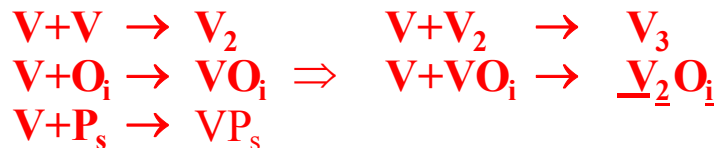
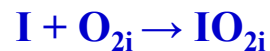
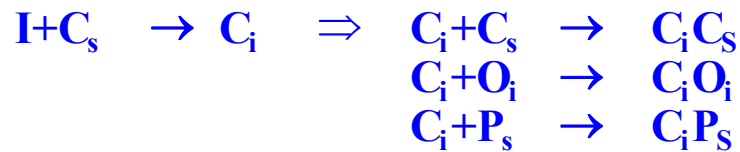
- Secondary defect generation

Dopants : P, B

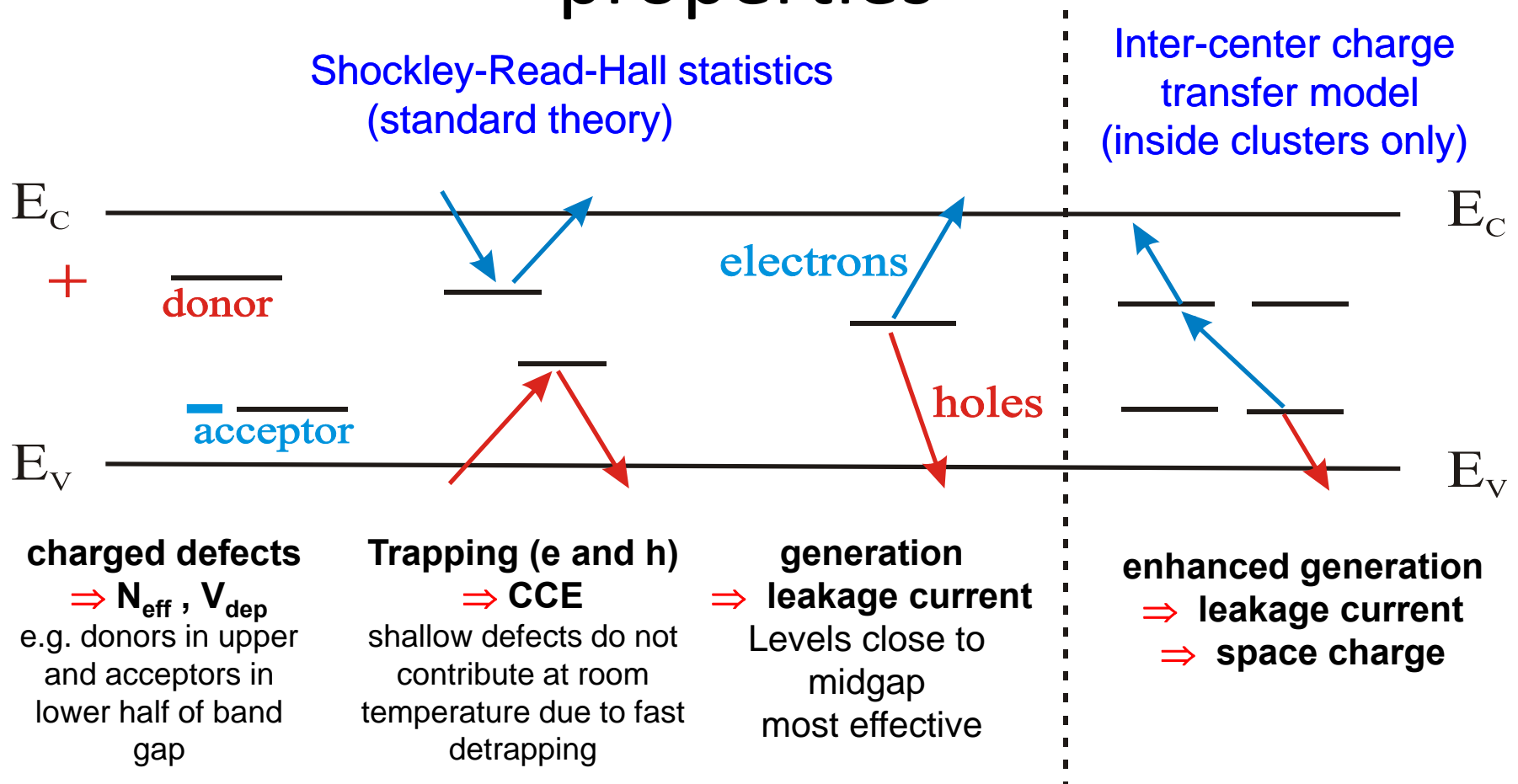
Main impurities in silicon: Carbon C_s

Oxygen O_i

Oxygen dimer: O_{2i}



Impact of Defects on Detector properties



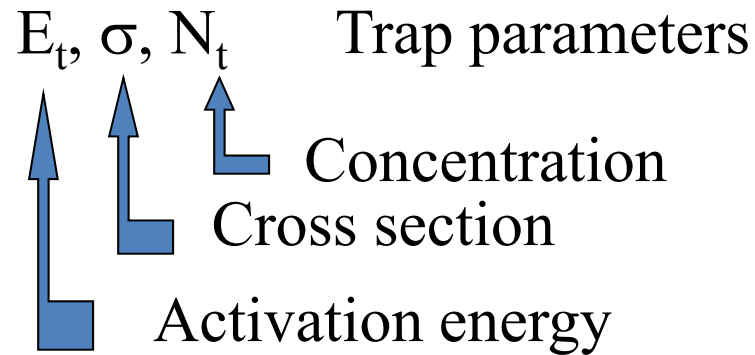
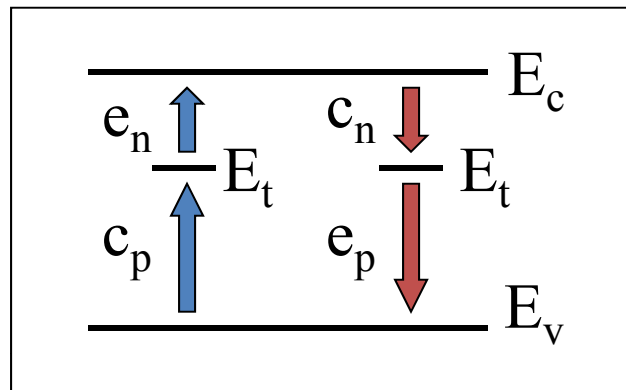
Impact on detector properties can be calculated if all defect parameters are known:

$\sigma_{n,p}$: cross sections

E_t : activation energy

N_t : concentration

Experimental techniques to analyse defects in semiconductor materials

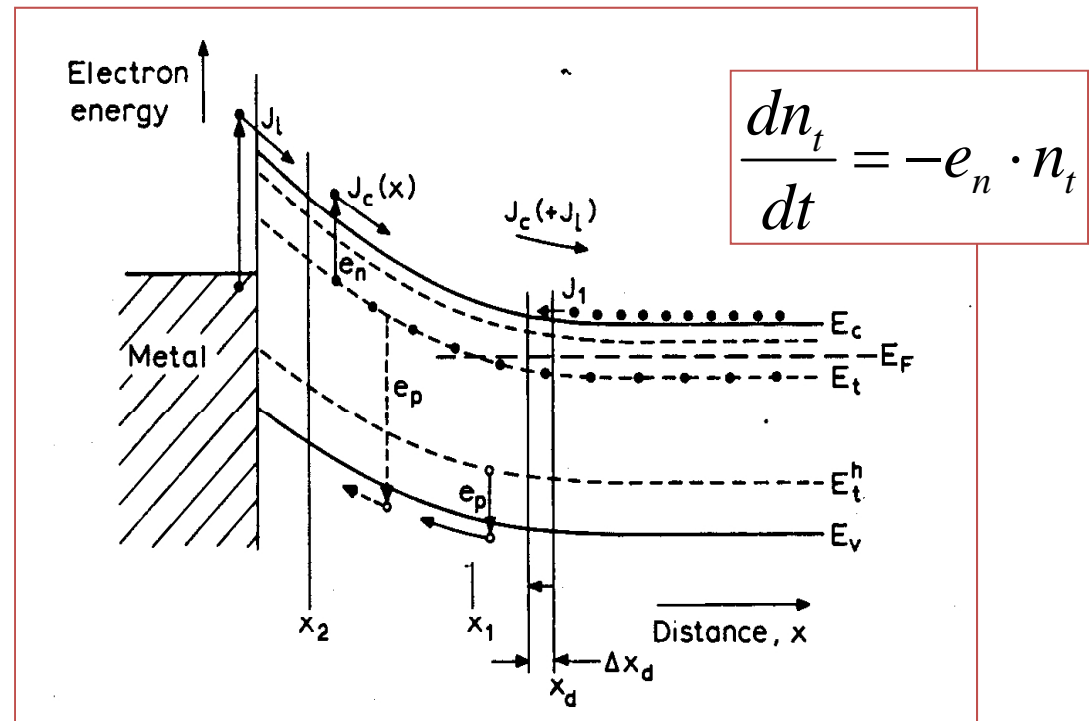


Emission coefficient:

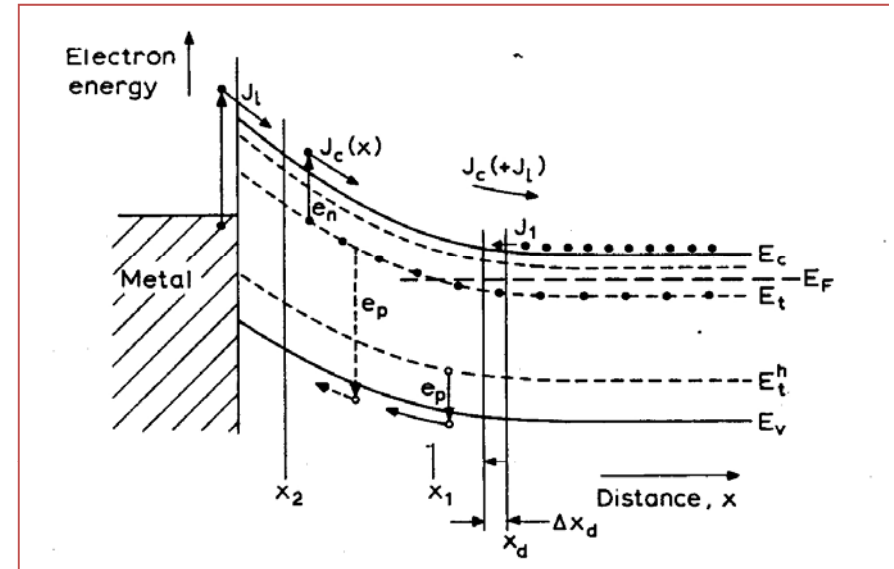
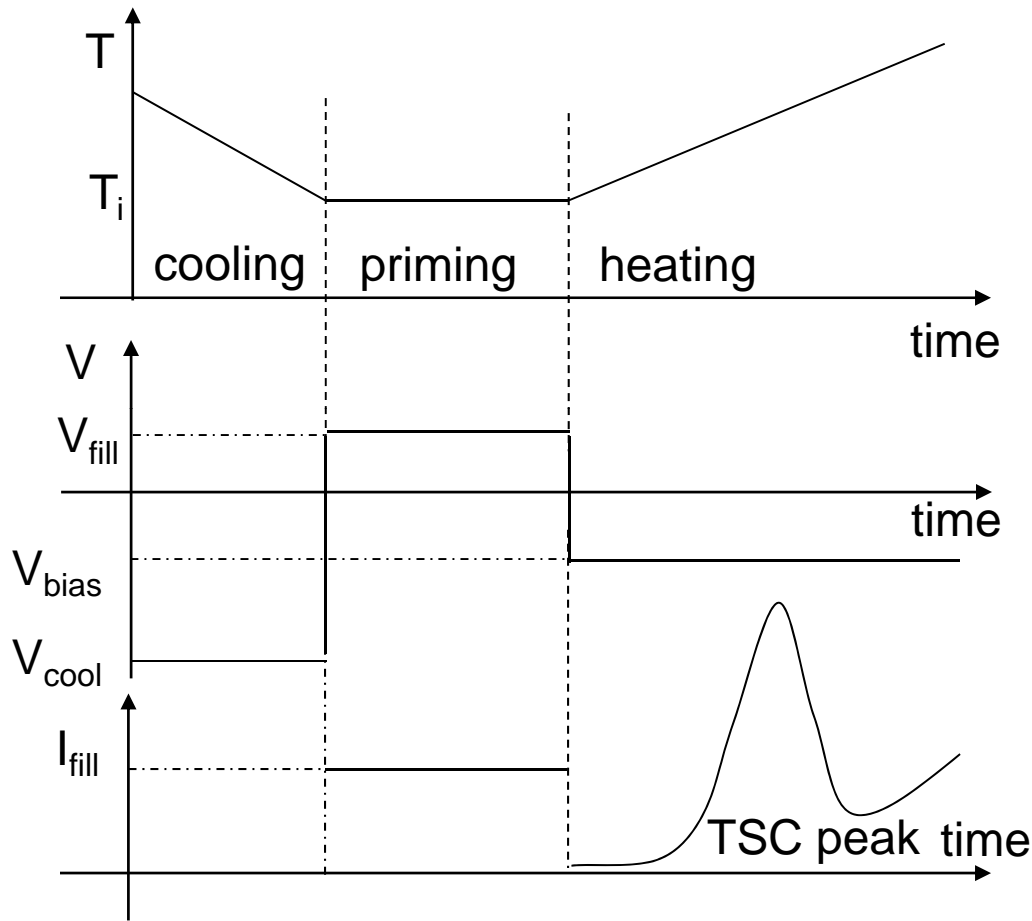
$$e_n = N_c \sigma_n v_{th} \cdot e^{-\frac{E_c - E_t}{KT}}$$

Capture coefficient :

$$c_n = n \sigma_n v_{th}$$



Thermally Stimulated Current: TSC



-Cooling with applied reverse V_{cool} or null bias

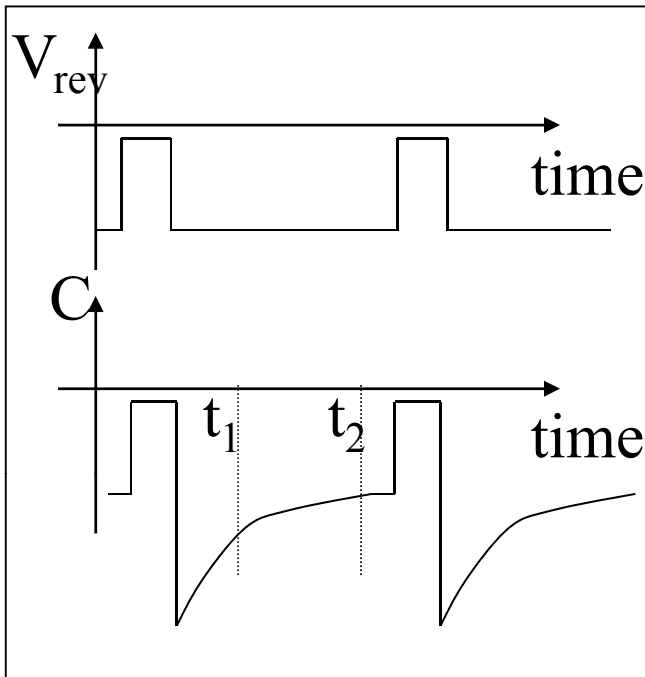
-Forward voltage applied V_{fill} at T_i or illumination with optical source

- V_{bias} applied

-Thermally stimulated current read-out

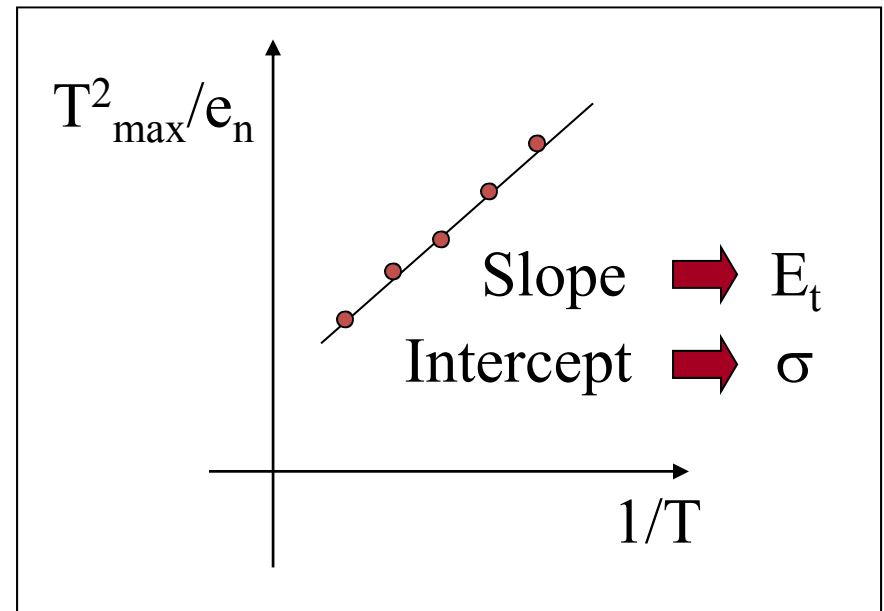
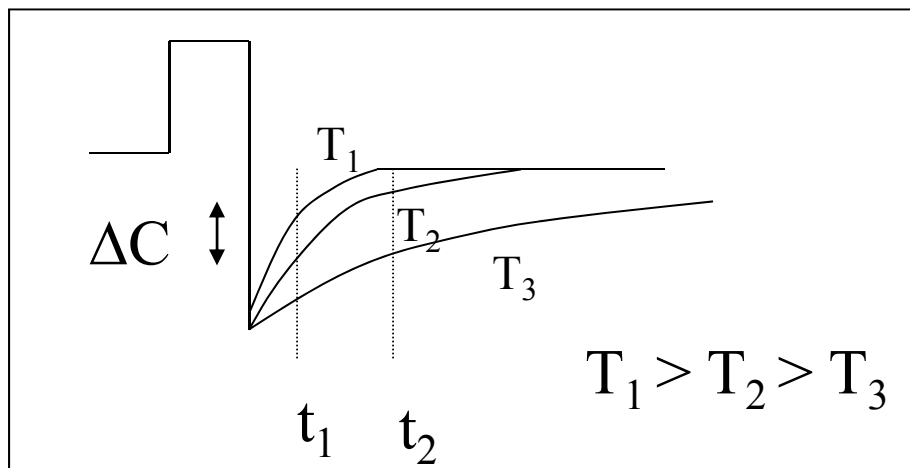
$$I_{TSC}(T) = -\frac{1}{2} q \cdot A \cdot N_t \cdot W \cdot e_n(T) \exp\left(-\frac{1}{b} \int_{T_i}^T e_n(T) dT\right)$$

Deep Level Transient Spectroscopy DLTS

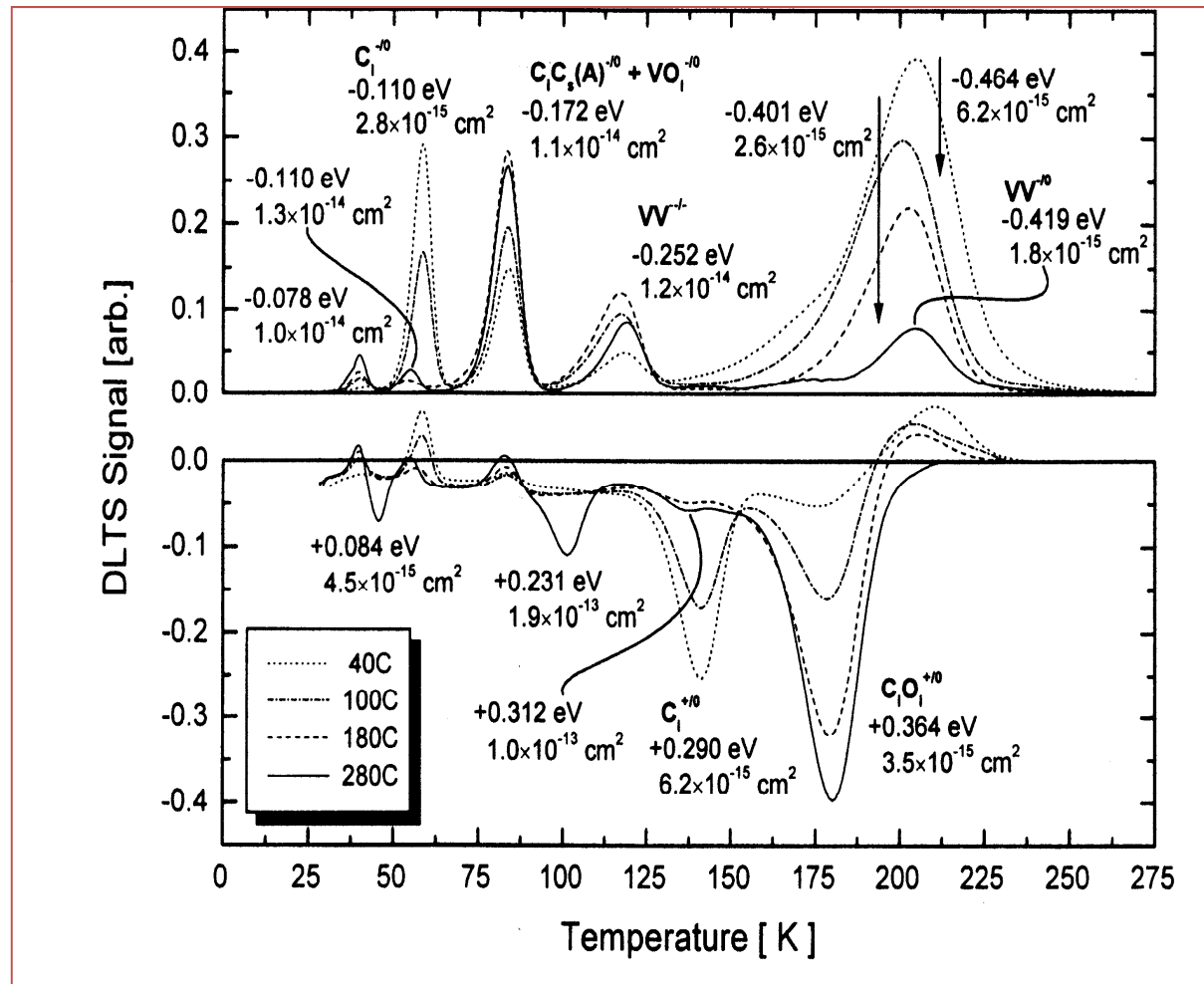


$$S = \Delta C_0 \left(e^{-e_n(T)t_1} - e^{-e_n(T)t_2} \right)$$

$$e_n(T_{\max}) = \frac{t_2 - t_1}{\ln(t_2 / t_1)} \alpha T_{\max}^2 \cdot e^{-E_t / KT_{\max}}$$



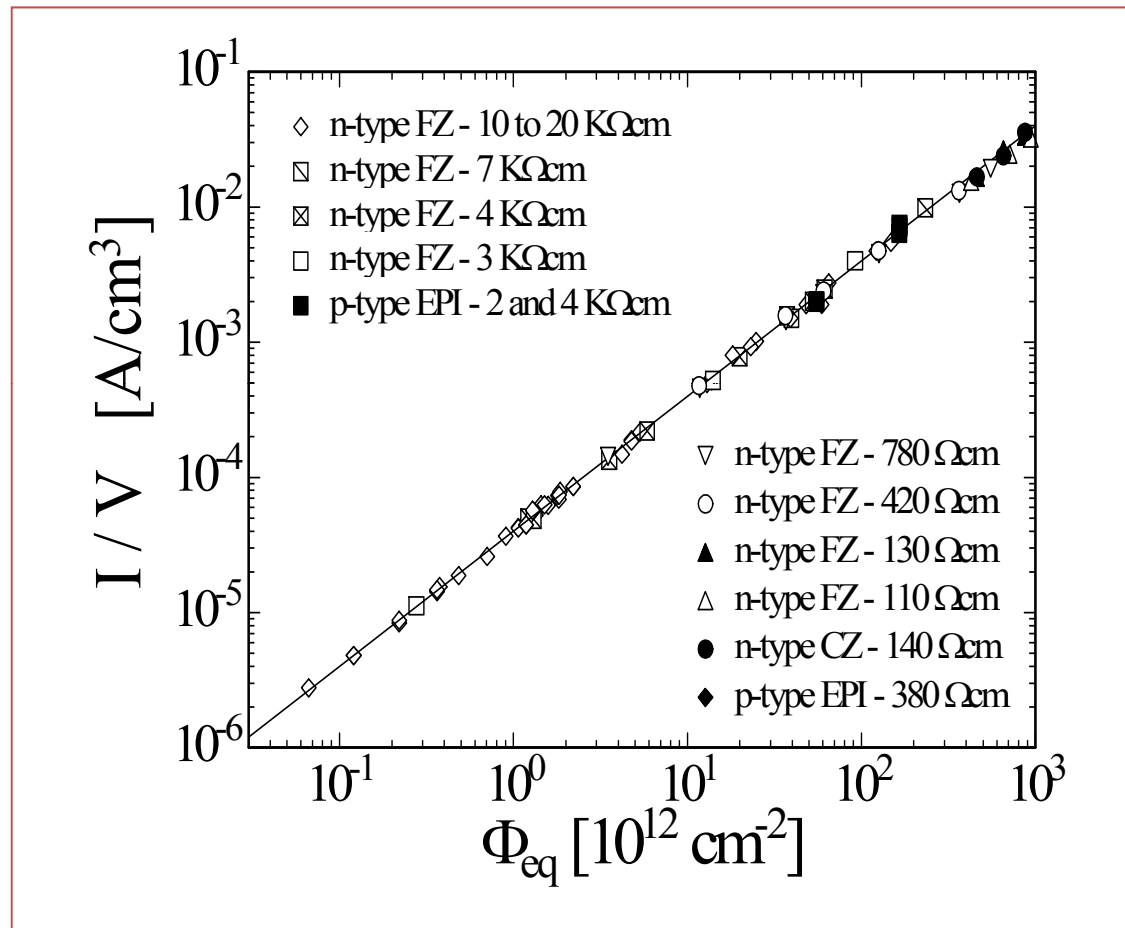
DLTS more powerful than TSC because can distinguish between acceptor-like and donor-like behaviour of traps BUT can be used only in the low fluence range due to insensitivity of capacitance at high fluence to high frequency signals



DLTS
 $f = 10^{11} \text{ ncm}^{-2}$
 ROSE Coll. NIM A
 466 (2001) 308

Radiation Damage: macroscopic parameters

I. Increase of leakage current with the fluence



- Damage parameter α (slope in figure):
Leakage current per unit volume and particle fluence

$$\alpha = \frac{\Delta I}{V \cdot \Phi_{eq}}$$

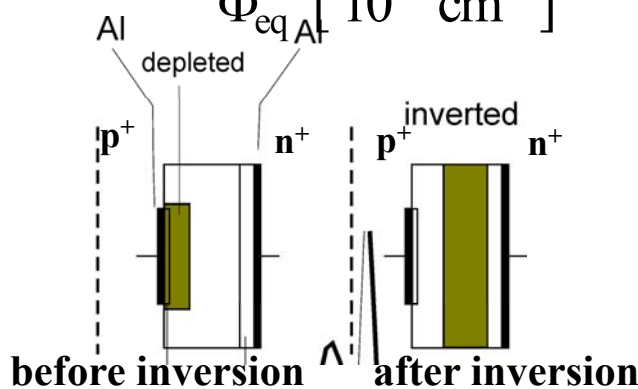
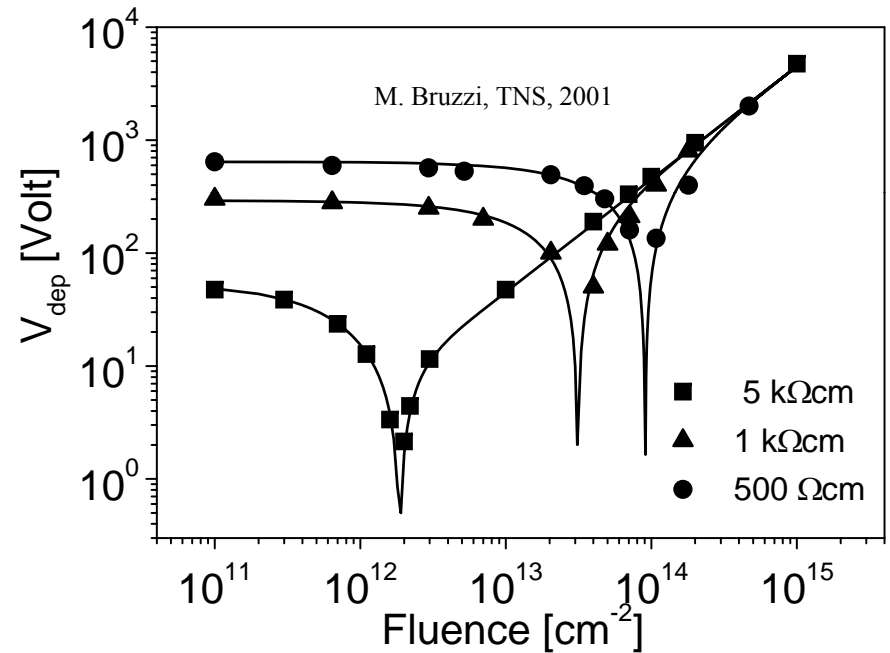
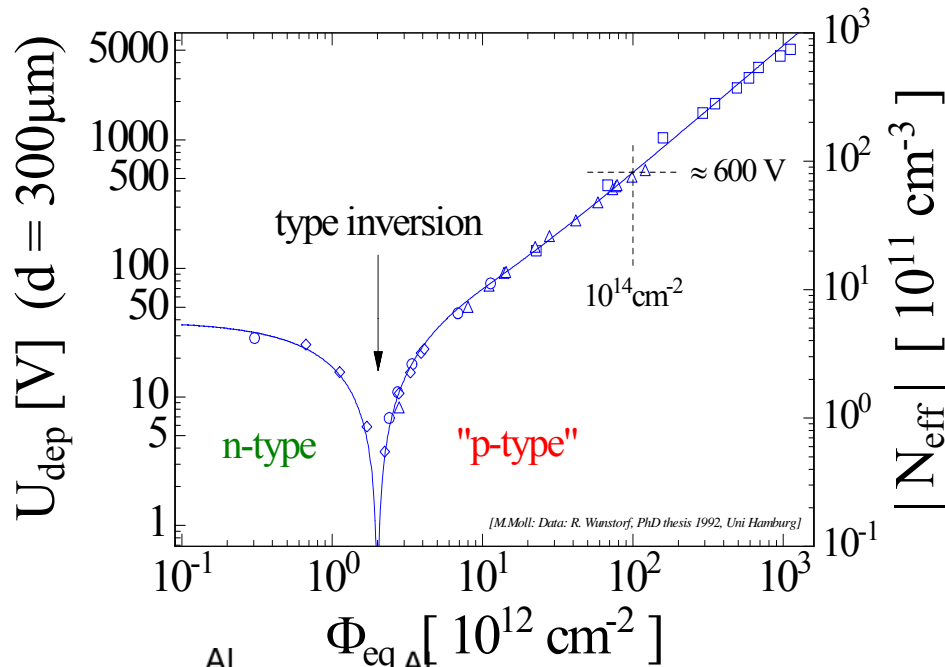
α independent of Φ_{eq} and impurities \Rightarrow used for
fluence calibration (NIEL-Hypothesis)

II. Change of V_{fd} and N_{eff} with fluence

$$\Delta N_{eff}(\Phi) = | N_{C0}(1 - e^{-c\Phi}) - \beta \cdot \Phi |$$

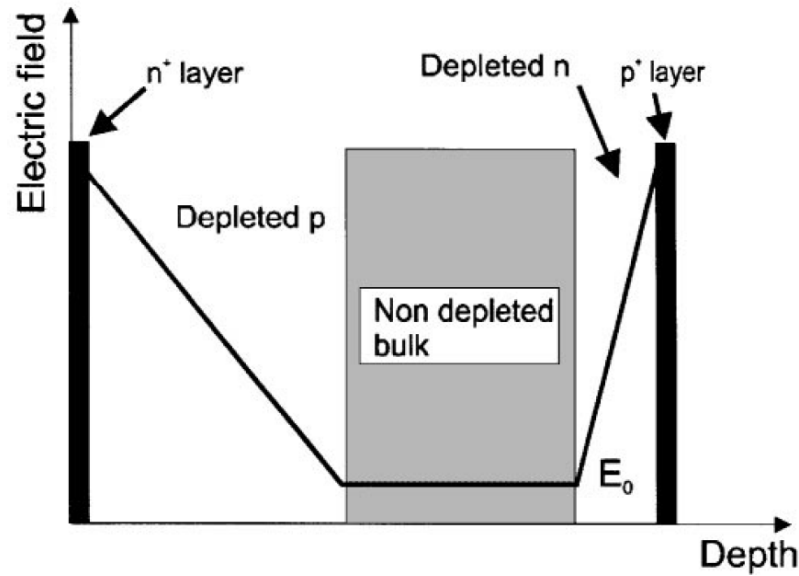
Production of acceptor like defect

Removal of the shallow dopant level



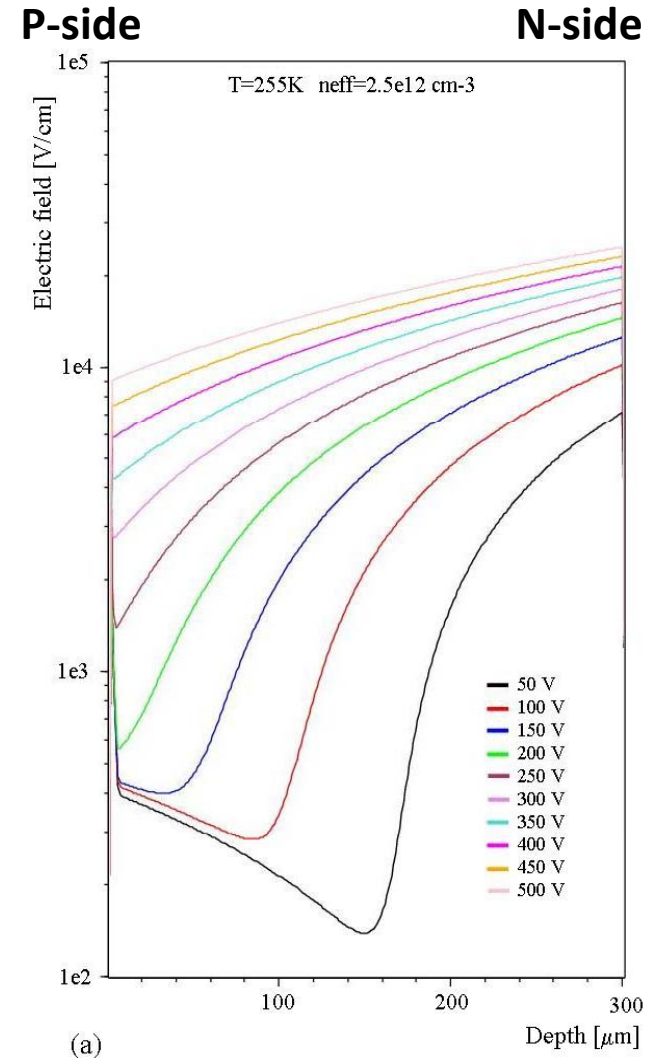
V_{dep} vs. fluence plot indicates an inversion of the Space Charge Sign at high fluences

Double Junction



In reality, after irradiation electric fields show a double junction structure with a non-depleted bulk in the middle of the sensor below the full depletion voltage

See G. Casse, et. al., NIMA 426 (1999) 140-146 and G. Kramberger, et. al., NIMA 579 (2007) 762-765 for details



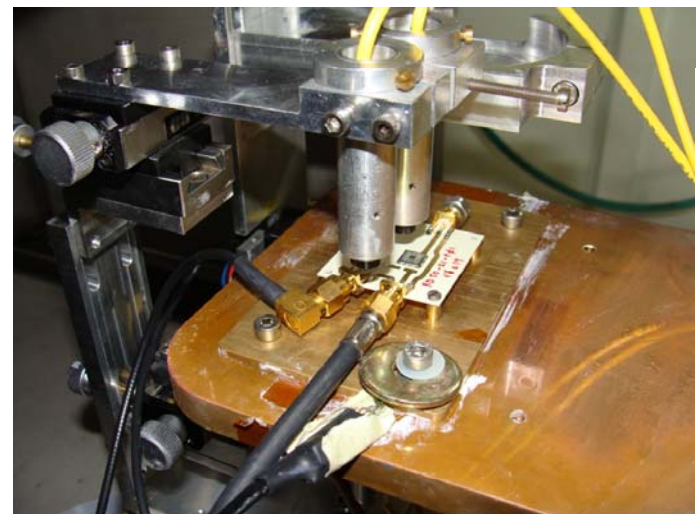
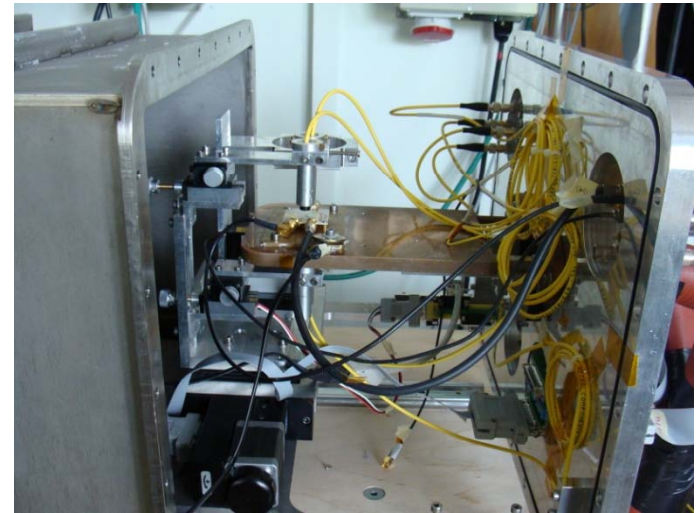
ISE-TCAD simulation after $6 \cdot 10^{14} \text{ p cm}^{-2}$

Experimental technique to analyze electric field

Transient Current Technique: TCT

- Cooling to -35 ± 0.5 C
- Red (665 nm) and Infrared (1060 nm) laser illumination
- FWHM pulse width 80 ps
- Miteq 1.5 GHz 44 dB low noise amplifier
- Agilent 2.5 GHz oscilloscope
- Detector bonded on thermally conductive PCB
- Front biasing, decoupling with 12 GHz BW Bias-Tee
- Laser delivery system with 4 focusers (front/back, red/IR)
- Humidity controlled: dry air atmosphere with dew point < -50 C

More on Laboratory :
Laser induced Signals
By Nicola Pacifico (CERN)
Gregor Kramberger (JSI, Ljubljana)



CERN TCT system

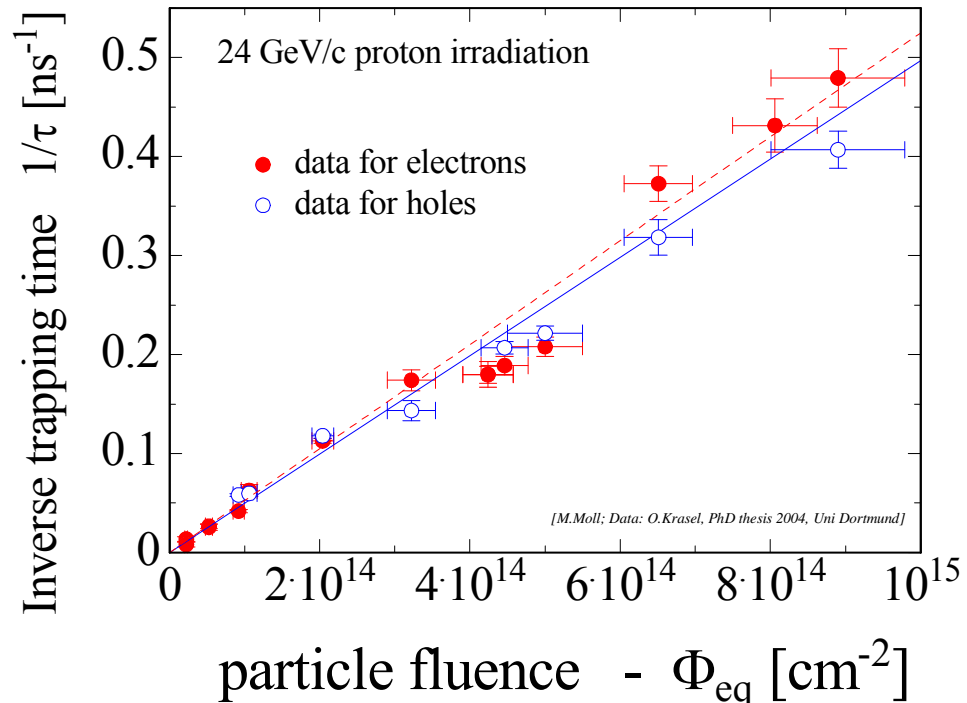
III. Charge Collection Efficiency (CCE) degradation due to trapping

CCE degradation is mainly due to partial depletion and trapping.

Effective trapping time τ_{eff} for electrons and holes:

$$Q_{e,h}(t) = Q_{0e,h} \exp\left(-\frac{1}{\tau_{\text{eff } e,h}} \cdot t\right) \quad \text{where} \quad \frac{1}{\tau_{\text{eff } e,h}} \propto N_{\text{defects}}$$

Increase of inverse trapping time ($1/\tau$) with fluence \longrightarrow



Expected signal from charge trapping

Effect of trapping on the Charge Collection Distance:

$$Q_{tc} \cong Q_0 \exp(-t_c/\tau_{tr}), 1/\tau_{tr} = \beta\Phi.$$

$$v_{sat,e} \times \tau_{tr} = \lambda_{av}$$

$$\beta_e = 4.2E-16 \text{ cm}^2/\text{ns}$$

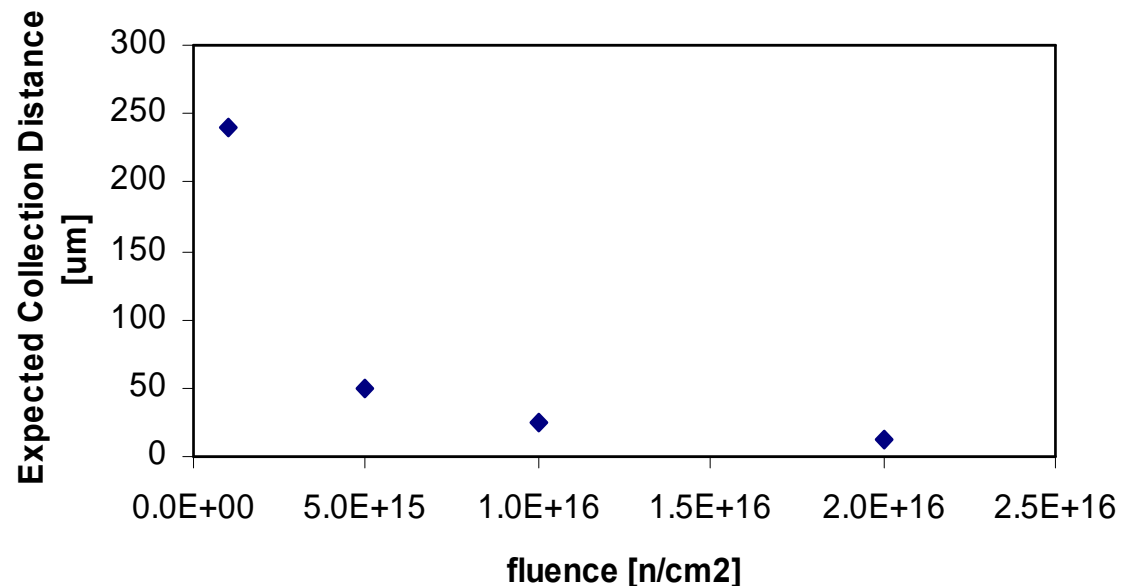
$$\beta_h = 6.1E-16 \text{ cm}^2/\text{ns}$$

G. Kramberger et al.,
NIMA 476(2002), 645-651.

Expected collection distance at saturation velocity λ_{av} :

after $1 \times 10^{15} \text{ n}_{eq} \text{ cm}^{-2}$: $240 \mu\text{m}$
expected charge $\sim 19 \text{ ke}$.

λ_{av} after $1 \times 10^{16} \text{ n}_{eq} \text{ cm}^{-2}$:
 $25 \mu\text{m}$
expected charge $< 1.3 \text{ ke}$.



Noise increase with irradiation

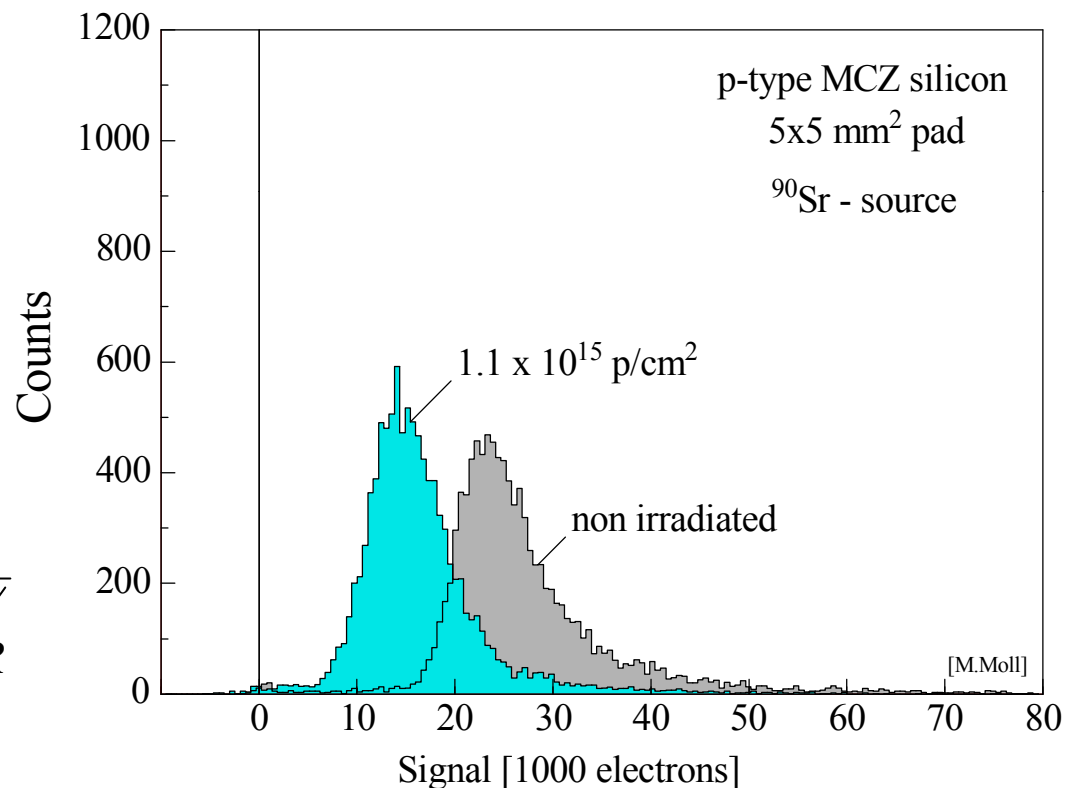
Figure of Merit: Signal-to-Noise Ratio S/N. Radiation damage severely degrades the S/N.

Noise sources:

- Capacitance $ENC \propto C_d$

- Leakage Current $ENC \propto \sqrt{I}$

- Thermal Noise (bias resistor) $ENC \propto \sqrt{k_B T / R}$

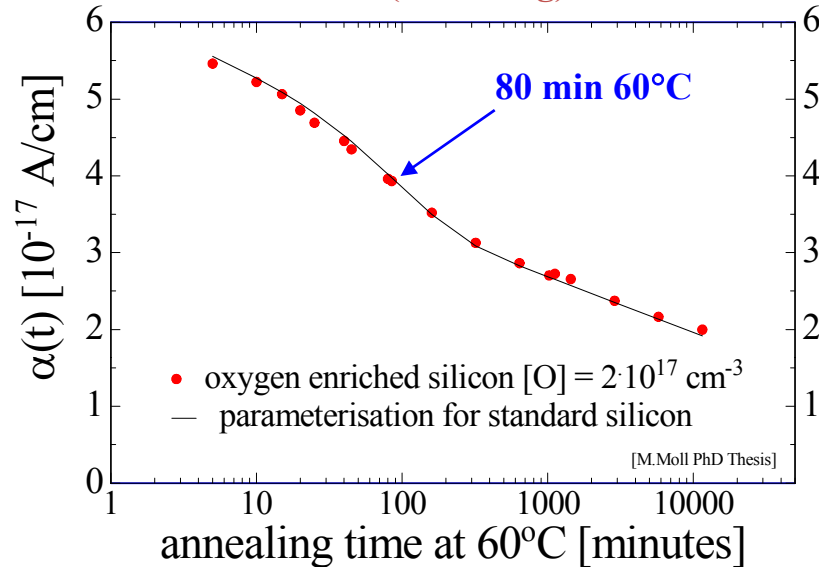


(ENC = Equivalent Noise Charge)

Changes with time and temperature after irradiation (annealing)

Leakage Current and N_{eff} (after hadron irradiation)

.... with time (annealing):



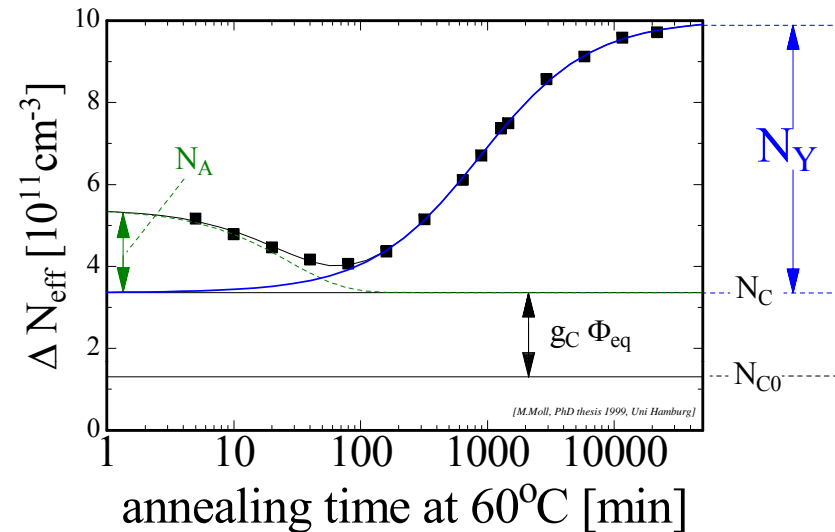
- Leakage current decreasing in time (depending on temperature)
- Strong temperature dependence

$$I \propto \exp\left(-\frac{E_g}{2k_B T}\right)$$

Consequence:

Cool detectors during operation!
Example: $I(-10^\circ\text{C}) \sim 1/16 I(20^\circ\text{C})$

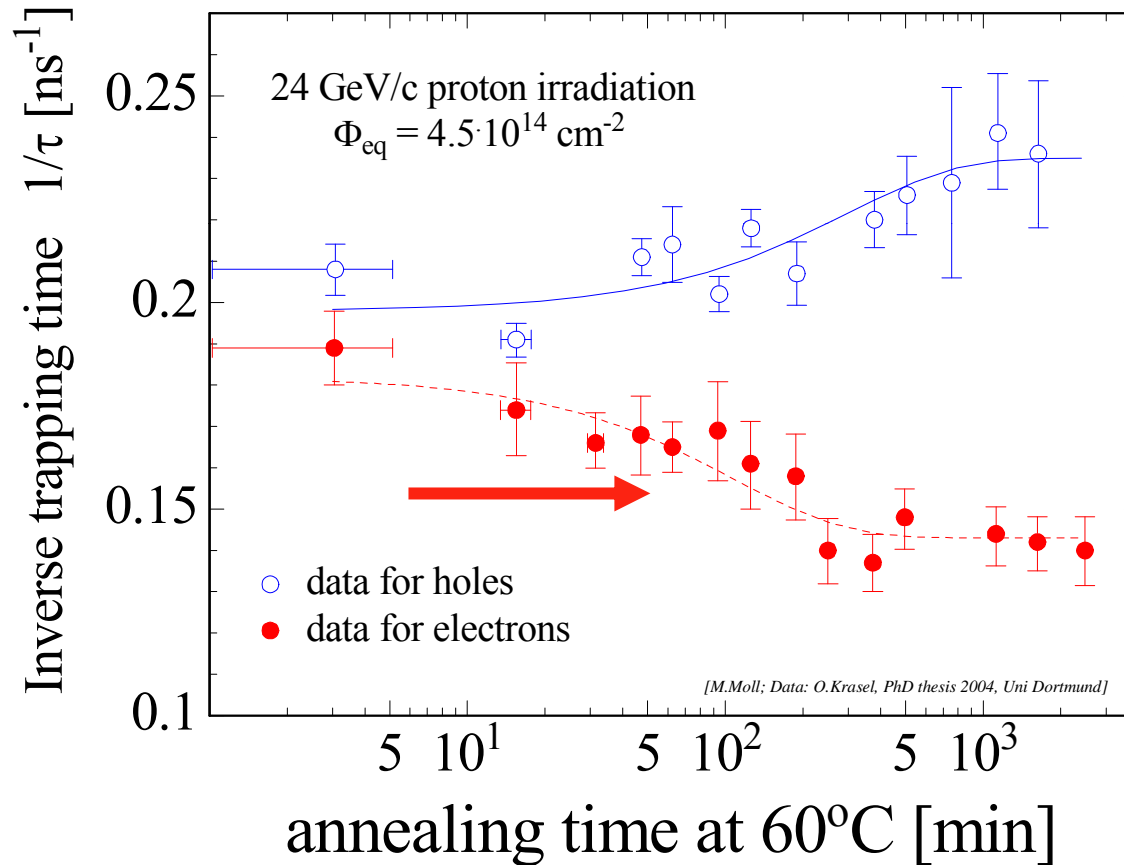
.... with time (annealing):



- Short term: “**Beneficial annealing**”
- Long term: “**Reverse annealing**”
- time constant depends on temperature:
 - ~ 500 years (-10°C)
 - ~ 500 days (20°C)
 - ~ 21 hours (60°C)
- Consequence: **Detectors must be cooled even when the experiment is not running!**

Change of inverse trapping time

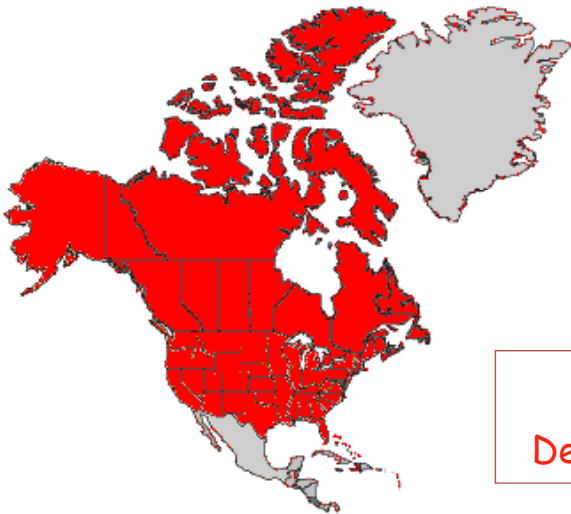
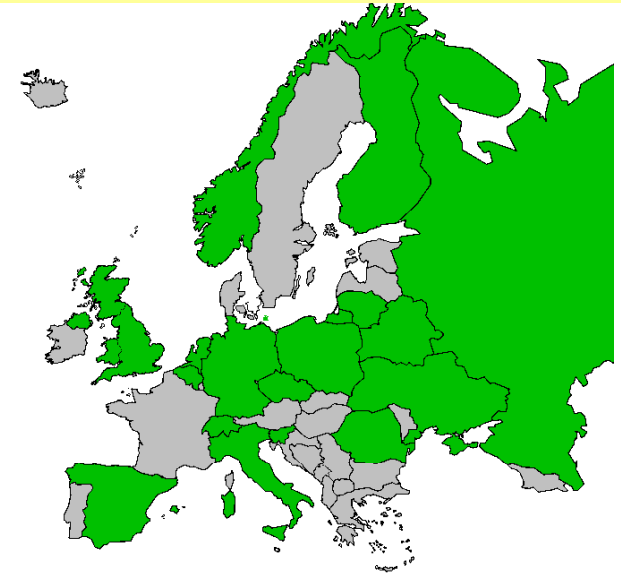
Decrease of inverse trapping time ($1/\tau$) with annealing for electrons



RD50 - Development of Radiation Hard Semiconductor Devices for High Luminosity Colliders

38 European institutes

Belarus (Minsk), Belgium (Louvain), Czech Republic (Prague (3x)), Finland (Helsinki, Lappeenranta), Germany (Dortmund, Erfurt, Freiburg, Hamburg, Karlsruhe, Munich), Italy (Bari, Florence, Padova, Perugia, Pisa, Trento), Lithuania (Vilnius), Netherlands (NIKHEF), Norway (Oslo (2x)), Poland (Warsaw(2x)), Romania (Bucharest (2x)), Russia (Moscow, St.Petersburg), Slovenia (Ljubljana), Spain (Barcelona, Valencia), Switzerland (CERN, PSI), Ukraine (Kiev), United Kingdom (Glasgow, Lancaster, Liverpool)



8 North-American institutes

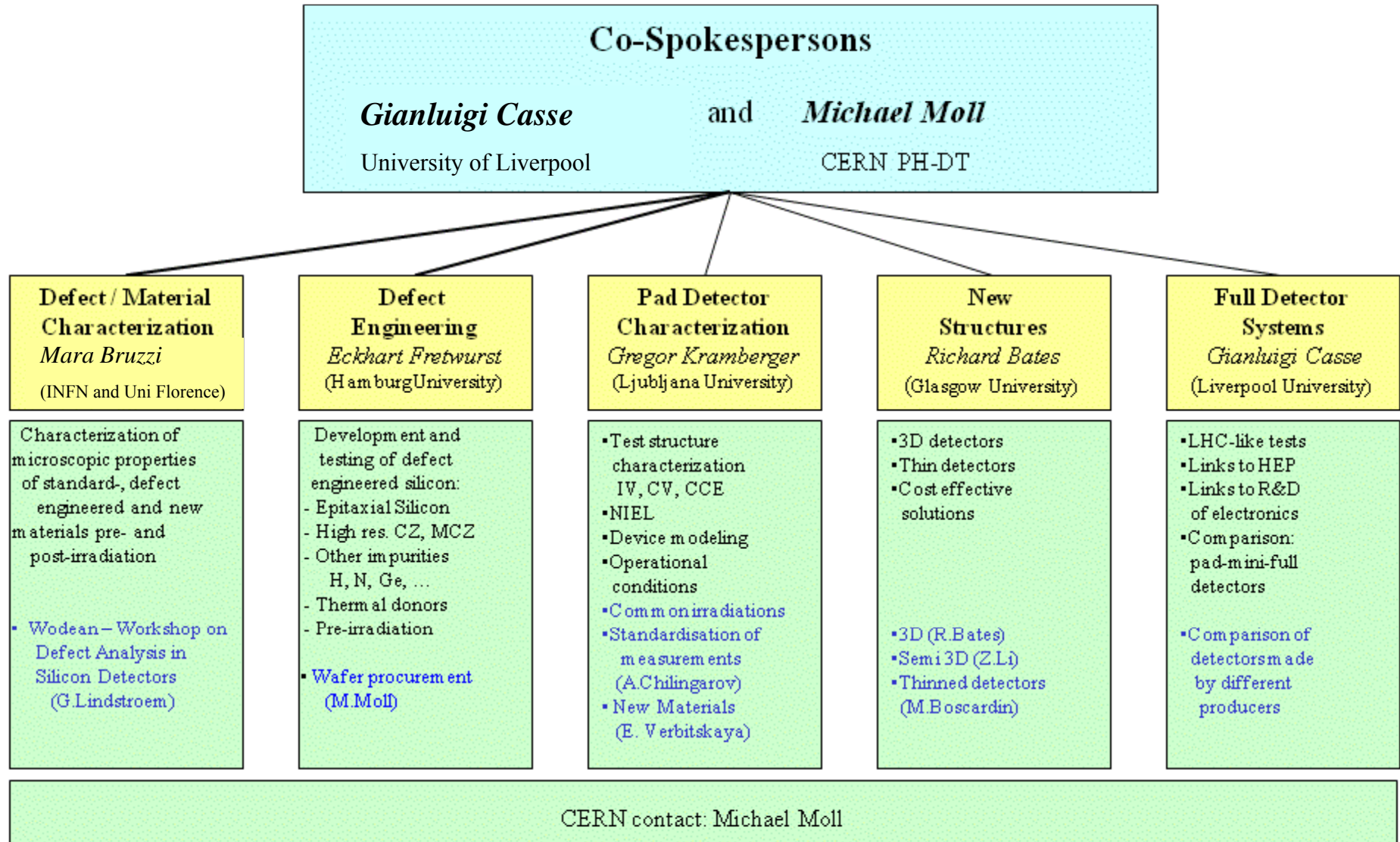
Canada (Montreal), USA (BNL, Fermilab, New Mexico, Purdue, Rochester, Santa Cruz, Syracuse)

1 Middle East institute

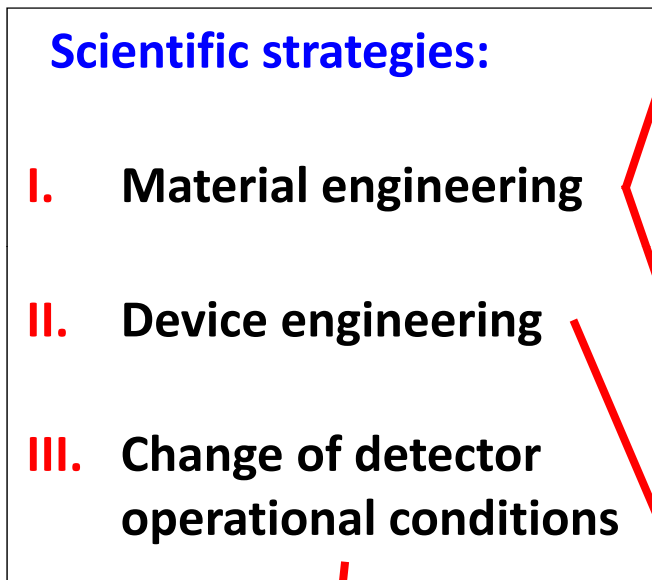
Israel (Tel Aviv)

257 Members from 47 Institutes

Detailed member list: <http://cern.ch/rd50>



Approaches to develop radiation harder solid state tracking detectors



CERN-RD39
“Cryogenic Tracking Detectors”
operation at 100-200K
to reduce charge loss

- Defect Engineering of Silicon

Deliberate incorporation of impurities or defects into the silicon bulk to improve radiation tolerance of detectors

- **Needs:** Profound understanding of radiation damage
 - microscopic defects, macroscopic parameters
 - dependence on particle type and energy
 - defect formation kinetics and annealing
- **Examples:**
 - Oxygen rich Silicon (DOFZ, Cz, MCZ, EPI)
 - Oxygen dimer & hydrogen enriched Si
 - Pre-irradiated Si
 - Influence of processing technology

- New Materials

- Silicon Carbide (SiC), Gallium Nitride (GaN)
- Diamond (CERN RD42 Collaboration)
- Amorphous silicon

- Device Engineering (New Detector Designs)

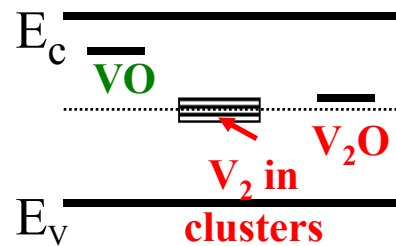
- p-type silicon detectors (n-in-p)
- thin detectors, epitaxial detectors
- 3D detectors and Semi 3D detectors, Stripixels
- Cost effective detectors
- Monolithic devices

Oxygen Enrichment for Radiation Hardening

RD48 (ROSE) and RD50 CERN Collaborations

Main Hypothesis: Oxygen beneficial as sink of vacancies

$V-O_i$ complex concentration increase \longrightarrow reduction of deeper levels
mainly divacancy related



Typical oxygen concentration in Si:

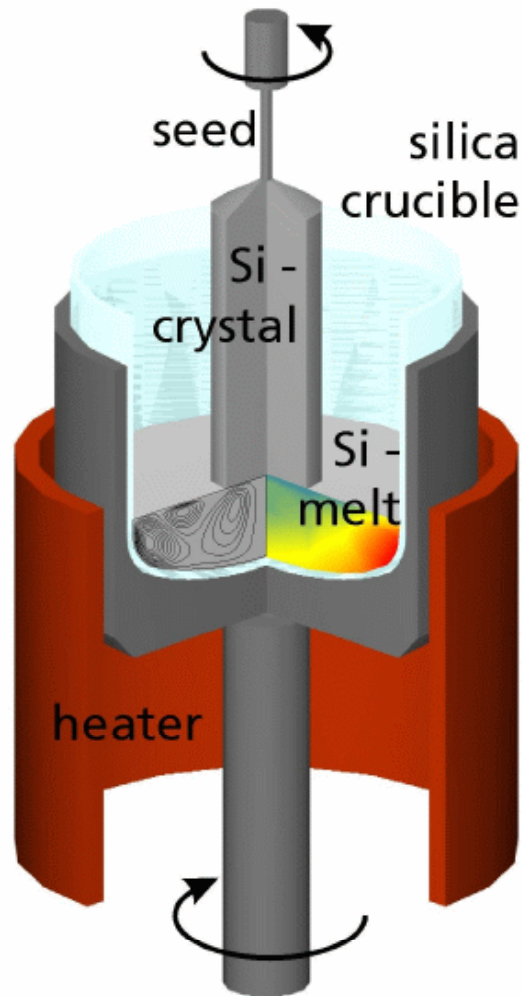
- FZ [O_i] 10^{15}cm^{-3}
- Diffusion oxygenated FZ : DOFZ [O_i] $10^{16}\text{-}10^{17}\text{cm}^{-3}$
- Czochralski Si: [O_i] up to 10^{18}cm^{-3}

Note: as VO is a point defect the beneficial effect of oxygen is expected especially when cluster formation by irradiation is less important than point defect formation.

RD50: Defect Engineering of Si

Czochralski silicon (Cz) & Epitaxial silicon (EPI)

■ Czochralski silicon



- Pull Si-crystal from a Si-melt contained in a silica crucible while rotating.
- Silica crucible is dissolving oxygen into the melt \Rightarrow high concentration of O in CZ
- Material used by IC industry (cheap)
- Recent developments (~5 years) made CZ available in sufficiently high purity (resistivity) to allow for use as particle detector.



■ Epitaxial silicon

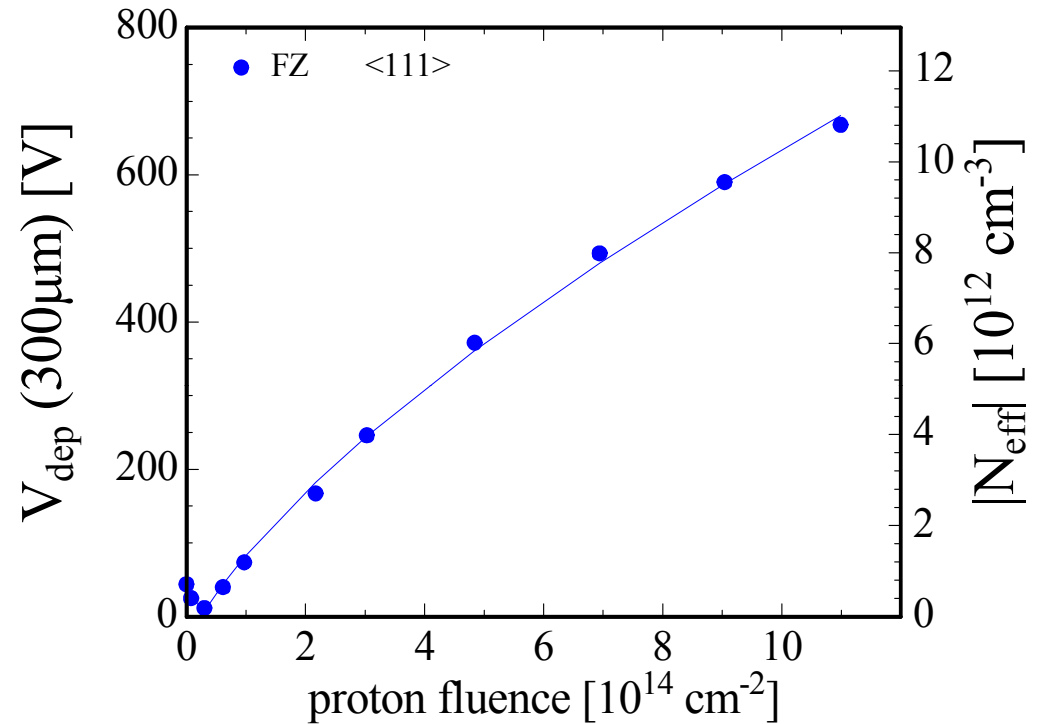
- Chemical-Vapor Deposition (CVD) of Silicon
- CZ silicon substrate used \Rightarrow in-diffusion of oxygen
- growth rate about $1\mu\text{m}/\text{min}$
- excellent homogeneity of resistivity
- up to $150\mu\text{m}$ thick layers produced (thicker is possible)
- price depending on thickness of epi-layer but not extending ~ 3 x price of FZ wafer

Standard FZ, DOFZ, MCz and Cz silicon

24 GeV/c proton irradiation

- **Standard FZ silicon**

- type inversion at $\sim 2 \times 10^{13}$ p/cm²
- strong N_{eff} increase at high fluence



Standard FZ, DOFZ, MCz and Cz silicon

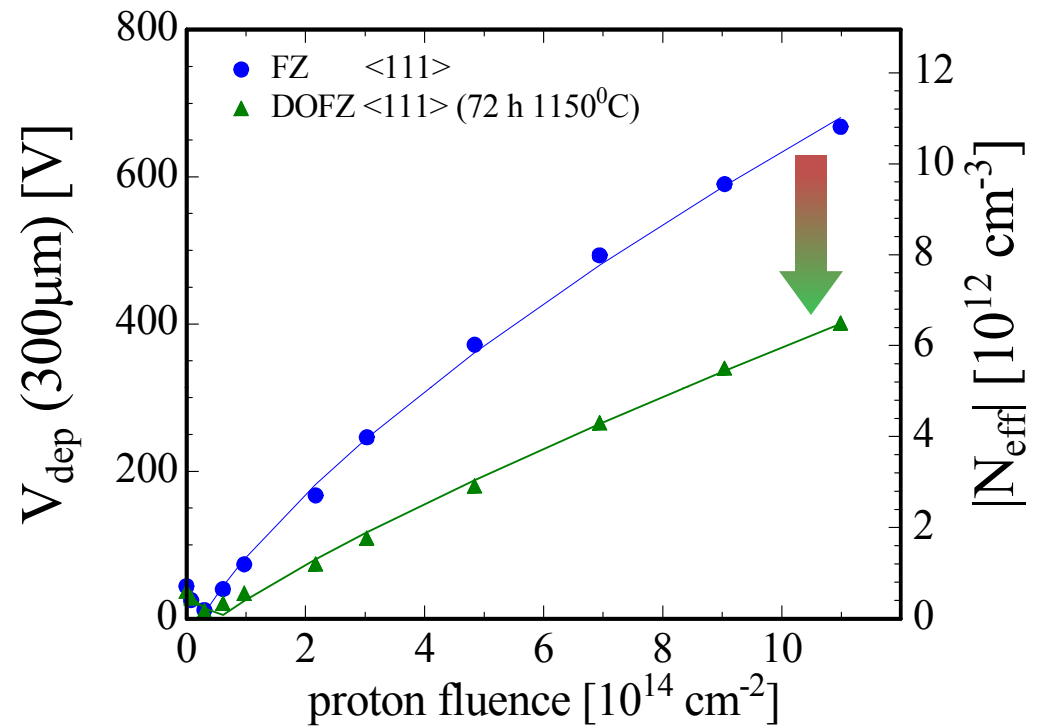
24 GeV/c proton irradiation

• Standard FZ silicon

- type inversion at $\sim 2 \times 10^{13}$ p/cm²
- strong N_{eff} increase at high fluence

• Oxygenated FZ (DOFZ)

- type inversion at $\sim 2 \times 10^{13}$ p/cm²
- reduced N_{eff} increase at high fluence



Standard FZ, DOFZ, MCz and Cz silicon

24 GeV/c proton irradiation

• Standard FZ silicon

- type inversion at $\sim 2 \times 10^{13}$ p/cm²
- strong N_{eff} increase at high fluence

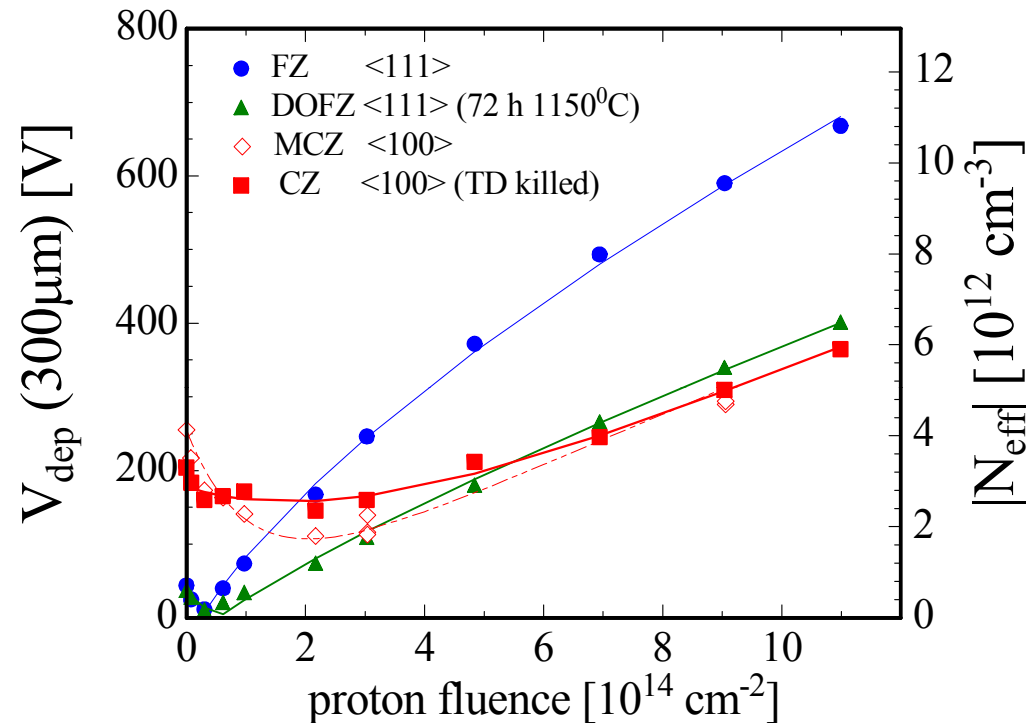
• Oxygenated FZ (DOFZ)

- type inversion at $\sim 2 \times 10^{13}$ p/cm²
- reduced N_{eff} increase at high fluence

• CZ silicon and MCZ silicon

- “no type inversion” in the overall fluence range

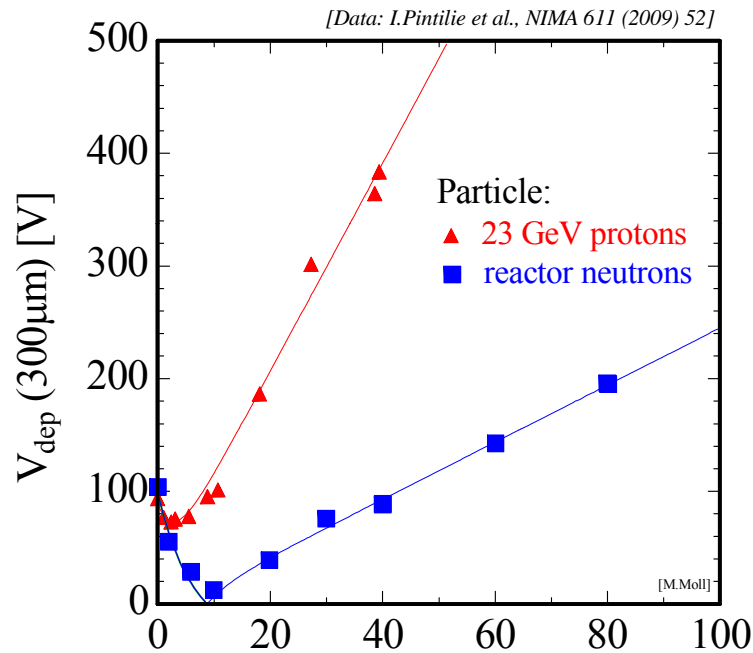
(for experts: there is no “real” type inversion, a more clear understanding of the observed effects is obtained by investigating directly the internal electric field; look for: TCT, MCZ, double junction)



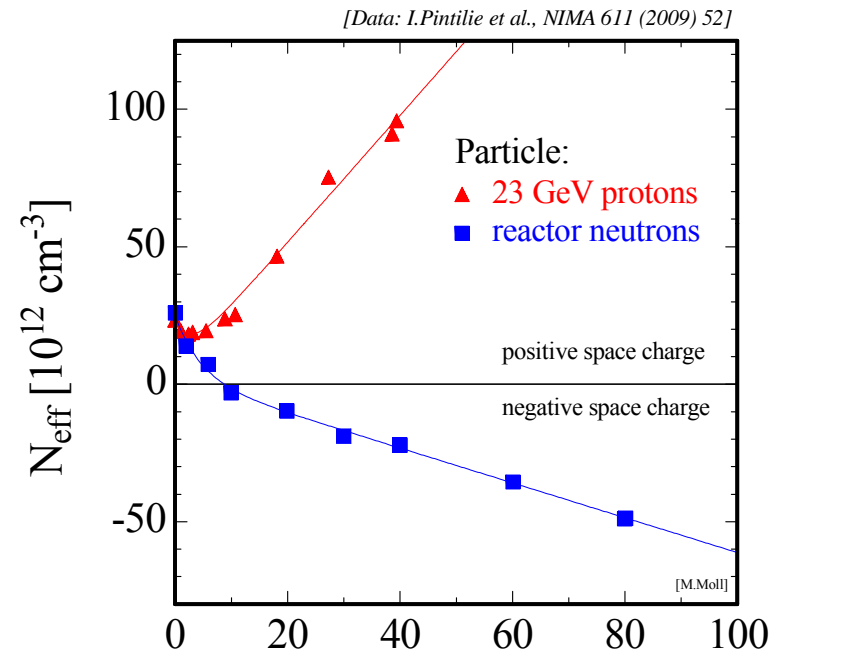
- **Common to all materials** *(after hadron irradiation, not after γ irradiation):*
 - reverse current increase
 - increase of trapping (electrons and holes) within $\sim 20\%$

Proton vs. Neutron irradiation of oxygen rich silicon

- Epitaxial silicon (*EPI-DO*, $72\mu\text{m}$, $170\Omega\text{cm}$, diodes) irradiated with 23 GeV protons or reactor neutrons



1 MeV neutron equivalent fluence $\Phi_{\text{eq}} [10^{14}\text{ cm}^{-2}]$



1 MeV neutron equivalent fluence $\Phi_{\text{eq}} [10^{14}\text{ cm}^{-2}]$

depletion voltage →

$$V_{\text{dep}} = \frac{q_0}{\epsilon\epsilon_0} \cdot |N_{\text{eff}}| \cdot d^2$$

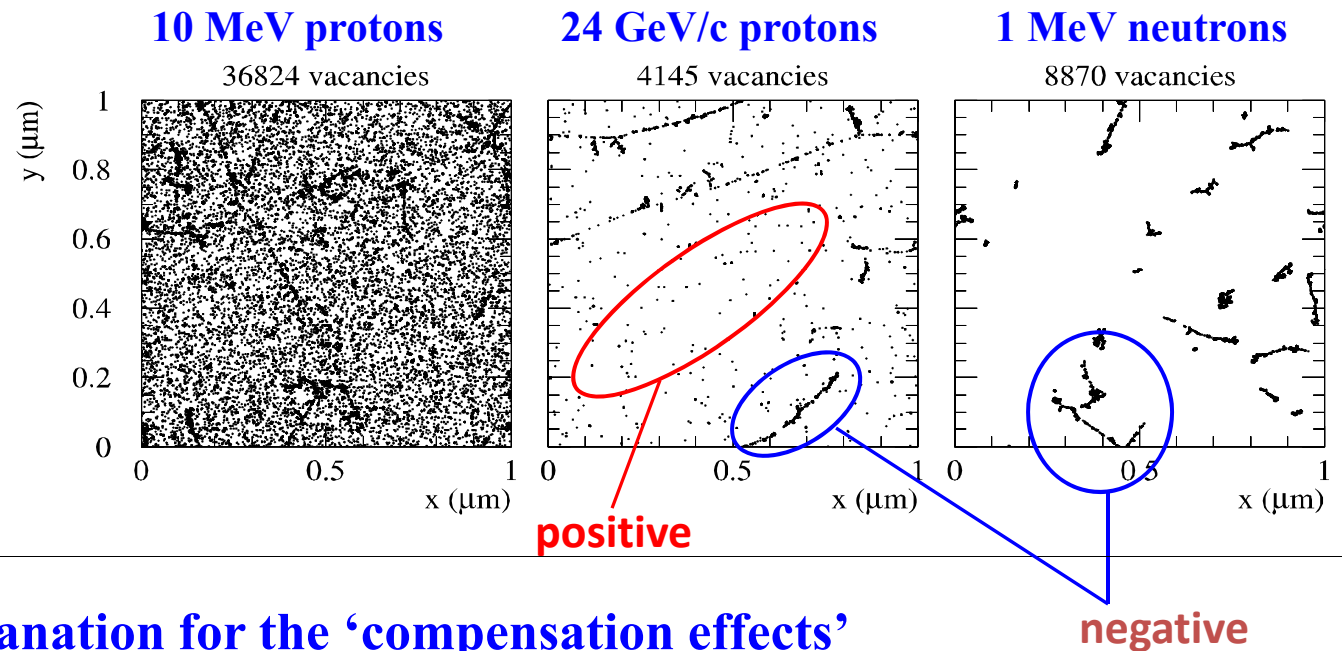
← *absolute effective space charge density*

Why is proton and neutron damage different?

Simulation:

Initial distribution of vacancies in $(1\mu\text{m})^3$ after 10^{14} particles/cm²

[Mika Huhtinen NIMA 491(2002) 194]

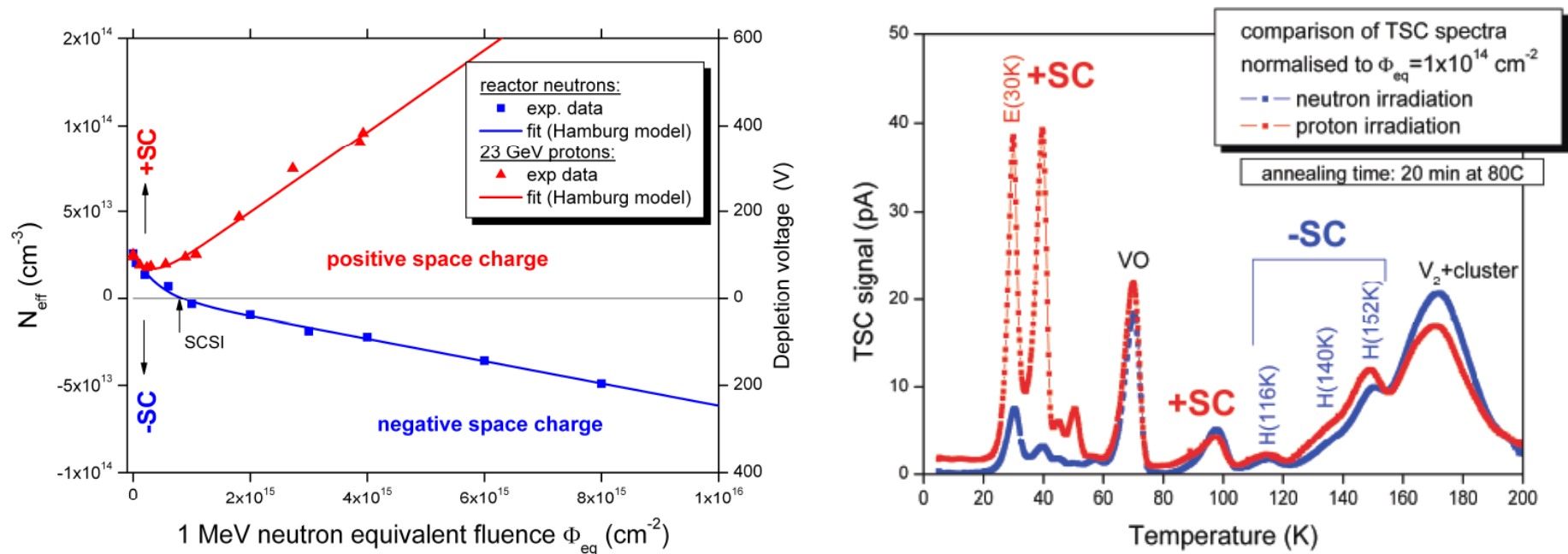


- A ‘simplified’ explanation for the ‘compensation effects’
 - Defect clusters produce predominantly **negative space charge**
 - Point defects produce predominantly **positive space charge** (in ‘oxygen rich’ silicon)

Note: NIEL violation

From microscopic to macroscopic: N_{eff} changes explained with TSC

Epi-Si irradiated with 23 GeV protons and reactor neutrons



[Pintilie, Lindstroem, Junkes, Fretwurst, NIM A 611 (2009) 52–68]

- SCSI "Type Inversion" after neutrons but not after protons
- donor generation enhanced after proton irradiation

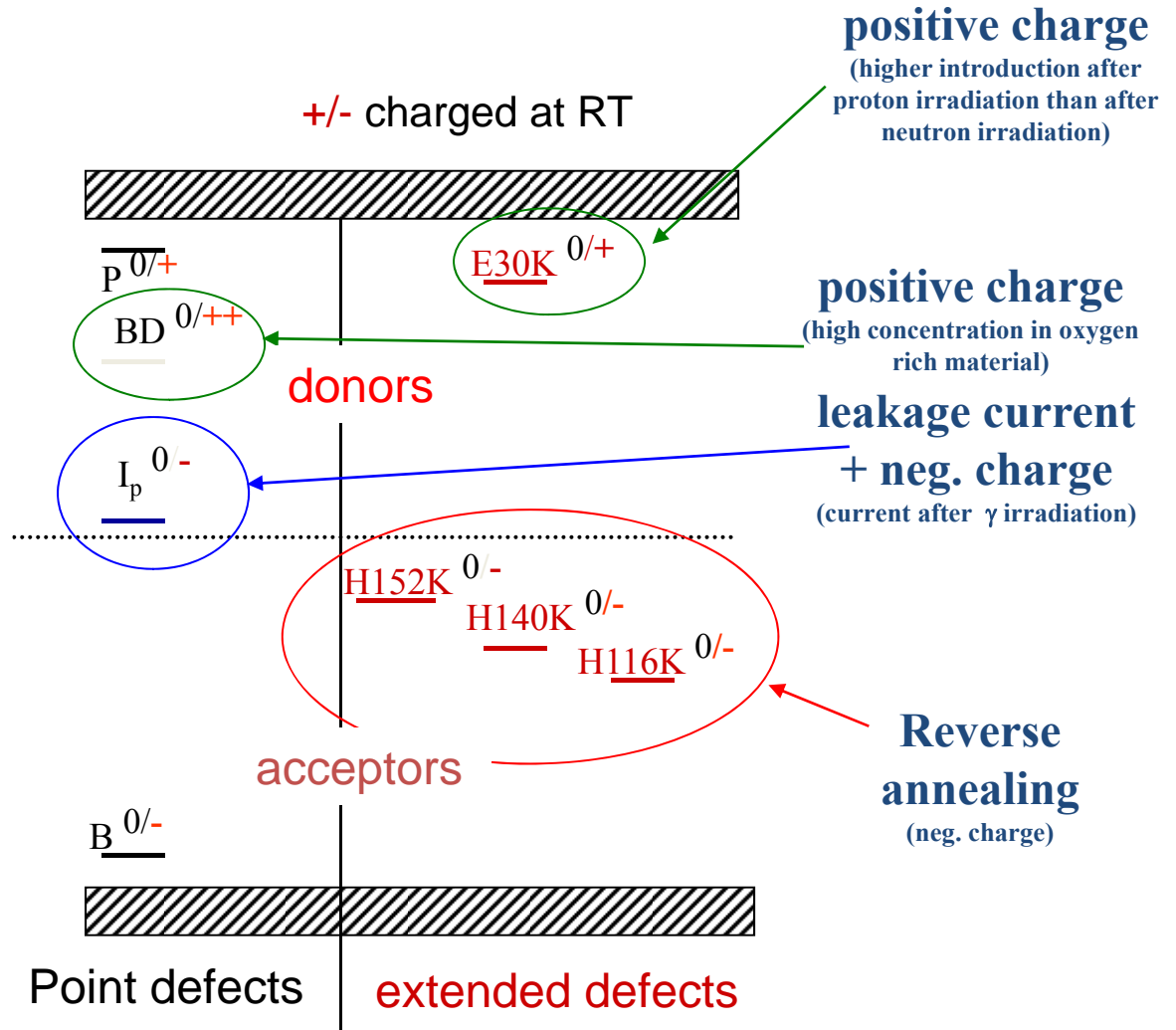
Main Defects Affecting the Device Properties

Point defects

- $E_i^{BD} = E_c - 0.225 \text{ eV}$
- $\sigma_n^{BD} = 2.3 \cdot 10^{-14} \text{ cm}^2$
- $E_i^I = E_c - 0.545 \text{ eV}$
 - $\sigma_n^I = 1.7 \cdot 10^{-15} \text{ cm}^2$
 - $\sigma_p^I = 9 \cdot 10^{-14} \text{ cm}^2$

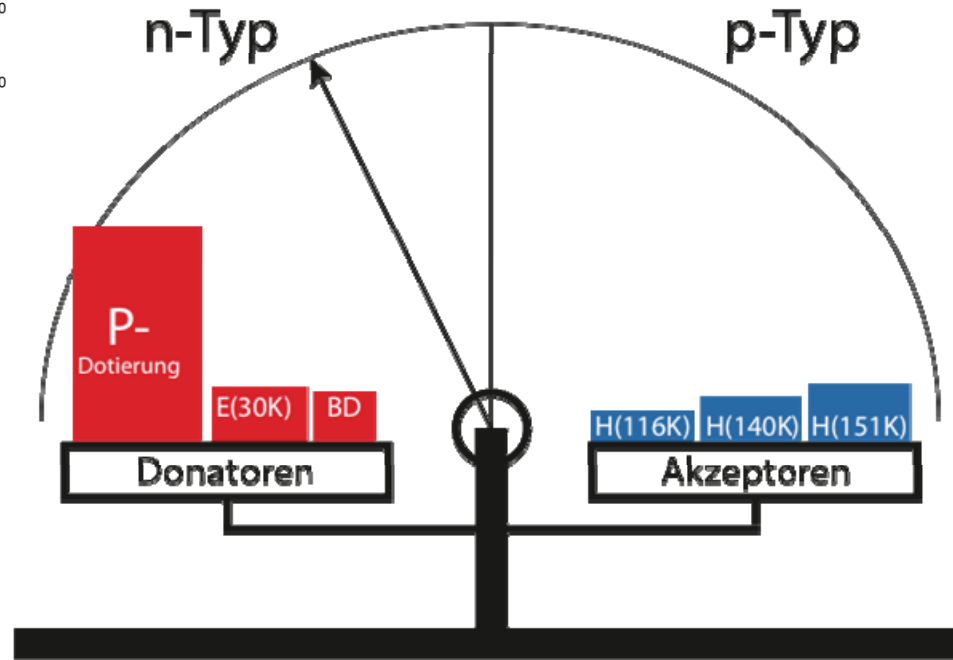
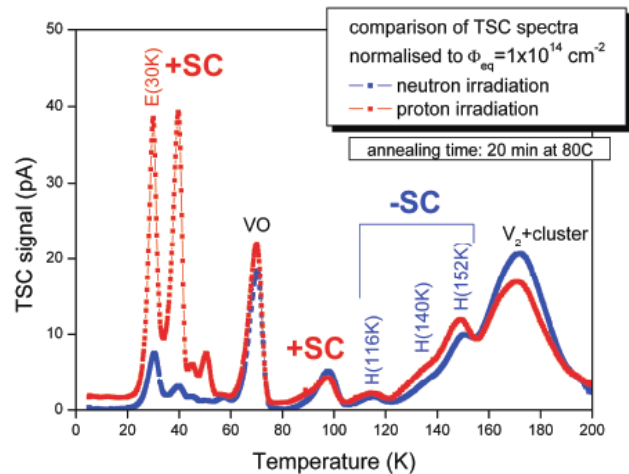
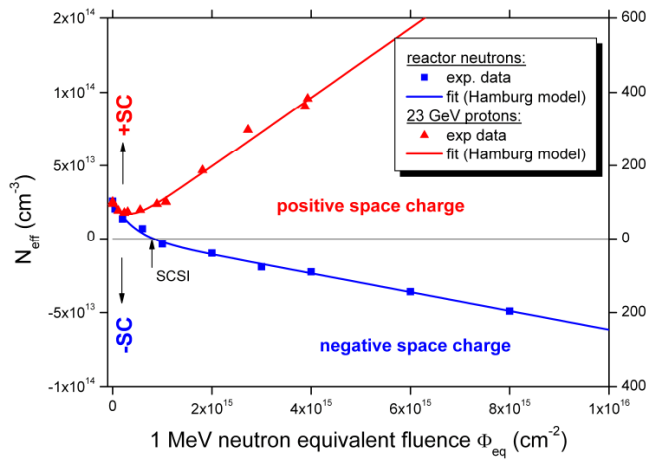
Cluster related centers

- $E_i^{116K} = E_v + 0.33 \text{ eV}$
- $\sigma_p^{116K} = 4 \cdot 10^{-14} \text{ cm}^2$
- $E_i^{140K} = E_v + 0.36 \text{ eV}$
- $\sigma_p^{140K} = 2.5 \cdot 10^{-15} \text{ cm}^2$
- $E_i^{152K} = E_v + 0.42 \text{ eV}$
- $\sigma_p^{152K} = 2.3 \cdot 10^{-14} \text{ cm}^2$
- $E_i^{30K} = E_c - 0.1 \text{ eV}$
- $\sigma_n^{30K} = 2.3 \cdot 10^{-14} \text{ cm}^2$



N_{eff} : Neutron irradiation

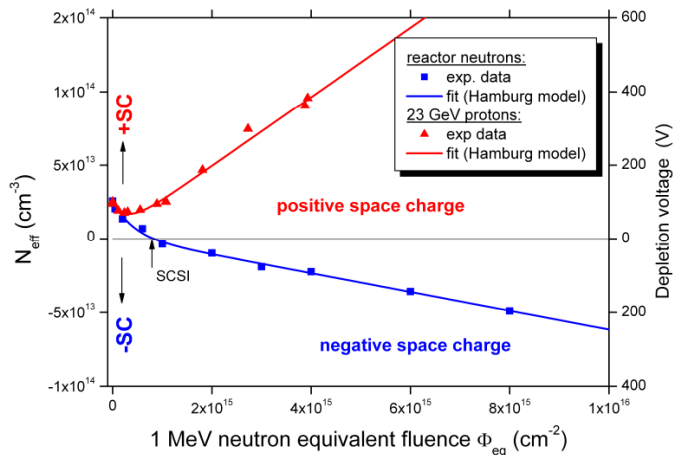
Epitaxial silicon (*EPI-DO*, $72\mu\text{m}$, $170\Omega\text{cm}$, diodes) irradiated with reactor neutrons



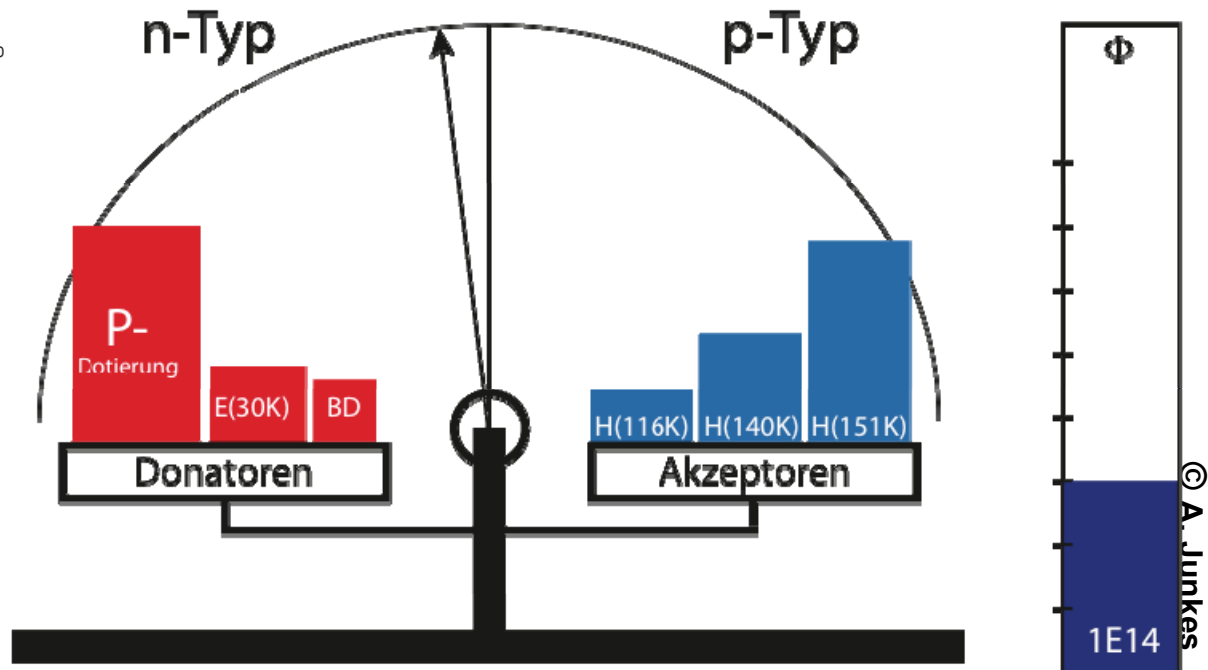
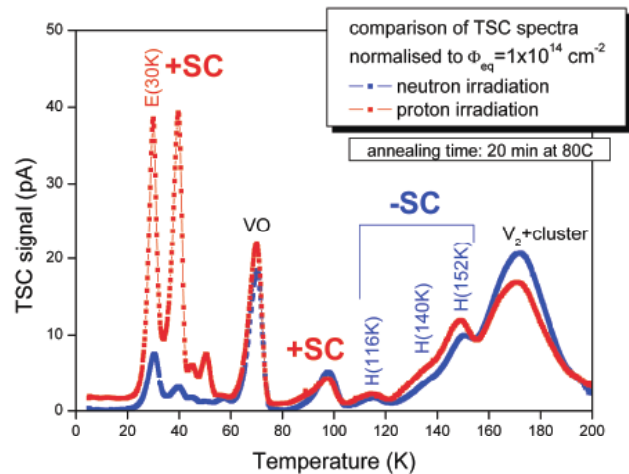
© A. Junkes

By A. Junkes, presented by U. Parzefal on behalf of the RD50 Collaboration, RESMDD10, Oct. 2010, Florence

N_{eff} : Neutron irradiation

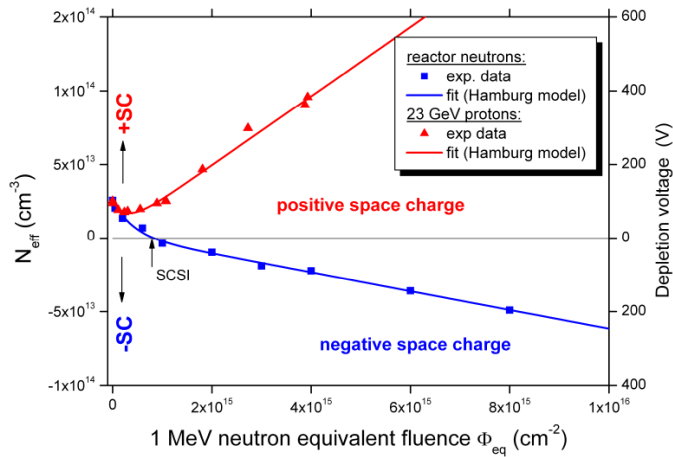


Epitaxial silicon (*EPI-DO*, $72\mu\text{m}$, $170\Omega\text{cm}$, *diodes*) irradiated with reactor neutrons

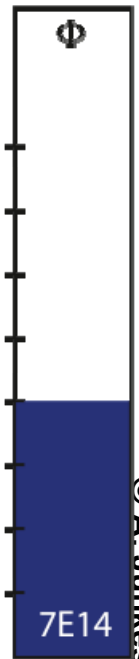
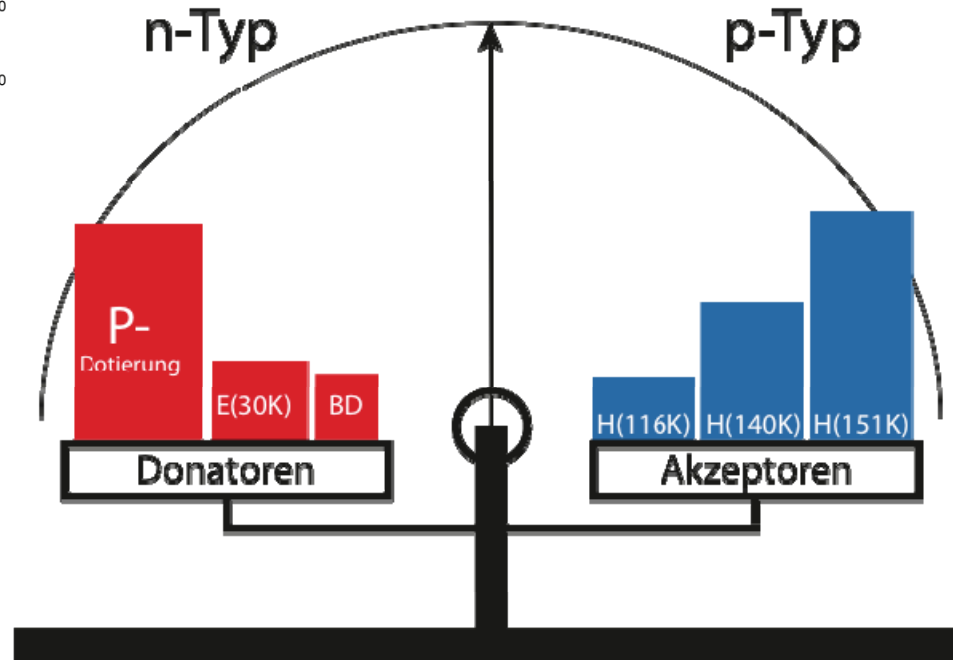
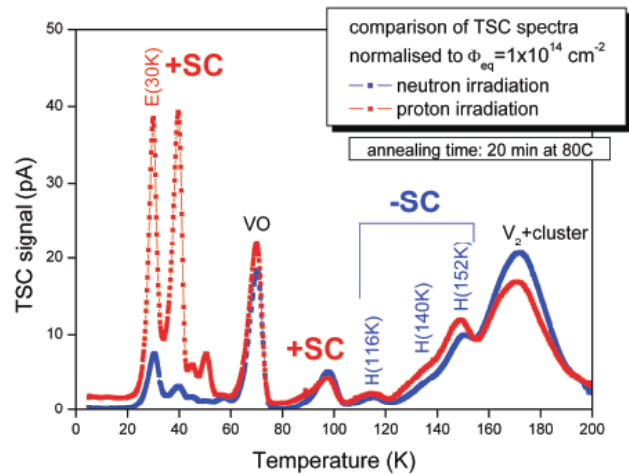


By A. Junkes, presented by U. Parzefal on behalf of the RD50 Collaboration, RESMDD10, Oct. 2010, Florence
 Radiation Tolerant Silicon Detectors, Mara Bruzzi, Gianluigi Casse, EDIT School, February 2011

N_{eff} : Neutron irradiation

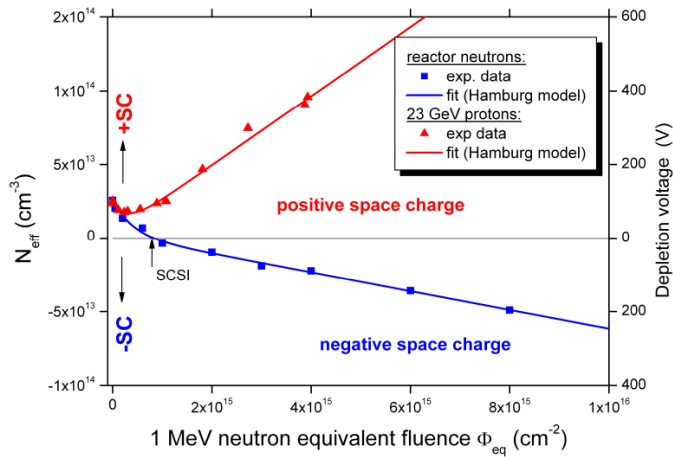


Epitaxial silicon (*EPI-DO*, $72\mu\text{m}$, $170\Omega\text{cm}$, *diodes*) irradiated with reactor neutrons

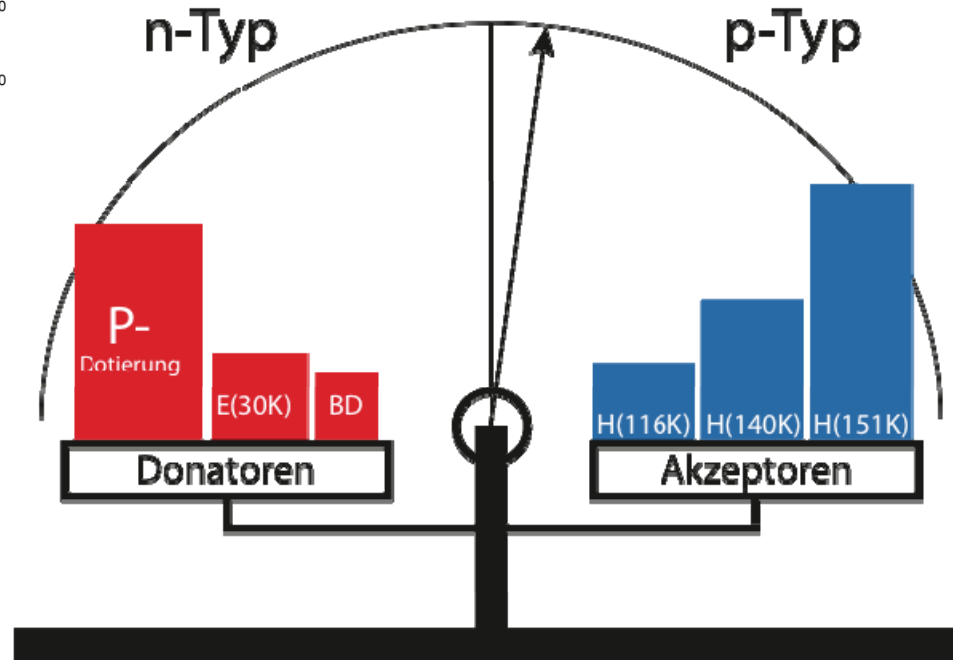
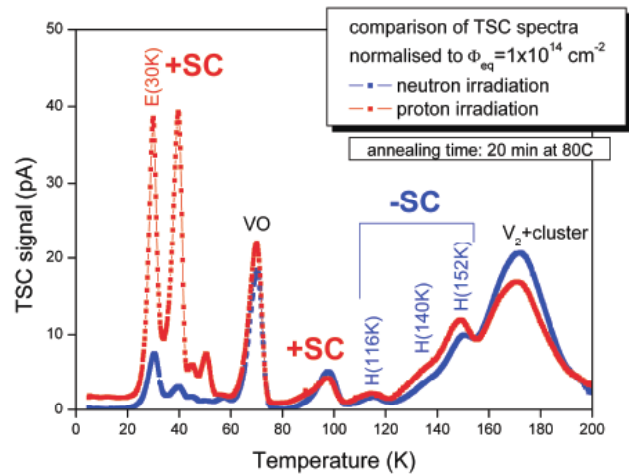


© A. Junkes

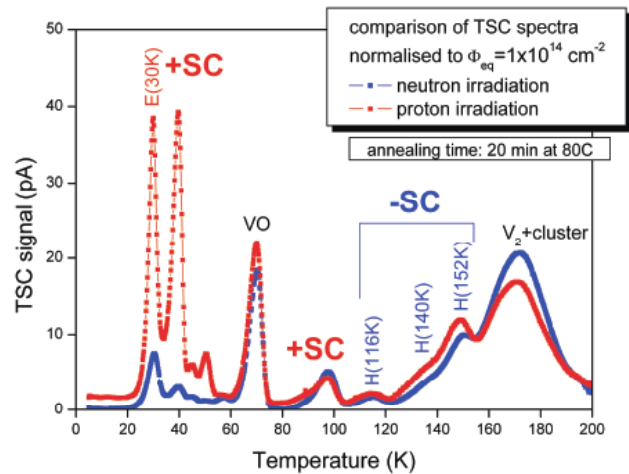
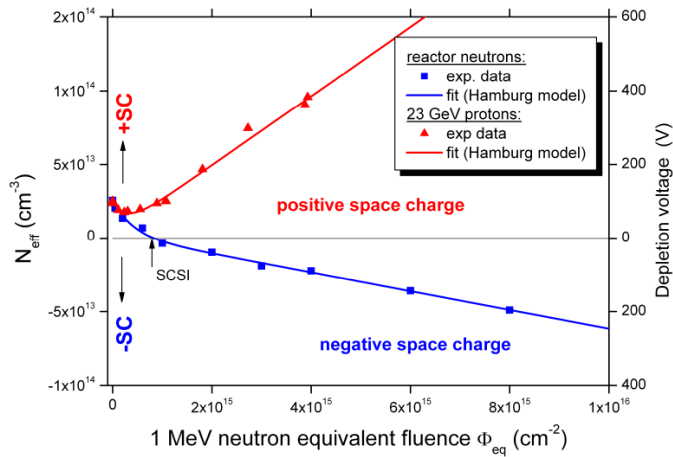
N_{eff} : Neutron irradiation



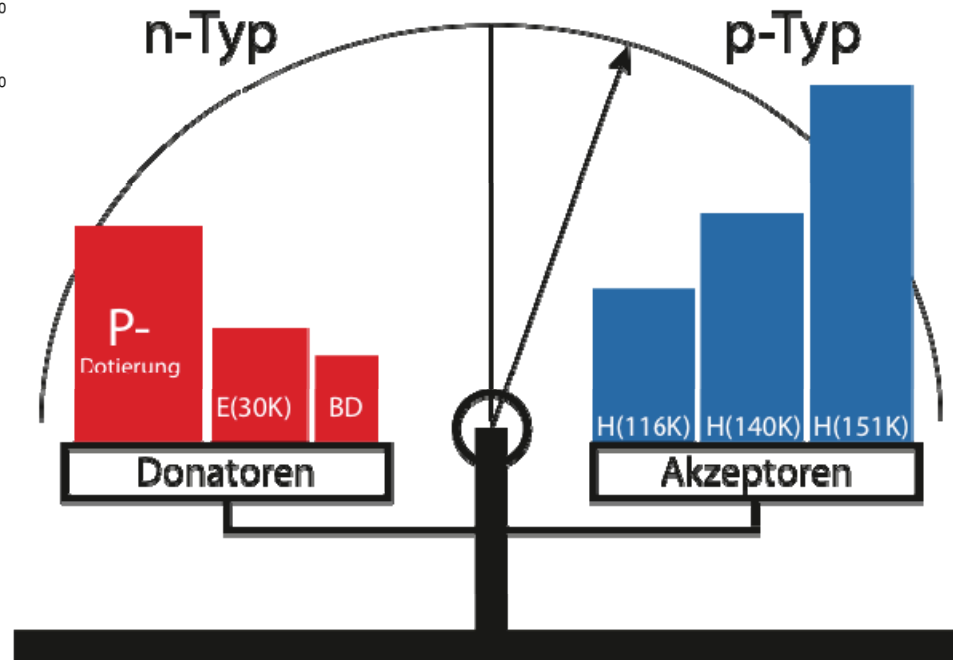
Epitaxial silicon (*EPI-DO*, $72\mu\text{m}$, $170\Omega\text{cm}$, *diodes*) irradiated with reactor neutrons



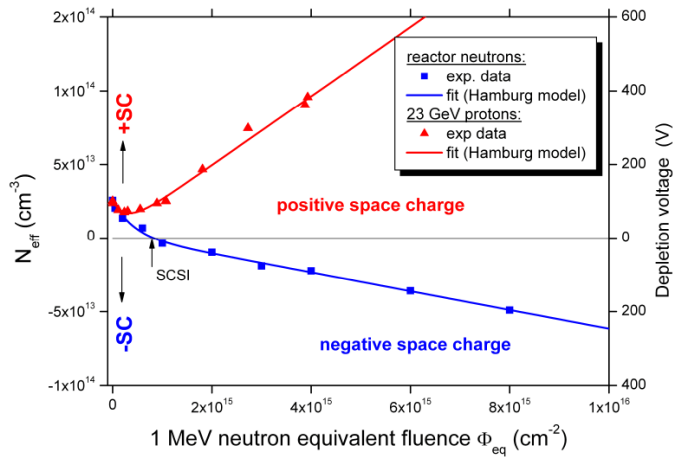
N_{eff} : Neutron irradiation



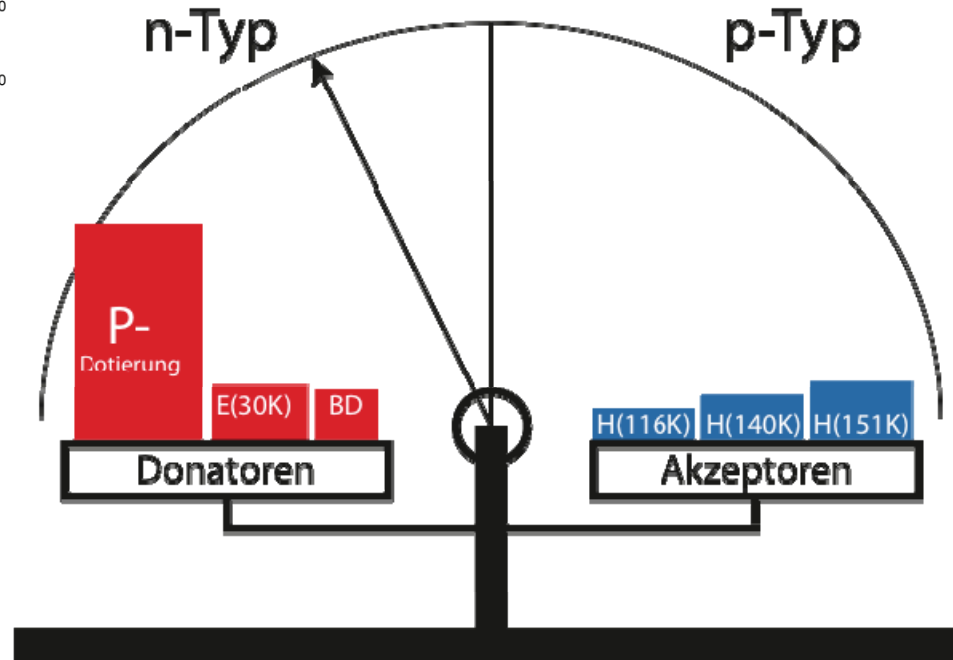
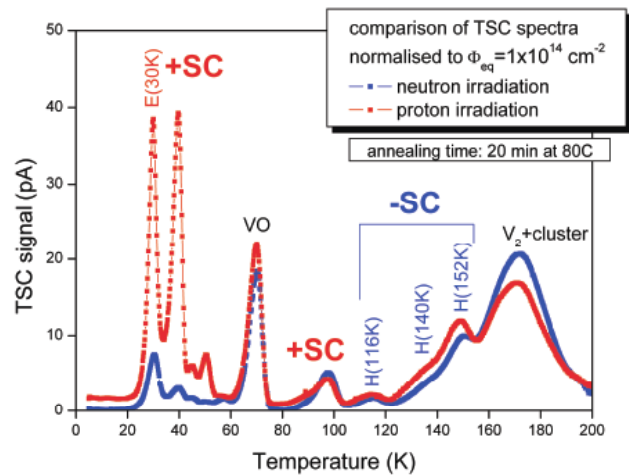
Epitaxial silicon (*EPI-DO, 72 μm , 170 Ωcm , diodes*) irradiated with reactor neutrons



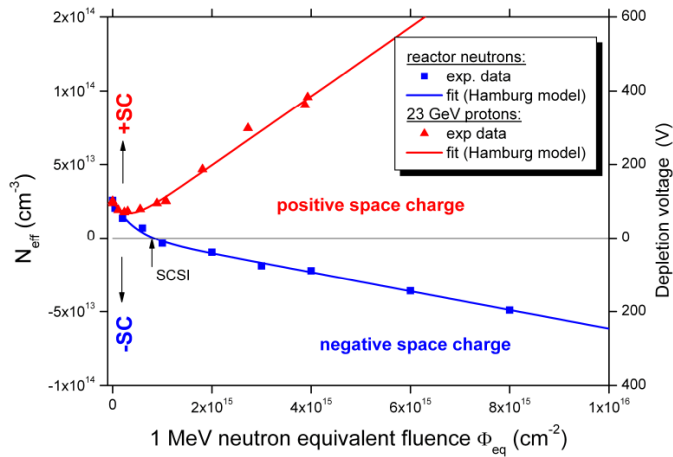
N_{eff} : Proton irradiation



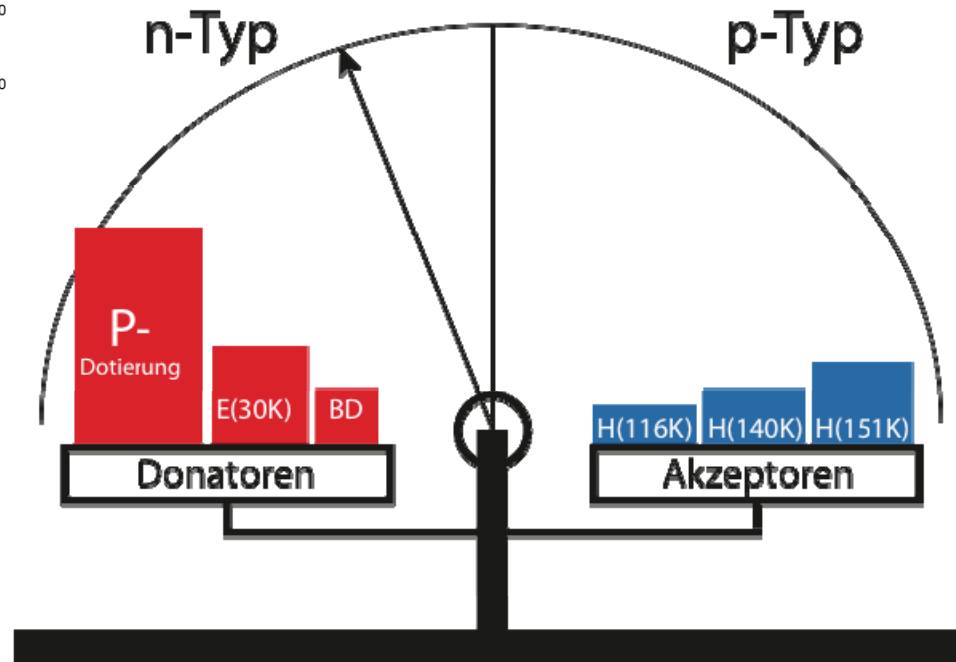
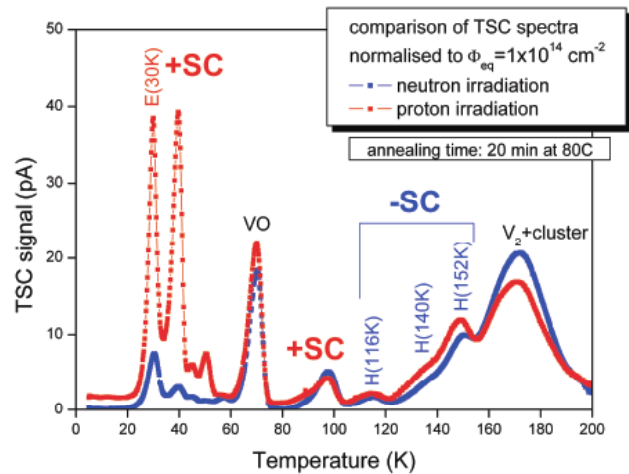
Epitaxial silicon (*EPI-DO*, $72\mu\text{m}$, $170\Omega\text{cm}$, *diodes*) irradiated with **23 GeV Protons**



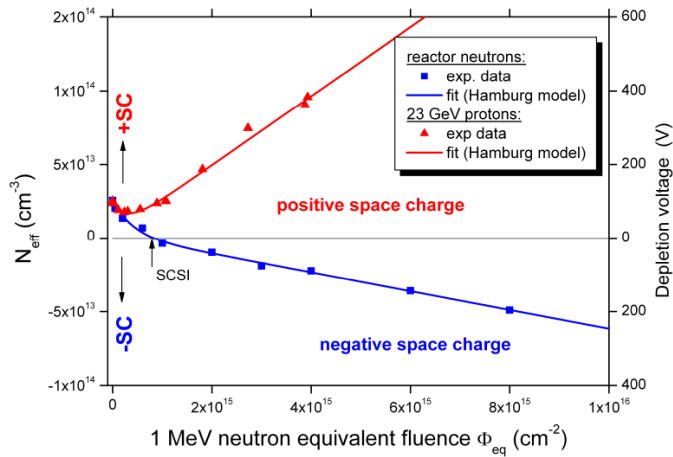
N_{eff} : Proton irradiation



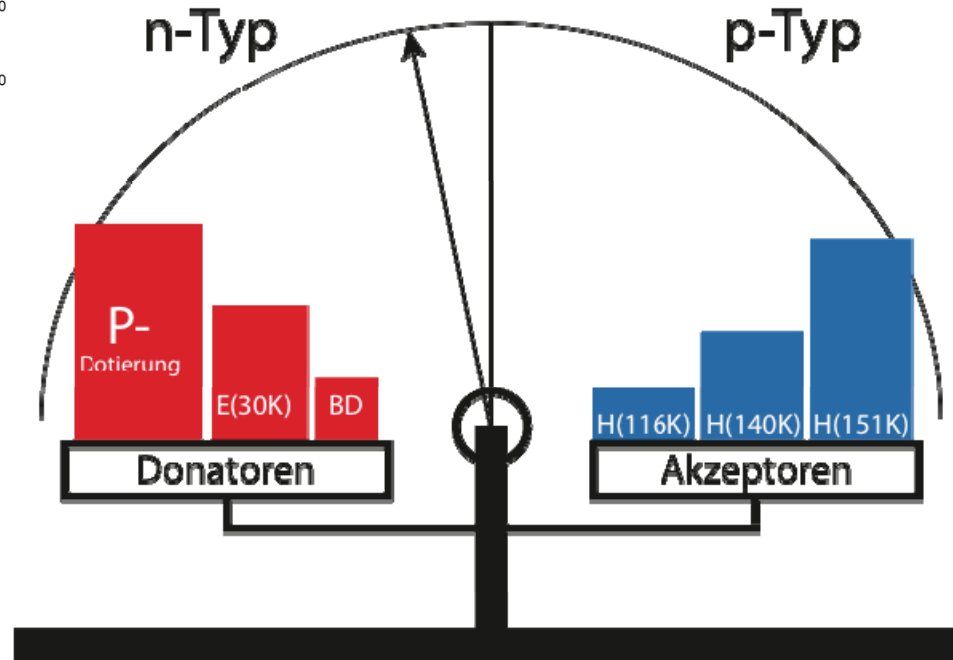
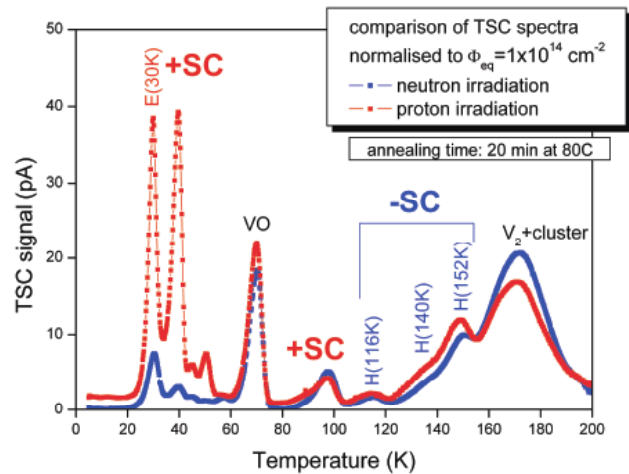
Epitaxial silicon (*EPI-DO*, $72\mu\text{m}$, $170\Omega\text{cm}$, *diodes*) irradiated with **23 GeV**
Protons



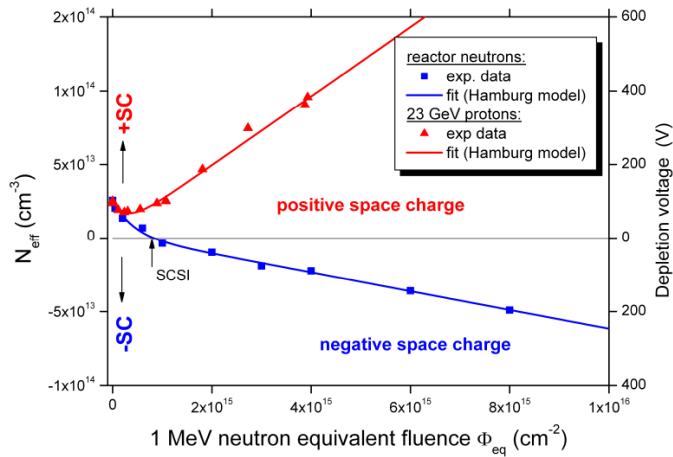
N_{eff} : Proton irradiation



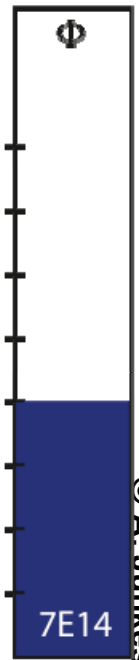
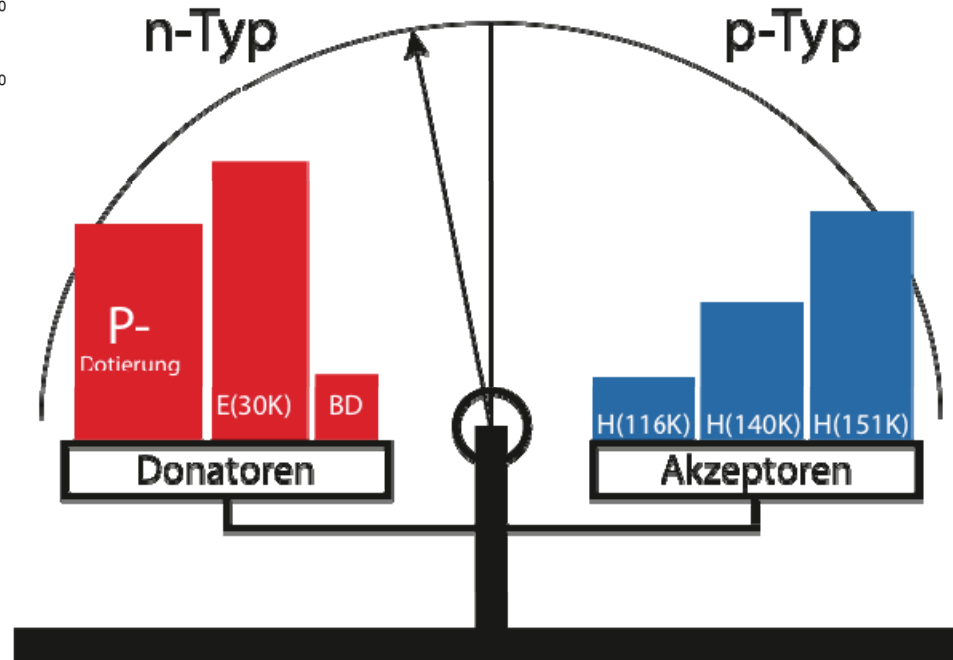
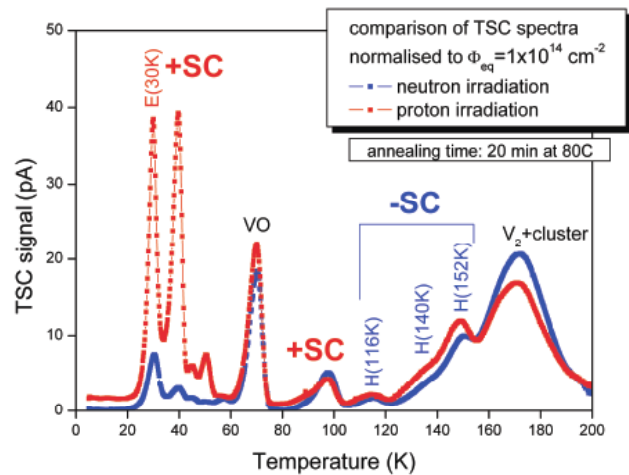
Epitaxial silicon (*EPI-DO*, $72\mu\text{m}$, $170\Omega\text{cm}$, *diodes*) irradiated with **23 GeV Protons**



N_{eff} : Proton irradiation

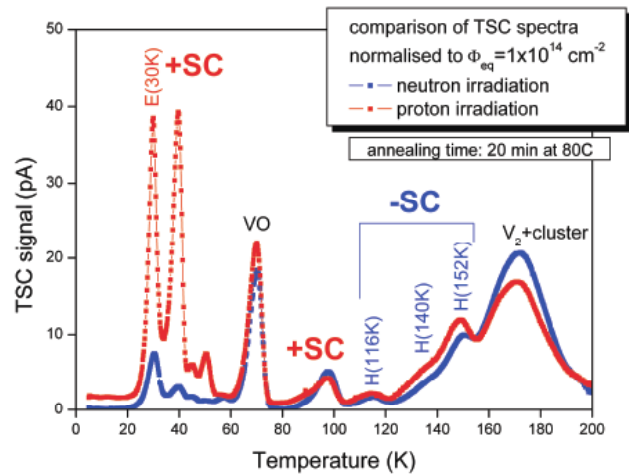
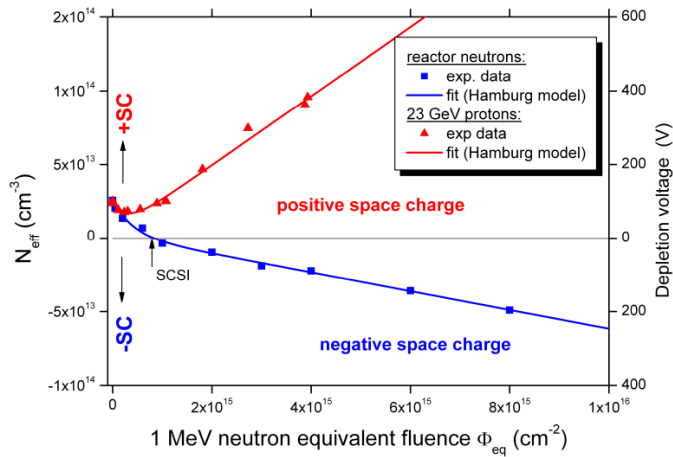


Epitaxial silicon (*EPI-DO*, $72\mu\text{m}$, $170\Omega\text{cm}$, *diodes*) irradiated with **23 GeV Protons**

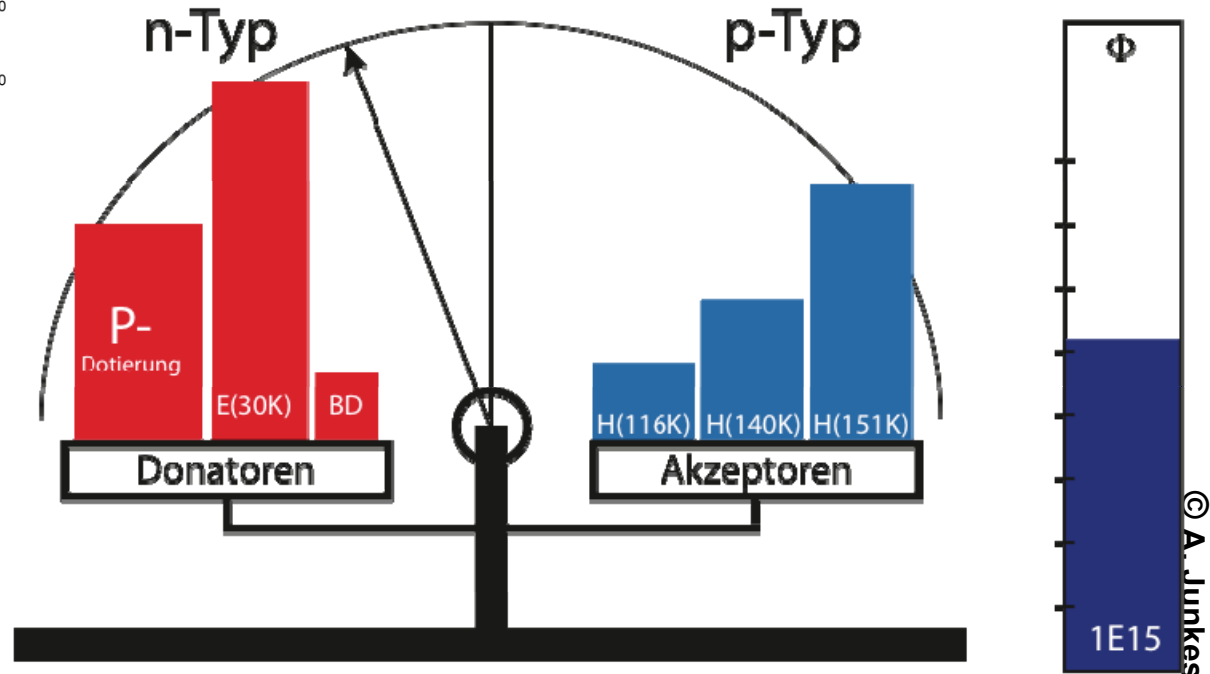


© A. Junkes

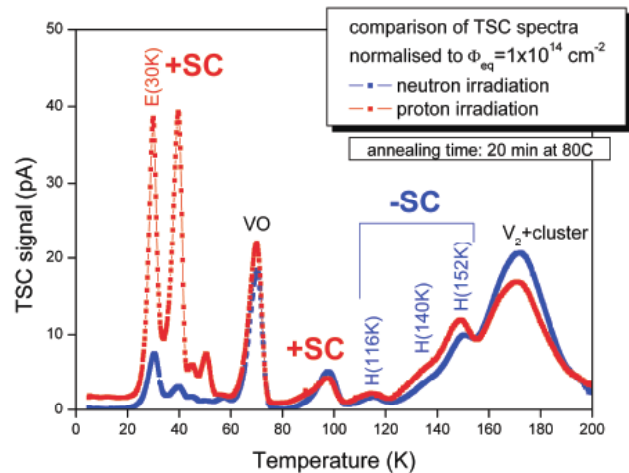
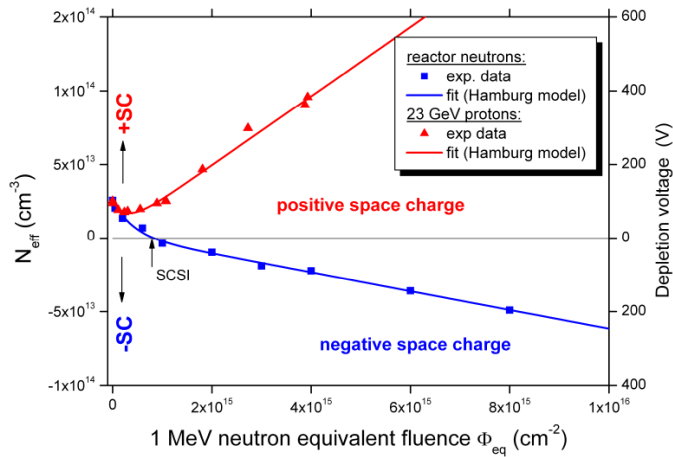
N_{eff} : Proton irradiation



Epitaxial silicon (*EPI-DO*, $72 \mu\text{m}$, $170 \Omega\text{cm}$,
diodes) irradiated with **23 GeV**
Protons

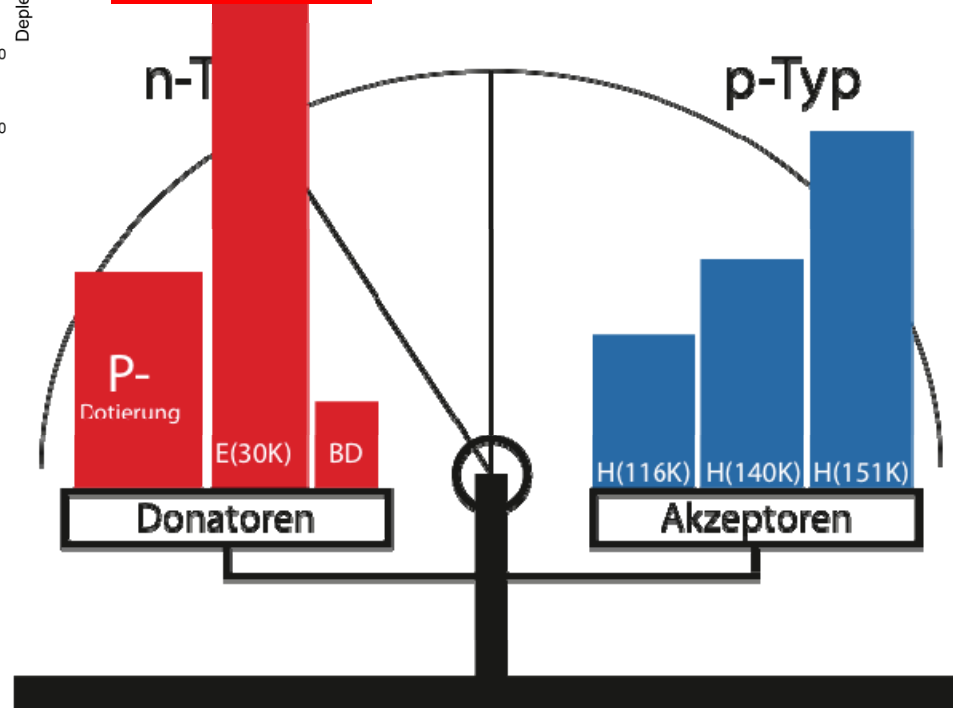


N_{eff} : Proton irradiation



Epitaxial silicon (*EPI-DO*, $72\mu\text{m}$, $170\Omega\text{cm}$, *diodes*) irradiated with **23 GeV**

Protons

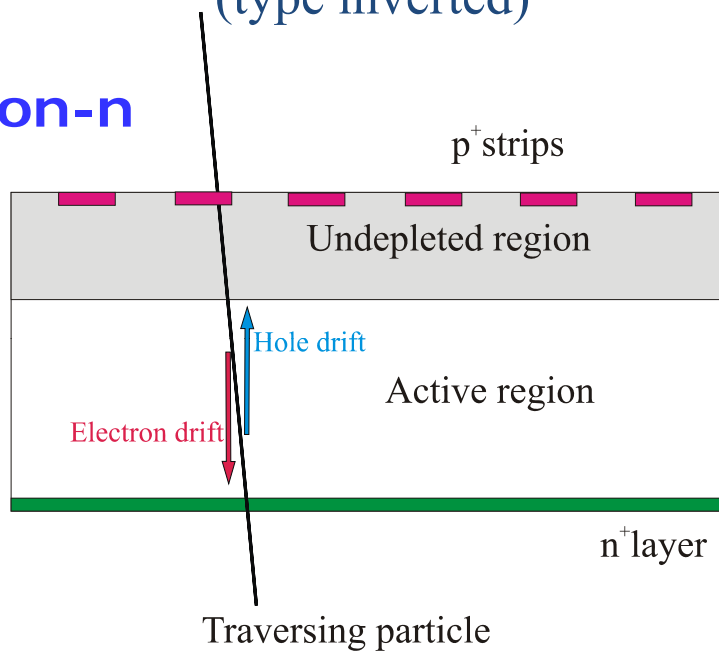


RD50: Device engineering

p-in-n versus n-in-p (or n-in-n) detectors

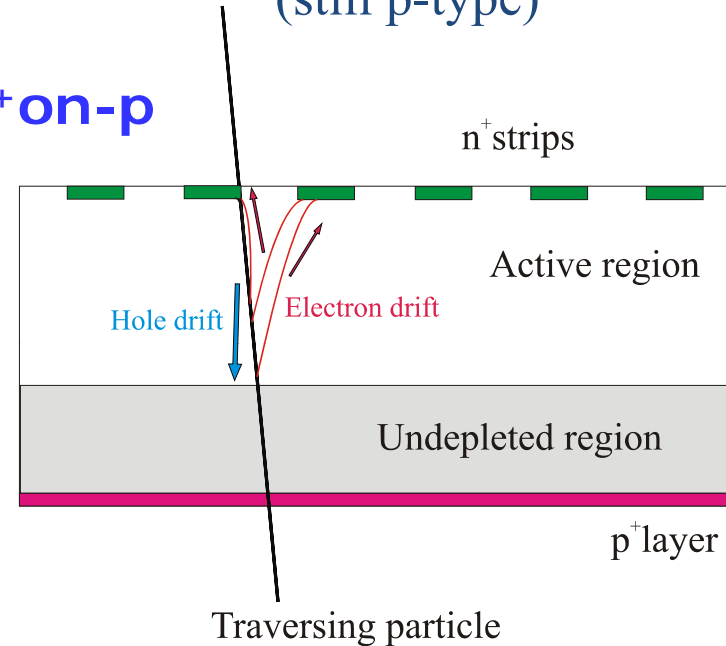
n-type silicon after high fluences:
(type inverted)

p⁺on-n



p-type silicon after high fluences:
(still p-type)

n⁺on-p



p-on-n silicon, under-depleted:

- Charge spread – degraded resolution
- Charge loss – reduced CCE

n-on-p silicon, under-depleted:

- Limited loss in CCE
- Less degradation with under-depletion
- Collect electrons (3 x faster than holes)

Comments:

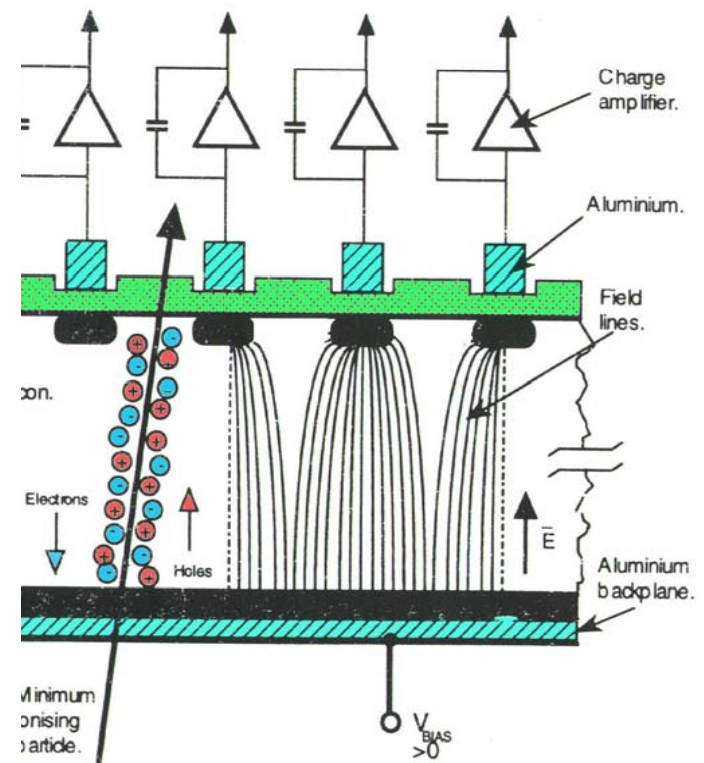
- Instead of n-on-p also n-on-n devices could be used

Charge Multiplication by impact ionization

Charge collected at electrodes in a semiconductor can not only be generated by ionising radiation but also by the acceleration of charge carriers by high electric fields, a phenomenon called **impact ionization**.

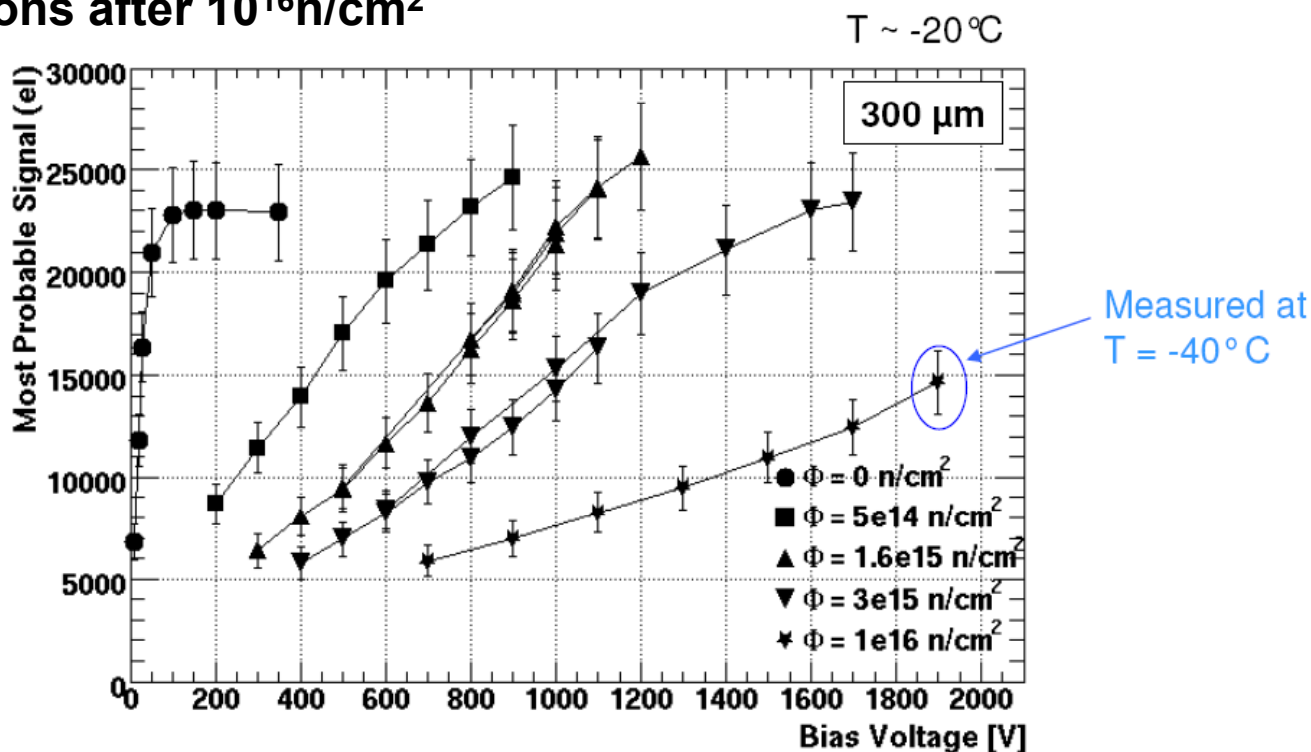
This way electrons and holes promoted in conduction/valence bands by ionising radiation (primary charge) attain enough energy to create new electron-hole pairs (secondary charge). This mechanism is also origin of current breakdown in diodes when very high reverse voltage are applied.

In a segmented device **electric field is increased in the nearby of the collecting electrode due to accumulation of field lines**. In irradiated devices the electric field is **also enhanced by radiation induced defects**.



Charge Multiplication

CCE measured with p-type Si microstrip detectors at very high fluences shows evidence of a charge multiplication effect: 100% CCE seen after $3 \times 10^{15} \text{ n/cm}^2$, 15000 electrons after 10^{16} n/cm^2



I. Mandić, RESMDD08, Florence, Italy, 15th -17th October 2008

7



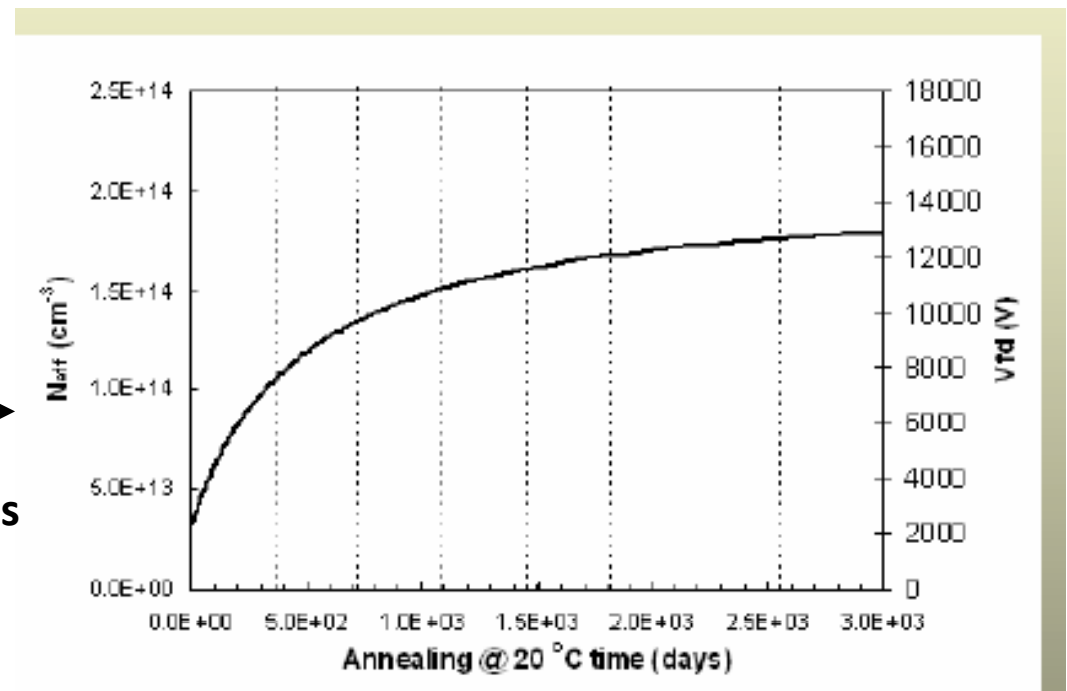
Origin: increase of the electric field close to the strips causing impact ionization/carrier when high concentrations of effective acceptors are introduced at very high fluences.

Annealing of irradiated microstrip detectors

Reverse annealing in irradiated Si microstrip detectors has been always considered as a possible cause of early failure in the experiments if not controlled by mean of low temperature (not only during operations but also during maintenance/shut down periods). This was originated by accurate measurements of the annealing behavior of the full depletion voltage in diodes measured with the CV method.

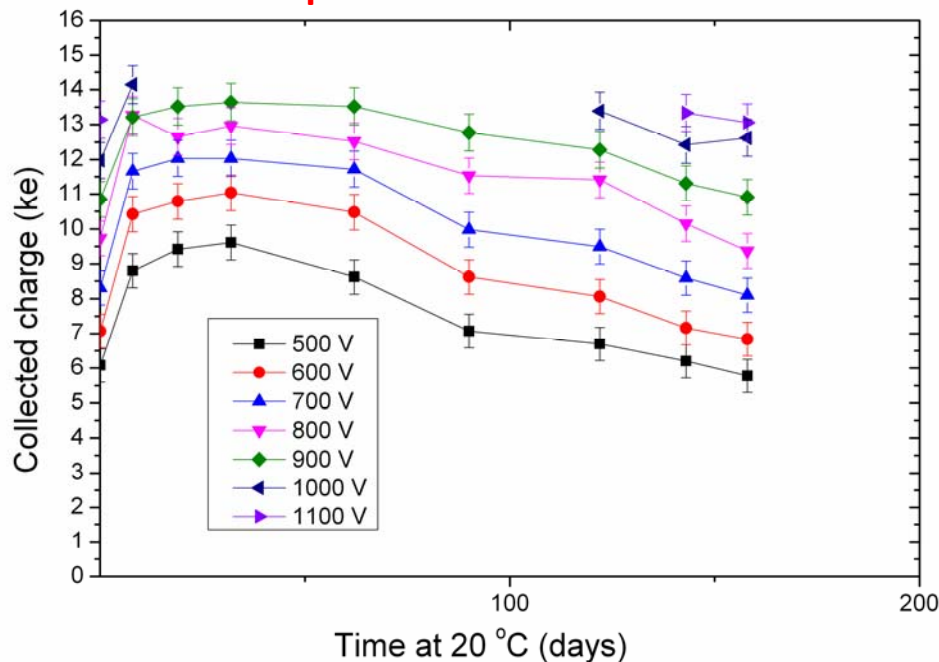
Expected changes of full depletion voltage with time after irradiation (as measured with the C-V method) for detector irradiated to $7.5 \cdot 10^{15} \text{ p cm}^{-2}$.

Please notice that according to CV measurements the so called V_{FD} changes from $<3\text{kV}$ to $>12\text{kV}$!

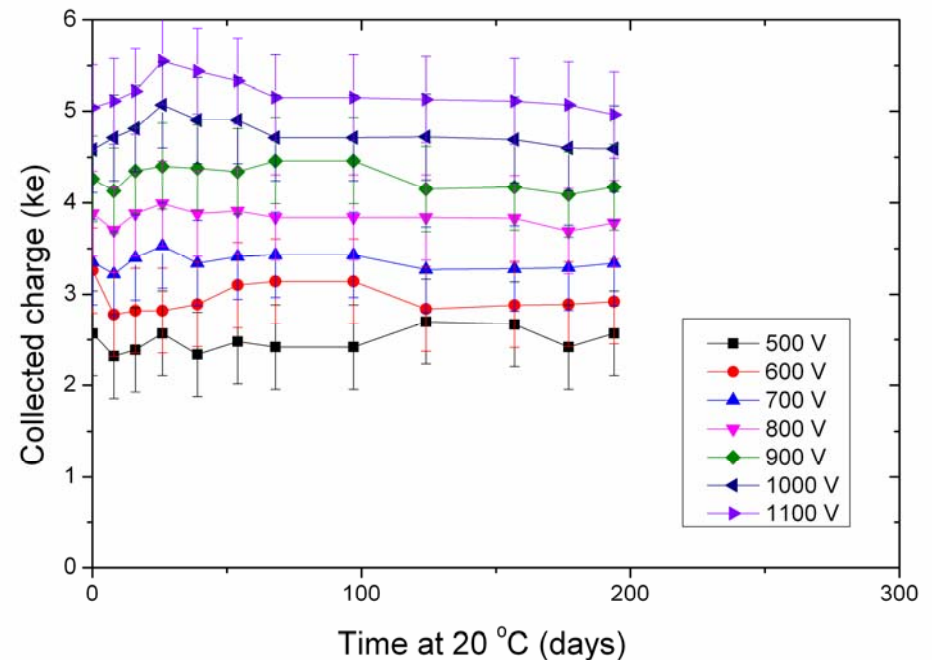


As a matter of fact, the annealing behaviour of the CCE measured with p-type Si microstrip detectors does not correspond to that measured by CV with diodes. **No reverse annealing is visible in the CCE measurement.**

HPK FZ n-in-p, $2E15 \text{ n cm}^{-2}$
26MeV p irradiation



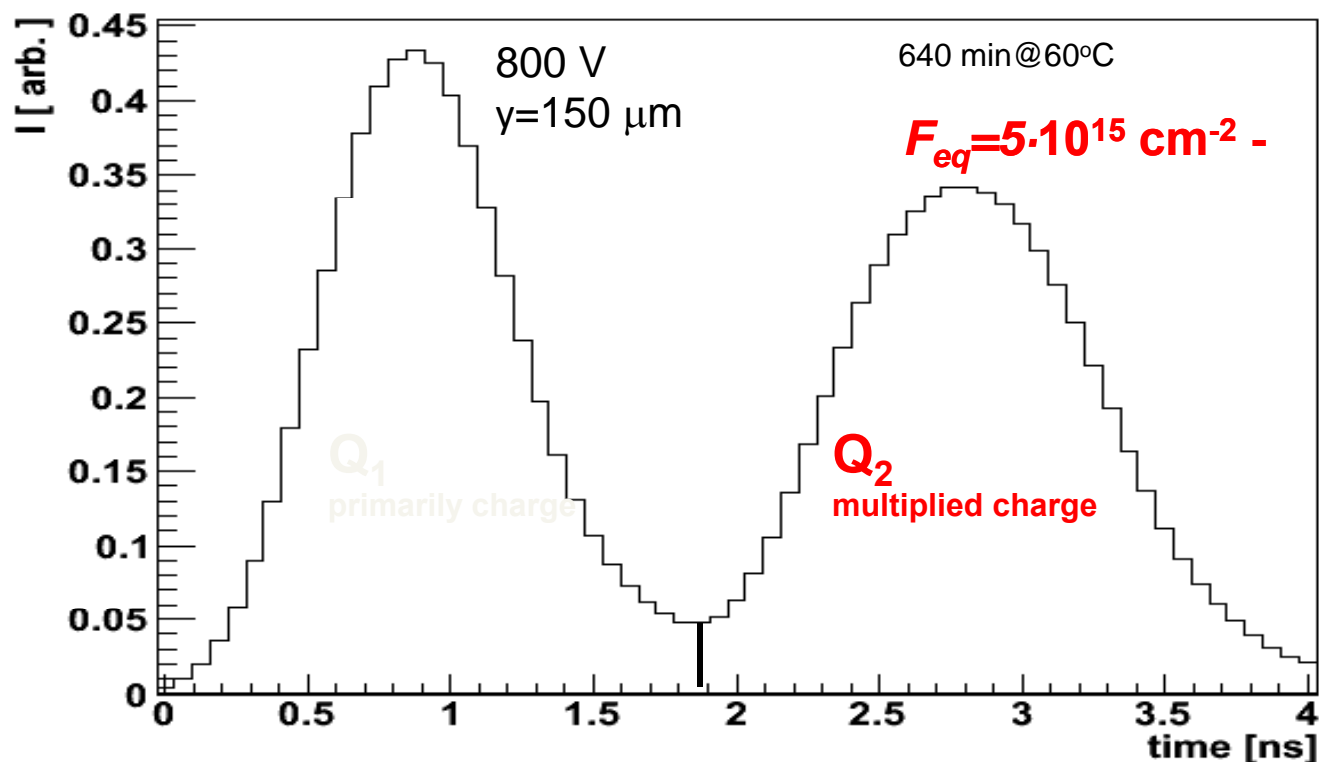
HPK FZ n-in-p,
 $1E16 \text{ n cm}^{-2}$ (26MeV p irradiation)



Origin of observed behaviour :

- Charge Multiplication due to increased electric field close to strips as concentration of acceptors grows with time/temperature;
- Reduction of the effective trapping probability of electrons with annealing.

Edge TCT: a way to visualize *Multiplication profiles*

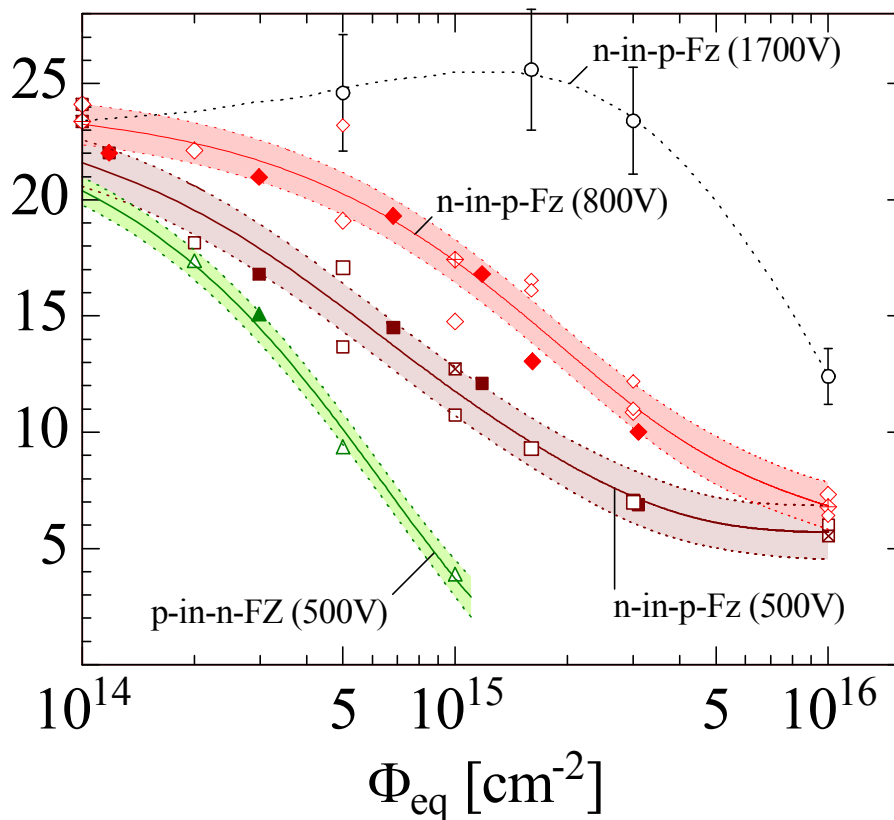


- 1st peak – current induced by the drift of primarily generated carriers
 - small change with annealing
- 2nd peak – current induced by the drift of multiplied holes
 - huge change with annealing

G. Kramberger, "Edge-TCT measurements with irradiated micro-strip silicon detectors", 8th RESMDD, Oct. 2010, Firenze, Italy

RD50 Planar Detector Compilation

Collected Charge [10^3 electrons]



FZ Silicon Strip Sensors

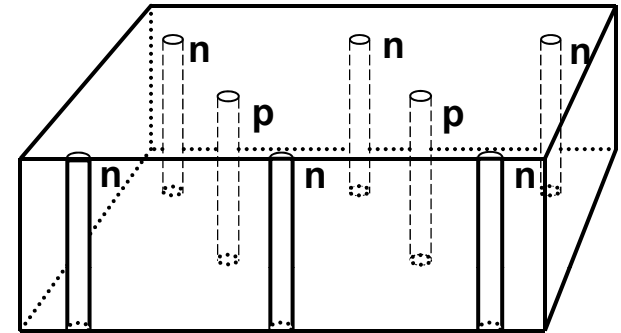
- n-in-p (FZ), 300 μm , 500V, 23GeV p
- n-in-p (FZ), 300 μm , 500V, neutrons
- ⊠ n-in-p (FZ), 300 μm , 500V, 26MeV p
- ◆ n-in-p (FZ), 300 μm , 800V, 23GeV p
- ◇ n-in-p (FZ), 300 μm , 800V, neutrons
- ◊ n-in-p (FZ), 300 μm , 800V, 26MeV p
- n-in-p (FZ), 300 μm , 1700V, neutrons
- ▲ p-in-n (FZ), 300 μm , 500V, 23GeV p
- △ p-in-n (FZ), 300 μm , 500V, neutrons

RD50 - M. Moll

- p-in-n fades away well before $10^{15} N_{eq}$
- n-in-p still gets 50% charge at $10^{16} N_{eq}$ at high bias voltages
- n-in-p benefits from charge multiplication (at high bias voltages)
- CM effect also seen for p-in-n (but less strong in partial depletion mode)
- n-in-p (n-in-n) superior material for high radiation environments

Device Engineering: 3D detectors

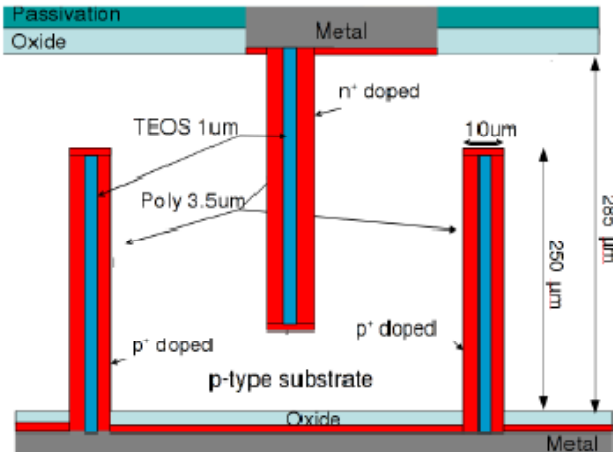
- Electrodes:
 - narrow columns along detector thickness-“3D”
 - diameter: $10\mu\text{m}$ distance: $50 - 100\mu\text{m}$
- Lateral depletion:
 - lower depletion voltage needed
 - thicker detectors possible
 - fast signal
- Hole processing :
 - Dry etching, Laser drilling, Photo Electro Chemical



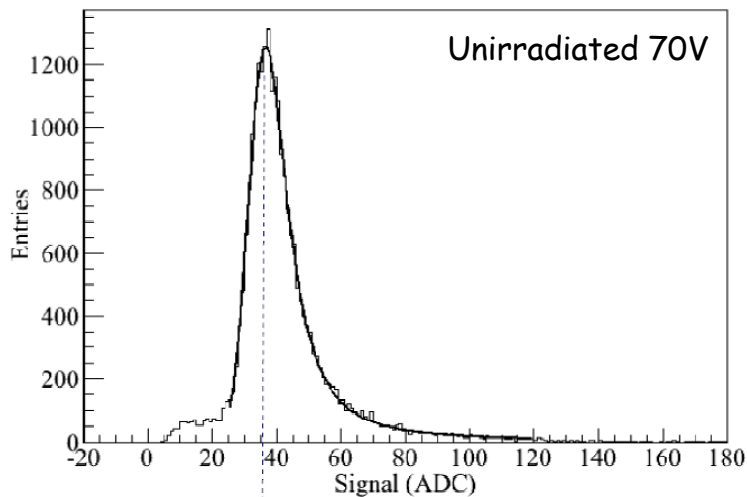
(Introduced by S.I. Parker et al., NIMA 395 (1997) 328)

Charge Collection of 3d Detectors: results from RD50

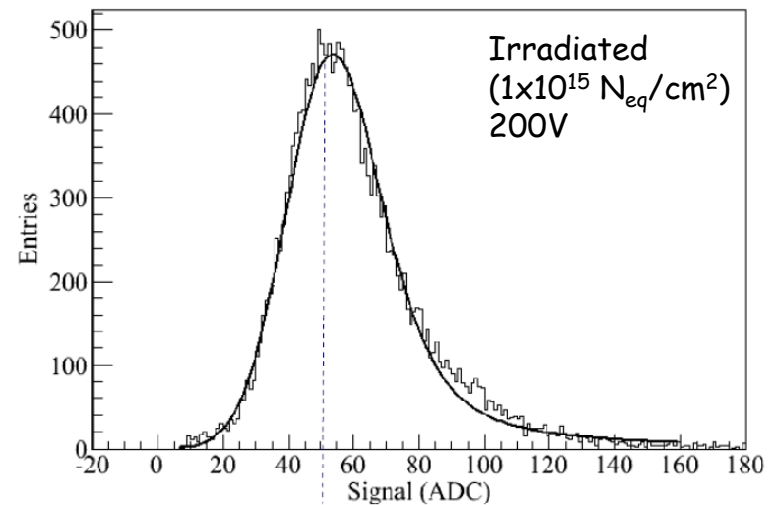
[M.Koehler et al., RD50 Workshop, May/June 2010]



- Double Sided 3d p-type sensors in SPS Testbeam
- Irradiation at the Karlsruhe cyclotron with 25MeV protons
- Higher signal after irradiation than before
→ Charge multiplication



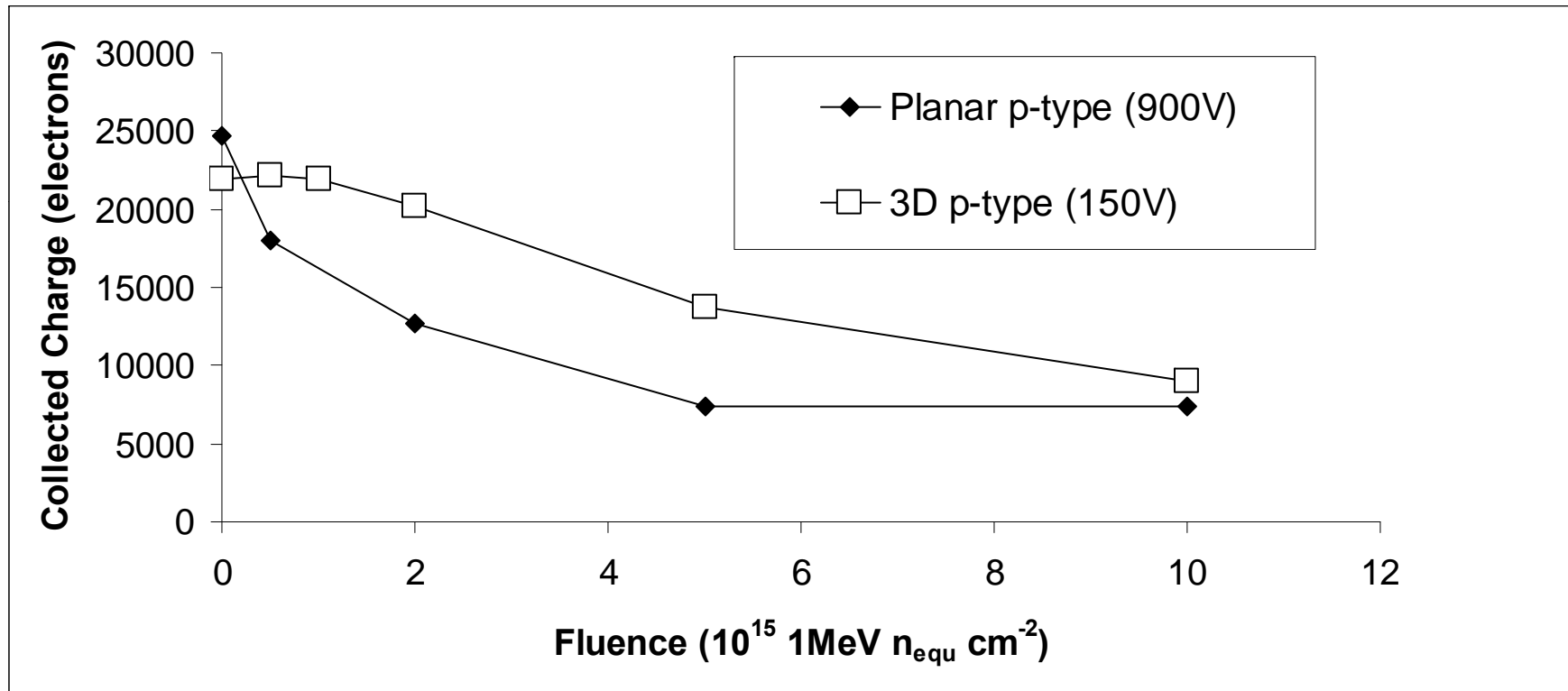
Landau MPV: 35 ADC



Landau MPV: 49 ADC

3D vs planar detectors

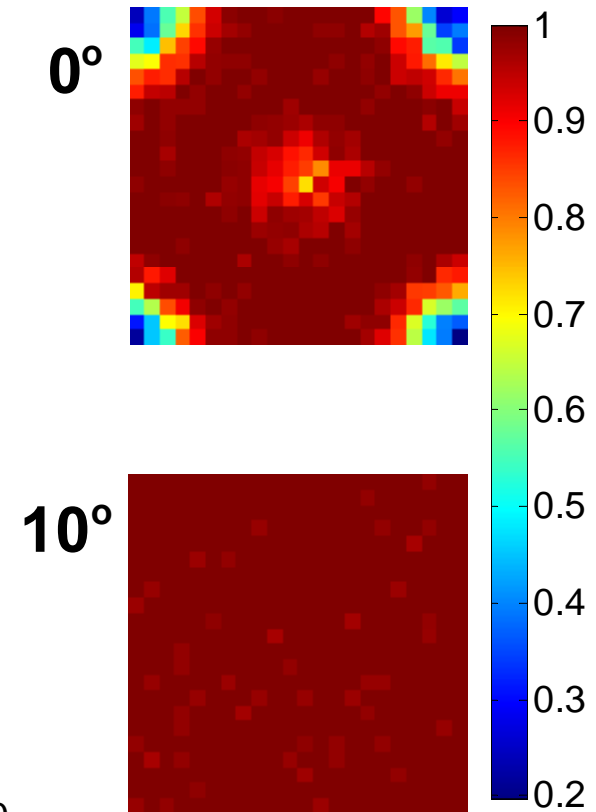
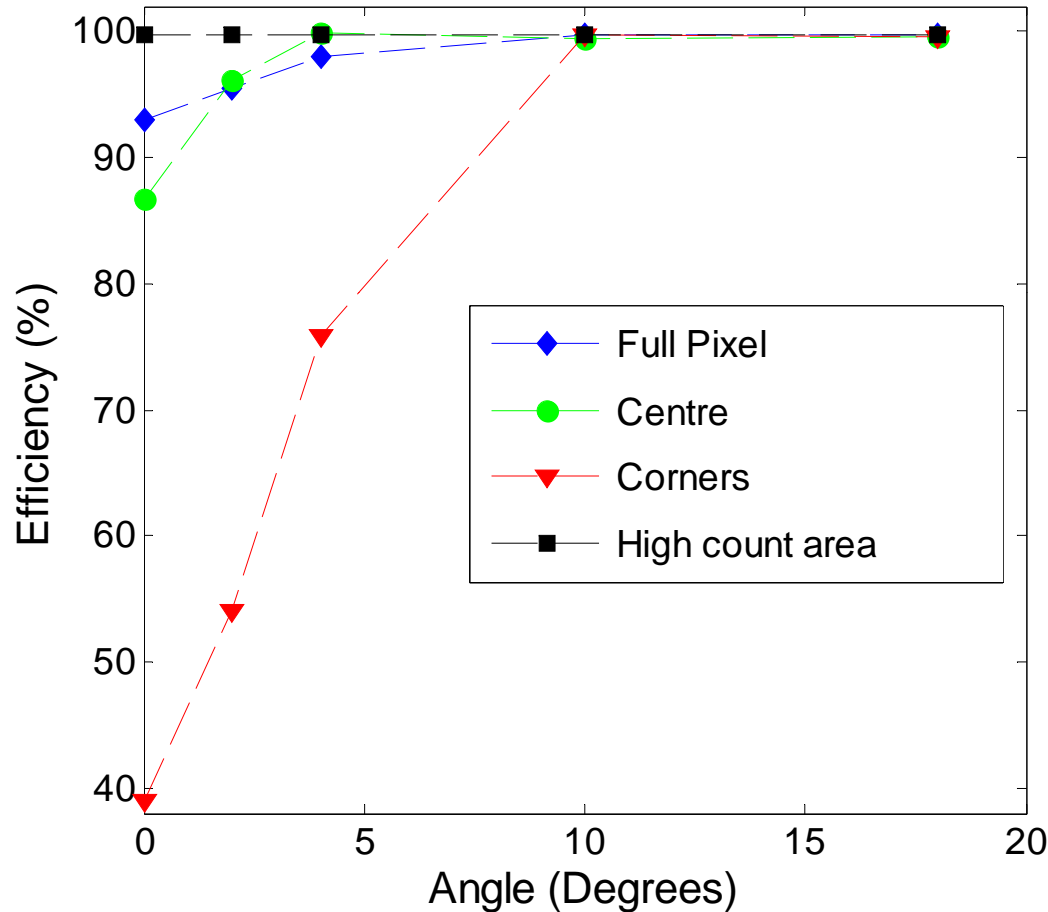
Collected charge as a function of fluence. Note 3D only 150V, high bias gets increase in charge due to multiplication



R. Bates et al. IEEE NSS 2009

R. Bates et al. IEEE Trans Nucl Sci To be published

Efficiency low in holes – reaches full efficiency at a track angle of 10degs



50um pitch (short side of ATLAS pixel)

C. Parkes et al. Submitted to JInst
P. Grenier et al. Submitted to NIMA

Conclusions

- Development of radiation-hard Silicon detectors for high-luminosity colliders, in particular the sLHC, is mandatory.
- RD50 is a forum to work on the subject inter-disciplinarily
- Microscopic view can explain radiation damage in detectors operative parameters. Large progress in understanding leakage current and effective doping concentration.
- Charge amplification and no annealing degradation observed on irradiated p-type Si microstrip sensors are beneficial to p-type Si detector performance especially at heavy fluence irradiations.
- N-on-p much better than standard n-on-p devices, good enough for most regions of the tracker.
- 3D Si can add extra radiation hardness if required for innermost sLHC tracking layer(s).